Title
Improvements for the in Vitro to in Vivo Extrapolation of Hepatic Clearance

Author
Bowman, Christine

Publication Date
2019

Peer reviewed|Thesis/dissertation

Improvements for the In Vitro to In Vivo Extrapolation of Hepatic Clearance

by
Christine Bowman

DISSERTATION
Submitted in partial satisfaction of the requirements for degree of
DOCTOR OF PHILOSOPHY

in

Pharmaceutical Sciences and Pharmacogenomics

in the

GRADUATE DIVISION
of the
UNIVERSITY OF CALIFORNIA, SAN FRANCISCO

Approved:

DocuSigned by:
Leslie Benet
336FEDB181AF457...

Leslie Benet
Chair

DocuSigned by:
Kathleen M. Giacomini

Kathleen M. Giacomini

DocuSigned by:
Rada Savic
7EC091D1336044E...

Rada Savic

Committee Members

ACKNOWLEDGEMENTS

I would like to deeply thank my mentors, family, and friends whose constant support made completing this thesis possible.

First I would like to thank my advisor and mentor Dr. Leslie Benet for his never-ending encouragement and support throughout my project. I will always appreciate not only learning from his scientific expertise, but also from his mentorship where he enourages creativity and independence, which has made me a more confident scientist. Les has unparalleled kindness and patience and is able to light up any room he walks into with his enthusiasm. I am so grateful to be a part of the Benet Lab family.

I would also like to thank Drs. Kathy Giacomini and Rada Savic, members of my thesis committee, for their very helpful feedback and advice throughout the development of this thesis. I appreciated the expertise of Drs. Matt Jacobson and Peter Turnbaugh, the other two members of my qualifying exam committee as well. I would also like to thank Dr. Deanna Kroetz, my program director, for her help with both my scientific and professional development starting on day one.

Being a part of the Benet Lab allowed me to have a great experience at UCSF. I would like to thank Dr. Hideaki Okochi for being such a helpful teacher and mentor especially with conducting my wet lab experiments. I would also like to thank our lab manager Alan Wolfe for always making the lab run seamlessly. I have learned a lot scientifically from both Hideaki and Alan. I would like to thank Frances Peterson as well for her constant support, positivity, and help with navigating graudate school. I would also like to thank all of the current and former members of the lab I have been lucky enough to interact with over the years who have not only been great sounding-boards, but also great friends.

I would also like to thank Drs. Yuan Chen, Jialin Mao, and everyone in the DMPK Department at Genentech for providing me the opportunity to do an internship there. I was lucky enough to have a project there that fit perfectly into my thesis work (Chapter 6) and it was a wonderful first experience working in the pharmaceutical industry.

I would also like to thank Dr. David Christianson, my former advisor and mentor at the University of Pennsylvania, and Dr. Ponzy Lu, my former program director, both of whom encouraged me to go to graduate school in the first place and helped with my decision to choose UCSF.

I would like to thank all of my PSPG classmates and the friends I have made over the years in San Francisco who have made the city feel like a second home. Finally, I would like to thank my parents and my entire family for their support throughout my life and especially during graduate school. They gave me the confidence to succeed in whatever I put my mind to, have always believed in me, and taught me the importance of education.

CONTRIBUTIONS

Chapter 2 was modified from "An examination of protein binding and protein-facilitated uptake relating to in vitro - in vivo extrapolation" as it was published in the European Journal of Pharmaceutical Science in October 2018. Christine Bowman wrote the manuscript with contributions from Leslie Benet.

Chapter 3 was modified from "Hepatic clearance predictions from in vitro-in vivo extrapolation and the Biopharmaceutics Drug Disposition Classification System" as it was published in Drug Metabolism and Disposition in November 2016. Christine Bowman and Leslie Benet contributed to study design. Execution and analyses were carried out by Christine Bowman. Christine Bowman wrote the manuscript with contributions from Leslie Benet.

Chapter 4 was modified from "In vitro-in vivo extrapolation and hepatic clearance dependent underprediction" as it was accepted in the Journal of Pharmaceutical Sciences in February 2019. Christine Bowman and Leslie Benet contributed to study design. Execution and analyses were carried out by Christine Bowman. Christine Bowman wrote the manuscript with contributions from Leslie Benet.

Chapter 5 was modified from "The presence of a transporter-induced protein binding shift: a new explanation for protein-facilitated uptake and improvement for in vitro-in vivo extrapolation" as it was published in Drug Metabolism and Disposition in April 2019. Christine Bowman, Hideaki Okochi, and Leslie Benet contributed to study design. Execution was carried out by Christine Bowman and Hideaki Okochi. Analyses were carried out by Christine Bowman, Hideaki Okochi, and Leslie Benet. Christine Bowman wrote the manuscript with contributions from Hideaki Okochi and Leslie Benet.

Chapter 6 was modified from a manuscript in preparation entitled “Organic anion transporting polypeptide (OATP) uptake predictions in HEK293 overexpressing cells in the presence and absence of human plasma”. Christine Bowman, Yuan Chen, and Jialin Mao contributed to study design. Execution was carried out by Christine Bowman, Eugene Chen, and Liuxi Chen. Analyses were carried out by Christine Bowman, Liuxi Chen, and Jialin Mao. Christine Bowman wrote the manuscript with contributions from Eugene Chen, Liuxi Chen, Xiaorong Liang, Matthew Wright, Yuan Chen and Jialin Mao.

Chapter 7 was modified from “Interlaboratory variability in human hepatocyte intrinsic clearance values and trends with physicochemical properties” as it was accepted in Pharmaceutical Research in May 2019. Christine Bowman and Leslie Benet contributed to study design. Execution and analyses were carried out by Christine Bowman. Christine Bowman wrote the manuscript with contributions from Leslie Benet.

Improvements for the In Vitro to In Vivo Extrapolation of Hepatic Clearance

Christine Bowman

ABSTRACT

Clearance, or a measure of the body's ability to remove drug, is a crucial pharmacokinetic parameter. Since clearance is linked to a drug's dosing regimen as well as its efficacy and toxicity, accurately predicting the parameter early in the drug discovery process is important to reduce the time and cost associated with drug development. To predict hepatic clearance, in vitro to in vivo extrapolation (IVIVE) is commonly used where an in vitro clearance measure generated in hepatocytes or microsomes is scaled to an in vivo prediction using biological scaling factors and a model of hepatic disposition.

The goal of this work was to evaluate the current state of IVIVE and examine ways to improve hepatic clearance predictions. After a literature search, we found that in human microsomes and hepatocytes, on average, 66.5% of drugs were predicted inaccurately (or fell outside two-fold of their in vivo clearance value). We also found that ≤ 25% of high extraction ratio compounds were predicted to have high extraction ratios. Examining the Biopharmaceutics Drug Disposition Classification System found that class 2 drugs have poorer predictions than class 1 drugs (81.9% vs. 62.3% inaccuracy), however these percentages of inaccuracy were still high in both cases. We conclude that the IVIVE of hepatic clearance needs to be improved through a better understanding of mechanisms.

We go on to propose a new hypothesis called a transporter induced protein binding shift (TIPBS) that is a new explanation for protein-facilitated uptake and can help mitigate current IVIVE error. When reviewing previous explanations for protein facilitated uptake, we noted that

the hypotheses did not include the potential role of hepatic uptake transporters, and the poorest IVIVE predictions often occur for compounds that have high protein binding and are substrates of transporters. We hypothesized that for highly protein bound drugs with high affinity to transporters, protein-binding may not actually be restricting the drug's access to the hepatocyte, which would lead to greater uptake and clearance values than currently predicted. We found support for our new TIPBS hypothesis by measuring the uptake of compounds in protein-free buffer vs. 100% plasma using rat hepatocytes as well as human embryonic kidney (HEK)293 cells overexpressing uptake transporters.

Finally we examined trends in clearance prediction accuracy with physiochemical and pharmacokinetic parameters. After noting high interlaboratory variability, we found that less lipophilic, lower intrinsic clearance, and lower protein binding compounds may yield more accurate predictions. These findings highlight the current errors associated with IVIVE and provide suggestions to improve predictions moving forward.

TABLE OF CONTENTS

LIST OF FIGURES

LIST OF TABLES

CHAPTER 1: Challenges with Hepatic Clearance Prediction

Since the current drug discovery and development process is lengthy and costly (1, 2), it is important to identify compound failures as early in the pipeline as possible to reduce inefficiency. When deciding which compounds to move forward, one of the most important pharmacokinetic parameters to estimate and consider is clearance (CL), or the measure of the body's ability to eliminate drugs, as the parameter is linked to drug exposure, half-life, and dosing interval (3). Most drugs are cleared hepatically and/or renally, and given that clearance is an additive process, predictions of all routes of clearance must be considered together to have an accurate estimate of total clearance.

Prediction Methods

Allometric scaling is one approach that can be taken for predicting human clearance using animal data. Using this method, the parameter of interest, clearance, is correlated with body size ($Y = aW^b$, where Y is clearance, W is body weight, and a and b are the allometric coefficient and exponent, respectively). While this approach has been shown to be useful in clearance predictions for drugs that are primarily cleared renally and is commonly used for such drugs, it is less useful for compounds cleared hepatically (4) as there can be species differences in the expression levels, substrate selectivity and activities of enzymes and transporters involved in hepatic drug clearance. Instead, in vitro - in vivo extrapolation (IVIVE) is commonly used to predict the hepatic clearance of compounds.

The typical IVIVE process involves determining the intrinsic clearance (CL_{int}) of a compound in vitro using rat or human microsomes or hepatocytes, which is then scaled to an in

vivo prediction for the corresponding species using physiologically based scaling factors as well as a model of hepatic disposition such as the well-stirred model shown below:

$$CL_H = \frac{Q_H \cdot f_{u,B} \cdot CL_{int,in\ vivo}}{Q_H + f_{u,B} \cdot CL_{int,in\ vivo}}$$

where CL_H is hepatic clearance, Q_H is hepatic blood flow and $f_{u,B}$ is the fraction unbound in blood (the fraction of drug not bound to proteins which is commonly measured with equilibrium dialysis). This process will be described in more detail in Chapter 2. Despite the common use of IVIVE, there is often underprediction that could be due to liver preparation process issues, cofactor depletion, ignoring the possibility of extra-hepatic metabolism, or errors in the measurement and/or understanding of protein binding (5). The overall IVIVE process and its current inaccuracy is depicted in Figure 1.1.

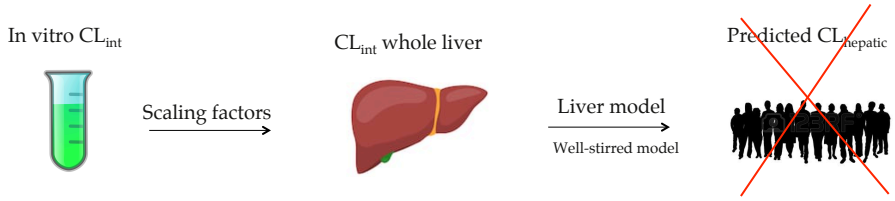

Figure 1.1: The traditional scale-up using IVIVE; however hepatic clearance is often not predicted accurately.

Understanding Plasma Protein Binding

Pharmaceutical scientists have long recognized the importance of plasma protein binding in pharmacokinetics and pharmacodynamics and the fraction unbound (f_u) term appears in equations for several fundamental parameters including clearance and volume of distribution (6). According to the traditional free drug theory, the unbound fraction of drug drives the efficacy of the molecule and is the portion that can undergo hepatic uptake followed by elimination.

According to the theory, protein binding is a rapid equilbirum process and drug concentration is the same on both sides of a membrane at steady state. However, after the transporter field emergered, it became clear that the assumption of instant equilbirum between the blood and an intracellular compartment is not valid for actively transported drugs where the intracellular free concentration would be higher than the free blood concentration. Other violations to the free drug theory have been suggested as well and it has been proposed that hepatic uptake may occur not only from the free drug, but also directly from the protein-drug complex. Studies found that highly protein bound ligands had more efficient hepatic uptake than could be accounted for by just their unbound concentrations, a phenomenon known as protein-facilitated uptake. The lack of recognition of protein-facilitated uptake could be leading to the underprediction seen with IVIVE.

Thesis Aims

This thesis aims to explore the current state of IVIVE and the underprediction commonly seen, to examine previous explanations of protein-facilitated uptake, and to propose a new hypothesis called a transporter-induced protein binding shift to mitigate IVIVE underprediction and reevaluate the role of protein binding.

The second chapter of this thesis reviews plasma protein binding and IVIVE in more detail and provides a balanced assessment of previous explanations of protein-facilitated uptake. Background and the current state of hypotheses including the possibility of a specific albumin receptor, rate-limiting dissociation of ligand from the albumin-ligand complex, rate-limiting diffusion of ligand through the unstirred water layer, and interactions with the hepatocyte cell surface are discussed.

The third chapter explores the accuracy of published in vitro intrinsic clearance values for the prediction of in vivo clearance. A literature search was conducted to assess IVIVE accuracy across several laboratories. The results of this search were further used to examine trends related to the Biopharmaceutics Drug Disposition Classification System (BDDCS) (7), which helps categorize transporter effects on drug disposition. BDDCS class 1 drugs, those that are extensively metabolized and highly soluble, are able to overwhelm transporters, while class 2 drugs, also extensively metabolized but poorly soluble, can be affected by efflux transporters in the gut, and both uptake and efflux transporters in the liver. Since in a previous study the poorest IVIVE predictions were found for drugs that have high plasma protein binding and are substrates of hepatic uptake transporters (8) examining BDDCS classification may help determine whether a drug's predicted in vitro hepatic clearance will be accurate or not.

Groups have also noticed poorer IVIVE predictions for compounds with high CL_{int} (9-11). The fourth chapter of this thesis examines if the trend also holds for compounds with high CL_H, as hepatic clearance, not CL_{int} alone, is the parameter used for first-in-human dose predictions.

The fifth and sixth chapters focus on our innovative hypothesis called a transporter-induced protein binding shift (TIPBS), which is a new explanation for protein-facilitated uptake and may help mitigate IVIVE underprediction. To evaluate the idea, we measured the uptake of high affinity transporter substrates with high and low protein binding in incubations with protein-free buffer vs. 100% plasma. Chapter 5 supports the hypothesis with rat hepatocyte data and chapter 6 supports it with human embryonic kidney (HEK)293 cell data.

Finally the seventh chapter aims to find physiochemical determinants of accurate IVIVE. It is expected that new hypotheses such as TIPBS that are being developed and implemented will

reduce the current IVIVE underprediction, but in the meantime, it is important to know which new compounds will yield accurate clearance predictions and which will not. By categorizing compounds based on physicochemical properties, the process of determining the data needed for a specific compound may be simplified.

References

(1) Hay M, Thomas DW, Craighead JL, Economides C and Rosenthal J (2014) Clinical development success rates for investigational drugs. *Nat Biotechnol* **32:**40-51.

(2) Parasrampuria DA, Benet LZ and Sharma A (2018) Why drugs fail in late stages of development: case study analyses from the last decade and recommendations. *AAPS J* **20:**46.

(3) Benet LZ (2010) Clearance (née Rowland) concepts: a downdate and an update. *J Pharmacokinet Pharmacodyn* **37:**529-539.

(4) Huh Y, Smith DE, and Feng MR (2011) Interspecies scaling and prediction of human clearance: comparison of small- and macro-molecule drugs. *Xenobiotica* **41:**972-987.

(5) Chiba M, Ishii Y and Sugiyama Y (2009) Prediction of hepatic clearance in human from in vitro data for successful drug development. *AAPS J* **11:**262-276.

(6) Schmidt S, Gonzalez D and Derendorf H (2010) Significance of protein binding in pharmacokinetics and pharmacodynamics. *J Pharm Sci* **99:**1107-1122.

(7) Wu CY and Benet LZ (2005) Predicting drug disposition via application of BCS: transport/absorption/elimination interplay and development of a biopharmaceutics drug disposition classification system. *Pharm Res* **22:**11-23.

(8) Soars MG, McGinnity DF, Grime K and Riley RJ (2007) The pivotal role of hepatocytes in drug discovery. *Chem Biol Interact* **168:**2-15.

(9) Hallifax D, Foster JA, and Houston JB (2010) Prediction of human metabolic clearance from in vitro systems: retrospective analysis and prospective view. *Pharm Res* **27:**2150-2161.

(10) Foster JA, Houston JB and Hallifax D (2011) Comparison of intrinsic clearances in human liver microsomes and suspended hepatocytes from the same donor livers: clearance-dependent relationship and implications for prediction of in vivo clearance. *Xenobiotica* **41:**124-136.

(11) Wood FL, Houston JB and Hallifax D (2017) Clearance prediction methodology needs fundamental improvement: trends common to rat and human hepatocytes/microsomes and implications for experimental methodology. *Drug Metab Dispos* **45:**1178-1188.

CHAPTER 2: An Examination of Protein Binding and Protein-Facilitated Uptake Relating to In Vitro-In Vivo Extrapolation[*]

Abstract

As explained by the free drug theory, the unbound fraction of drug has long been thought to drive the efficacy of a molecule. Thus, the fraction unbound term, or f_u, appears in equations for fundamental pharmacokinetic parameters such as clearance, and is used when attempting in vitro to in vivo extrapolation (IVIVE). In recent years though, it has been noted that IVIVE does not always yield accurate predictions, and that some highly protein bound ligands have more efficient uptake than can be explained by their unbound fractions. This review explores the evolution of f_u terms included when implementing IVIVE, the concept of protein-facilitated uptake, and the mechanisms that have been proposed to account for facilitated uptake.

[*] Modified from the publication: Bowman CM and Benet LZ (2018) An examination of protein binding and protein-facilitated uptake relating to in vitro - in vivo extrapolation. *Eur J Pharm Sci* **123:**502-514.

[*]Modified from the publication: Bowman CM and Benet LZ (2016) Hepatic clearance

Introduction

Beginning as early as 1949 with Goldstein's review of the interactions between drugs and proteins (1), pharmaceutical scientists have recognized the importance of plasma protein binding (PPB) in pharmacokinetics and pharmacodynamics. Appearing in equations for several parameters including clearance and volume of distribution, it is one of the most fundamental properties in the field (2). The widely accepted free drug theory (FDT) (Fig. 2.1) explains that plasma protein binding is a rapid equilibrium process allowing a constant concentration of free drug, and in the absence of energy-dependent processes, this free drug concentration is the same on both sides of a membrane at steady state (3). The other main principle of FDT is that only free drug can reach the site of action (or metabolism), and therefore the free drug concentration is what drives the pharmacological effect of a molecule (4).

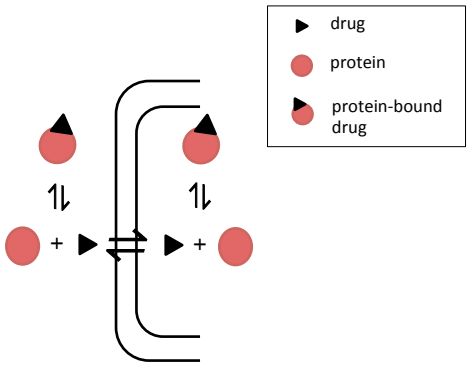

Figure 2.1: Free drug theory. According to free drug theory only free drug can reach the site of action or metabolism, and at steady state, the unbound drug concentration is the same on both sides of the membrane.

While PPB is one of the most fundamental properties, it is often misinterpreted and compounds are wrongfully "optimized" based on protein binding measurements (4, 5). Hueberger et al. (6) nicely summarize the answer to the question they pose in their paper entitled, "When Is Protein Binding Important?". In the final section they discuss the use of f_u, the

unbound fraction of drug, in the in vitro-in vitro extrapolation (IVIVE) of hepatic clearance. This review expands upon the questions surrounding protein binding, protein-facilitated uptake, and IVIVE.

Plasma Protein Binding

Major Drug Binding Proteins

While there are several drug-binding components in plasma including lipoproteins and globulins, human serum albumin (HSA) and α-1-acid glycoprotein (AAG) have been the most extensively studied and are present in large enough amounts to have an effect on drug action.

HSA, a 66 kDa globular protein containing 585 amino acids including a large amount of charged residues, is present in the body at a relatively constant concentration of 600 μM (7). It is the most abundant protein in human plasma and accounts for 50% of total plasma protein content (8). Physiologically HSA maintains colloid osmotic pressure, and is capable of binding both endogenous ligands (such as fatty acids and bilirubin) as well as xenobiotics (7). Composed of 3 homologous domains (I-III) each with two sub-domains (A and B) (7), HSA has several low affinity binding sites and at least two high affinity drug binding sites (Sudlow site I and Sudlow site II) with a bias for binding acidic drugs (9). The protein undergoes different transitions depending on pH: the neutral-fast (N-F) transition between pH 5.0-3.5 that causes elongation, the fast-elongated (F-E) or acid expansion transition below pH 3.5 that causes further expansion, and the neutral-base (N-B) transition between pH 7.0-9.0 that causes enhanced binding at site I (10, 11).

AAG, a 38-48 kDa acidic protein containing 204 amino acids, can have more variable concentrations in the body. In healthy subjects it is typically present at 12-31 μM, however as an

acute-phase protein synthesized in the liver, it can be as high as 60 μM in some disease states (3). In other disease states, while levels of AAG are unchanged, its binding capacity is reduced (12). AAG binding has also been shown to be dependent on age, gender, ethnicity, obesity, pregnancy, and diurnal changes (13). While multiple binding sites have been reported, only one appears to be important for drug binding, and it has a preference for basic and neutral drugs (12). The lower baseline levels of AAG as well as its possibility to fluctuate can readily cause drug-binding effects.

The association and dissociation of the drug-protein complex is rapid (2) and at equilibrium can be described as:

$$[D] + [P] \underset{k_{off}}{\overset{k_{on}}{\rightleftharpoons}} [DP]$$

where k_{on} and k_{off} are the association and dissociation rate constants, and the affinity of the drug for binding to the protein can be described by the association constant, K_a, or its inverse, the dissociation constant, K_d:

$$K_a = \frac{[DP]}{[D] \cdot [P]} = \frac{1}{K_d}$$

Methods to Measure Plasma Protein Binding

While there are several methods used to measure protein binding and in depth reviews comparing them (13, 14) the three most widespread methods measuring equilibrium binding in vitro will be briefly summarized here (Fig. 2.2).

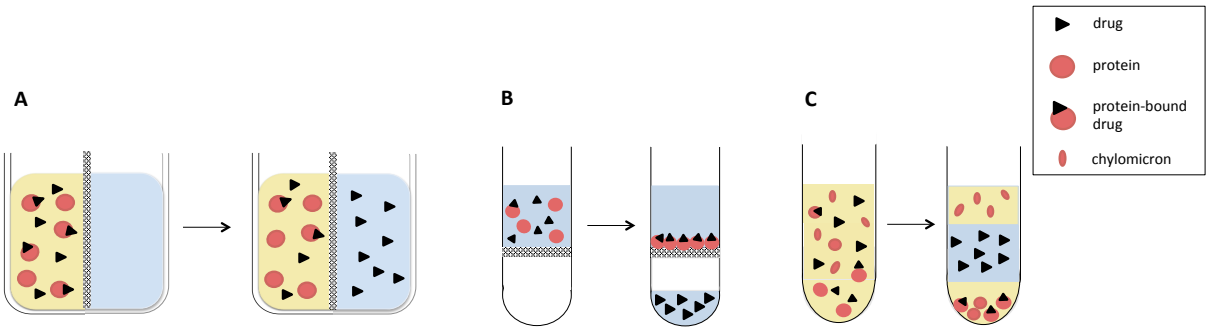

Figure 2.2: In vitro methods for measuring f_u. The fraction unbound can be determined with A) equilibrium dialysis B) ultrafiltration or C) ultracentrifugation.

The most commonly used technique to measure protein binding in the pharmaceutical industry is equilibrium dialysis (Fig. 2.2A). Using a device with two chambers separated by a semipermeable membrane, the protein-drug solution is added on one side, while buffer is added on the opposing side. When equilibrium is reached, the free fraction can be determined by measuring the total drug concentration in the protein chamber and the free drug concentration in the buffer chamber. Despite its ease of use, equilibrium dialysis still has disadvantages that must be considered including nonspecific binding to the membrane and the apparatus, volume shifts due to colloidal osmotic pressure, Gibbs-Donnan effects where charged particles near the membrane do not distribute evenly on both sides of the membrane, protein leakage across the membrane if the integrity of the membrane is compromised, and the need to determine the time required to reach equilibrium (14).

Other commonly used methods are ultrafiltration and ultracentrifugation. Ultrafiltration uses centrifugal force and a semipermeable membrane to separate a protein-free phase from a drug-protein solution (Fig. 2.2B). With this method the drug-protein solution is placed in the upper chamber of the two-chambered device and centrifugation (~2,000g) is used to move the unbound drug into the lower chamber (13). Here the total drug concentration is measured before

centrifugation, and the free drug concentration is measured in the lower chamber at the end of the process. Similar to equilibrium dialysis, nonspecific binding to the membrane and the apparatus, Gibbs-Donnan effects, and protein leakage must be considered. In addition, more rigorous temperature and pH control are needed, and molecular sieving, where plasma water passes though the membrane faster than drug molecules, must be recognized (14).

Ultracentrifugation separates a drug-protein solution into several phases by using a high centrifugal force (~500,000g) for a long period of time (10-24hr) (13) (Fig. 2.2C). While this method avoids the membrane issues encountered with equilibrium dialysis and ultrafiltration, it has its own challenges. After centrifugation, three distinct layers are formed: a top layer containing very low-density lipoproteins and chylomicrons, a middle layer of free drug, and a bottom layer containing high-density molecules including albumin, AAG, and lipoproteins. To determine the free fraction, total drug concentration is measured before centrifugation and free drug concentration is measured from the middle layer at the end of the process. By having distinct layers, binding to specific proteins such as low-density lipoproteins vs. albumin can be determined (15). The three layers can lead to the experimental difficulties since the top lipid layer must not be disrupted during sampling, and it is necessary to use the correct centrifugation parameters to ensure a truly protein-free middle layer (16). Additionally, free drug can sediment depending on its shape, size, and the run temperature, while back diffusion of drugs from the protein-free layer is possible (13).

While these three methods are among the most commonly used, reviews summarize additional methods including gel filtration, chromatography, capillary electrophoresis, erythrocyte partitioning, surface plasmon resonance, and microdialysis (13, 14). Despite advances in technology, there is still uncertainty in the f_u values generated using these standard

methodologies for highly bound drugs. Recent DDI guidelines reflect the low confidence in measured f_u values as regulatory agencies decided that the lower limit should be 0.01, regardless of the actual measured value, to avoid false negative DDI predictions (17). However, approximately one third of experimental drugs have high protein binding (≥ 99%), and using warfarin and itraconazole as examples, Di et al. (17) show that fu ≤ 0.01 may be accurately measured using appropriate methods.

IVIVE and Protein Binding

Given that the current drug development process is expensive and time-consuming (18), it is important to identify failures as early in the pipeline as possible to reduce inefficiency. When deciding which new chemical entities (NCE) to move forward, one of the most important pharmacokinetic parameters to consider is clearance as it is linked to drug exposure, half life, and dosing interval (19). In vitro - in vivo extrapolation is commonly used to predict the hepatic clearance of compounds and accurately understanding f_u is crucial for these predictions.

The typical IVIVE process involves determining the intrinsic clearance (CL_{int}) of a compound in vitro using microsomes or hepatocytes, which can then be scaled to an in vivo prediction using physiologically based scaling factors as well as a model of hepatic disposition such as the well-stirred model. CL_{int} is a measure of the body's ability to remove drug in the absence of protein binding or blood flow limitations (20, 21), and in vitro CL_{int} is commonly measured by either uptake or substrate depletion assays (22, 23).

Rane et al. (24) first suggested the use of in vitro uptake assays for hepatic clearance prediction and determined CL_{int} under low substrate concentrations ([S] <<K_m) using the following:

$$CL_{int,in\ vitro} = \frac{V_{max}}{K_m}$$

where V_{max} represents the maximum velocity of metabolism and the Michaelis-Menten constant, K_m, is the concentration of drug at half V_{max} (24). For substrate depletion assays, the metabolic rate parameter, k, can be determined from the slope of the linear regression of the log percentage of drug remaining versus time, and CL_{int} can then be determined using:

$$CL_{int,in\ vitro} = k \cdot V_{inc}$$

where V_{inc} is the volume of the in vitro incubation (25, 26).

$CL_{int,in\ vitro}$ can then be scaled to $CL_{int,in\ vivo}$ using scaling factors (SF) that typically include 40 mg microsomal protein/g liver (27) or 120 million hepatocytes/g liver (28) as well as 21.4 g liver/kg bodyweight (28):

$$CL_{int,in\ vivo} = SF \cdot CL_{int,in\ vitro}$$

Following this scale-up, a model of hepatic disposition such as the well-stirred model (20, 21) shown below:

$$CL_H = \frac{Q_H \cdot f_{u,B} \cdot CL_{int,in\ vivo}}{Q_H + f_{u,B} \cdot CL_{int,in\ vivo}}$$

(where Q_H is hepatic blood flow and $f_{u,B}$ is the fraction unbound in blood), the parallel tube model (29), or the dispersion model (30) is commonly applied. It has been shown that clearance predictions are similar among the three models except for high clearance drugs, where the well-stirred model will cause underprediction (31). However, our lab recently derived the theoretical basis for the extraction ratio and found that when organ clearance is calculated as the product of the extraction ratio (ER) and blood flow (Q) to the organ, it is only consistent with the well-stirred model (32). The paper goes on to explain why comparisons of the different models are not possible and IVIVE can only potentially work for the well-stirred model. Within the well-stirred model, it is important to note that total drug concentrations must be measured in blood and the fraction unbound is in reference to blood since the liver is capable of removing drug from both plasma and blood cells (33).

Despite the common use of IVIVE, underprediction has been noted and proposed explanations include preparation process issues, cofactor depletion, and the possibility of extra-hepatic metabolism (31). Heuberger et al. (6) discuss that one of the other major questions regarding IVIVE scale-up is which f_u terms to include, which we elaborate on here.

Nonspecific Binding & $f_{u,inc}$

As mentioned earlier, the widely accepted free drug theory says that only unbound drug can exert pharmacological effects, and thus when doing IVIVE the unbound drug concentrations in plasma, tissue, and assays should be considered (34). It has been well recognized that when inputting data into the well-stirred model, the fraction unbound in blood ($f_{u,B}$) must be used, or the fraction unbound in plasma ($f_{u,p}$) divided by the blood to plasma ratio (R_B) (Yang et al., 2007). More recently the idea that the fraction unbound in the in vitro assay may need to be incorporated as well has begun to be implemented (35-38).

Since nonspecific binding may occur in the in vitro system if drug binds to the incubation plate, to proteins in the assay media, or to proteins and lipids of microsomes or cells, another binding term, $f_{u,inc}$, or the fraction of drug unbound in the incubation, can be included as shown in the equation below. As Obach (35) explained, "Thus, most K_m and K_i values reported in the literature that use impure in vitro systems are artifactual overestimates, because they are based on total substrate or inhibitor concentration added to the incubation (i.e., the nominal concentration) and not the free substrate or inhibitor available to bind to the enzyme."

$$CL_H = \frac{Q_H \cdot \left(\frac{f_{u,B}}{f_{u,inc}}\right) \cdot CL_{int,in\ vivo}}{Q_H + \left(\frac{f_{u,B}}{f_{u,inc}}\right) \cdot CL_{int,in\ vivo}}$$

$f_{u,inc}$ Measured In Vitro

The same assays for measuring PPB as mentioned previously can also be used for measuring $f_{u,mic}$, the fraction unbound in a microsomal incubation, and $f_{u,hep}$, the fraction unbound in a hepatocyte incubation. Equilibrium dialysis is again commonly used and to

measure binding to microsomes, drug and microsomes without cofactors (NADPH/UDPGA) are added to one chamber, and buffer is added to the other (25). The value of $f_{u,mic}$ can be determined as the ratio of the concentration on the buffer side to the concentration on the microsome plus drug side. Unlike PPB measurements, volume shifts due to osmotic forces are not observed (25).

Measuring $f_{u,hep}$ is not quite as simple as excluding cofactors. Hepatocytes that have been deactivated at room temperature and subject to freeze/thaw cycles are commonly used to minimize the complication of simultaneous metabolism (39). An alternative method is to use live hepatocytes preincubated with metabolic inhibitors such as 1-amino-benzotriazole and salicylamide for the assay, however equilibrium dialysis time vs. half-life of metabolism of the compounds must be considered (40). Furthermore, although the presence of specific, saturable binding sites did not appear to fit microsomal binding data (41), the test compound binding to hepatocytes could potentially be displaced by the inhibitors. Using only metabolic inhibitors also does not provide direct information about whether the measured binding is truly binding to the cell wall, or is actually intracellular accumulation from uptake. Despite the potential disadvantages, when comparing the use of live hepatocytes with inhibitors vs. dead hepatocytes for $f_{u,hep}$ measurements, overall there was no statistically significant difference for a dataset of 17 compounds (40).

When running assays for both $f_{u,inc}$ and CL_{int} determinations, it is important to note that nonspecific binding increases as phospholipid concentration, microsomal protein concentration, or cell density increases (39, 42, 43). This is particularly relevant as microsomal protein concentrations can vary as much as 200-fold among laboratories (42). To try to avoid nonspecific binding, very low microsomal concentrations can be used; however under certain

conditions such as investigating phase II metabolic reactions or intestinal metabolism, higher concentrations are needed (44).

After proposing the incorporation of a $f_{u,inc}$ term for IVIVE (35), Obach (26) tested the idea on data collected from 29 drugs in human microsomes. IVIVE prediction accuracy was examined when when only $f_{u,B}$ was included in the scale up (Fig. 2.3A), when both $f_{u,B}$ and $f_{u,inc}$ terms were used (Fig. 2.3B), and when no binding terms were used (under the assumption the values of $f_{u,B}$ and $f_{u,inc}$ would cancel) (Fig. 2.3C). However, as Kalvass et al. (42) mention, "Since the free fraction in microsomes is determined, in part, by the choice of microsomal concentration in the incubation, equivalent free fractions between plasma and microsomes should be considered coincidental." Obach (26) reports that predictions were best for acidic compounds when both the $f_{u,B}$ and $f_{u,inc}$ binding terms were included and basic compounds when no f_u terms were included, with which we agree. Obach (26) also states that for neutral compounds, no binding terms gave better predictions, but we believe both methods were comparable in accuracy although no binding terms overpredicts and both binding terms underpredicts. Note in Figure 2.3 that since AFE values on the y-axis are represented on a log scale, visual comparisons must be validated with numerical values. Riley et al. (45) also saw similar trends with hepatocytes. Overall, predictions were best when both binding terms were included for acidic, basic, and neutral compounds. The worst accuracy occurred if no f_u terms were included and in this scenario, predictions were very poor for acidic drugs and better for basic and neutral drugs where $f_{u,inc}$ may be large and cancel with $f_{u,B}$.

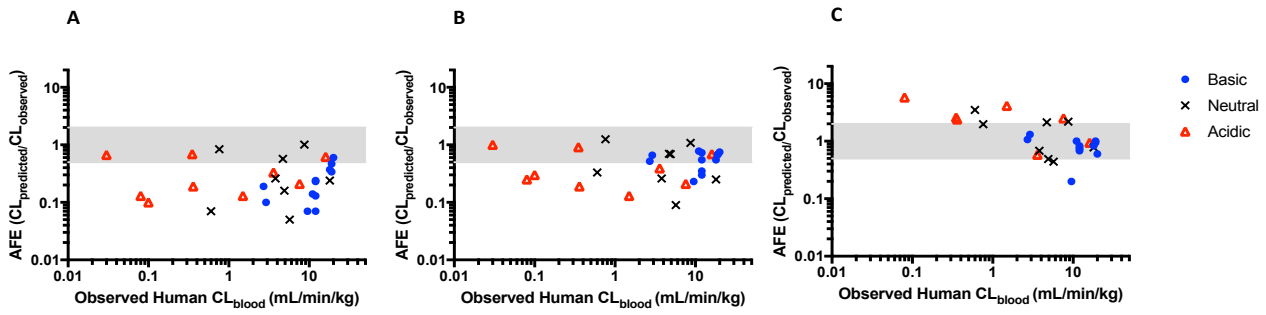

Figure 2.3: Accuracy of predictions from Obach (26) using the well-stirred model. The accuracy is examined using: A) the traditional model with $f_{u,B}$ only; B) both $f_{u,B}$ and $f_{u,inc}$; and C) no binding terms assuming $f_{u,B}$ and $f_{u,inc}$ cancel. The shaded area highlights predictions falling within two fold of observed values.

$f_{u,inc}$ Estimated In Silico

Given that the experimental methods for measuring $f_{u,inc}$ are not high-throughput, in silico models for predicting the value have been proposed (46). Since it is believed that the phospholipid component is the primary contributor to nonspecific binding (43), the extent of binding would increase with increasing lipophilicy as proposed by Austin et al. (41).

Noting that basic compounds have enhanced binding over neutral and acidic compounds of similar lipophilicity (thought to be due to favorable electrostatic interactions between the protonated base and the phosphate groups), Austin et al. (41) suggested using logP for basic compounds and $logD_{7.4}$ for acidic and neutral compounds. Based on data from 37 compounds with $f_{u,mic}$ values of <0.9, the following equation was developed to predict $f_{u,inc}$ based only on ionization and lipophilicy ($r^2 = 0.82$):

$$f_{u,mic} = \frac{1}{1 + C \cdot 10^{0.56logP/D - 1.41}}$$

where C is the microsomal protein concentration in mg/mL.

The equation was created based on both rat and human in vitro microsome binding data, but as Austin et al. (41) mention, it has been shown that $f_{u,mic}$ is usually independent of species (25, 47).

Other groups have built on this relationship and Hallifax and Houston (48) proposed a quadratic equation (n=92, $r^2 = 0.75$) for determining $f_{u,mic}$:

$$f_{u,mic} = \frac{1}{1 + C \cdot 10^{0.072logP/D^2 + 0.067logP/D - 1.126}}$$

Using an expanded dataset of 127 compounds, no major differences were seen between the two equations for $f_{u,mic}$ predictions for low and high lipophilicity drugs. However, for intermediate drugs (logP/D values between 2.5 – 5.0) the Hallifax and Houston equation was more accurate (44). For compounds with logP/D <0, where there is expected to be negligible interaction with microsomal protein, predictions from the Austin et al. (41) equation are expected to be accurate, and it would be inappropriate to use the Hallifax and Houston (48) equation due to the nonlinear nature (44).

While these in silico predictions can be useful, Gertz et al. (44) saw that minor variation in logP predictions could lead to high variations in $f_{u,mic}$ predictions, and in certain cases $f_{u,mic}$ should still be determined experimentally. However, they did find good agreement between using predicted logP values from software packages and experimental determinations.

A similar equation was later proposed for $f_{u,hep}$ prediction (40, 49):

$$f_{u,hep} = \frac{1}{1 + 125 \cdot V_R \cdot 10^{0.072logP/D^2 + 0.067logP/D - 1.126}}$$

where V_R is the ratio of cell volume to incubation volume and is 0.005 at a cell concentration of 10^6 cells/mL.

Groups continue to try to improve $f_{u,inc}$ predictions (50) and there are reviews that discuss the nuances of the methods more in detail (46, 50-52). However, while many studies support the incorporation of $f_{u,inc}$, there are still some that question its utility (53). Even when both $f_{u,inc}$ and $f_{u,B}$ terms are incorporated in IVIVE, there are still inconsistencies that need to be solved.

pH Difference and F1

Berezhkovskiy (54) proposed adding an ionization factor, F1, to account for the difference in pH of extra- and intracellular water in hepatocytes (pH 7.4 vs. 7.0). F1 is defined as the ratio of the unbound, unionized (neutral) drug fractions in plasma and intracellular tissue water, and is added into the well-stirred model as a product of CL_{int} as shown below:

$$CL_H = \frac{Q_H \cdot f_{u,p} \cdot R_B \cdot CL_{int} \cdot F1}{Q_H + f_{u,p} \cdot R_B \cdot CL_{int} \cdot F1}$$

where $F1 = \frac{f_p^n}{f_{IW}^n}$

and f_p^n is the neutral drug fraction in plasma (or the concentration of unbound neutral drug in plasma divided by the concentration of unbound drug in plasma) and f_{IW}^n is the neutral drug fraction in intracellular water. These ratios can be calculated as:

$$f^n = 1 \text{ for neutral compounds}$$

$$f^n = 1/[1+(10^{\text{pH-pKa}})] \text{ for monoprotic acids}$$

$$f^n = 1/[1+(10^{\text{pKa-pH}})] \text{ for monoprotic bases}$$

If the pH were the same or if the compound were neutral then F1 equals 1. For basic drugs where F1 >1, CL predictions will be higher (up to 6.3 fold for diprotic bases, 15 fold for triprotic bases) helping with IVIVE underprediction, and conversely for acidic drugs where F1 <1, CL predictions will be lower, helping with IVIVE overprediction. The largest difference in predictions is expected for low extraction ratio drugs where the prediction is directly proportional to F1.

When measuring CL_{int} with hepatocytes, if buffer with a pH of 7.4 is utilized, and assuming the intracellular pH is maintained at 7.0, there would be no need to account for F1 in doing IVIVE. However, the pH gradient appears to be disrupted as the fraction of buffer in the incubation is larger than the fraction of extracellular water in the liver (55). When measuring CL_{int} with microsomes, it would always be necessary to account for F1 since the cellular integrity does not exist. A preliminary test of the method with microsomal data from 25 highly bound drugs did not completely cancel the underprediction seen, but showed improvement (56).

Protein Facilitated Uptake

Baker and Bradley (57) were first to suggest violations of the free drug theory and that hepatic uptake may occur directly from the albumin-drug complex, not just from free drug. Later studies also noted that highly protein bound ligands had more efficient hepatic uptake than could be accounted for by just their unbound concentrations. This phenomenon became known as albumin-mediated uptake. The idea gained traction in the 1980's when single-pass liver perfusion studies with various ligands including taurocholate (58), rose bengal (59), oleate (60), and warfarin (61) demonstrated the facilitated uptake. More recently it has been noted that as $f_{u,p}$ decreases, underprediction with traditional IVIVE increases (62). This trend may also be seen with data from human hepatocytes compiled by Wood et al. (63) (Fig. 2.4). While only 9 drugs with $f_{u,p}$ values ranging from 0.001-0.01 were included, the AFE may be higher in this range.

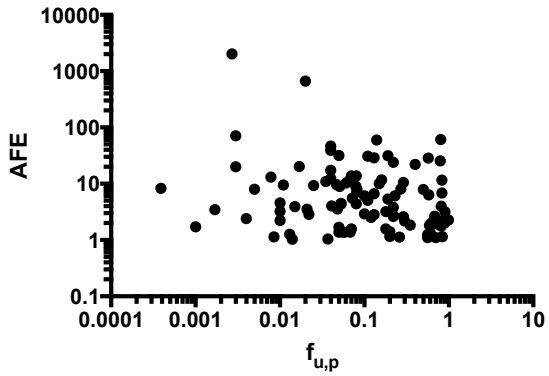

Figure 2.4: IVIVE prediction error and $f_{u,p}$. Examining the accuracy of predictions from human hepatocytes taken from Wood et al. (63), as $f_{u,p}$ decreases to the 0.001-0.01 range, average fold error (AFE) may increase. If AFE <1, the reciprocal is plotted.

Accordingly, some have tried using total rather than free drug concentrations in clearance equations to eliminate the underprediction (26, 45), which conceptually supports the idea of albumin-mediated uptake. When conducting in vitro studies, groups have also found that adding HSA or plasma to microsome and hepatocyte incubations can cause decreases in K_m values and

improved IVIVE results (62, 64-74). Poulin et al. (75) have nicely summarized several of these studies. When proteins are added to the incubations, the drug uptake rates decrease less than would be expected with the decrease in unbound drug concentrations.

While there are now several examples suggesting that perhaps total drug, not unbound drug, can drive hepatic uptake and clearance and should be considered when doing IVIVE, the mechanism explaining why has not yet been agreed upon. We review here the state of past and present hypotheses (Fig. 2.5).

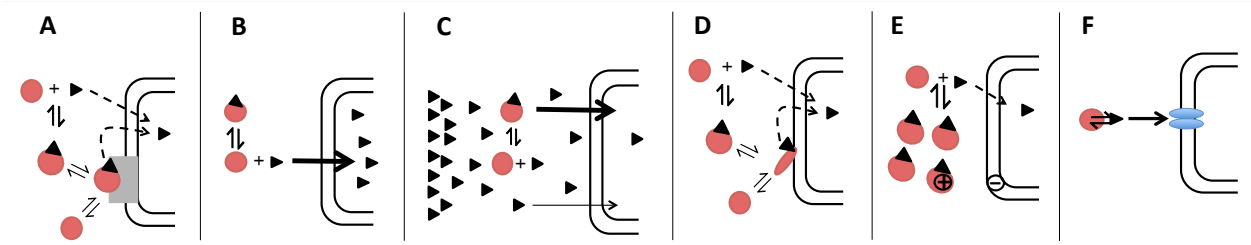

Figure 2.5: Hypotheses to explain albumin-facilitated uptake. A) Presence of an albumin receptor where uptake can occur due to direct uptake of unbound ligand or after specific interaction of the albumin-ligand complex with its receptor; B) Rate-limiting dissociation where free ligand uptake is faster than ligand dissociation from albumin; C) Rate-limiting diffusion of ligand through the UWL where the slow diffusion of unbound ligand is supplemented with the diffusion of more soluble bound ligand; D) Conformational change where uptake occurs from the direct uptake of unbound ligand in plasma or after a conformational change of the albumin-ligand complex due to cell membrane binding catalyzing the release of drug; E) Ionic interactions with the cell membrane where the diffusional distance for unbound ligand is decreased; and F) Transporter-induced protein binding shift where a high affinity transporter may strip ligand from the ligand-drug complex.

Specific Albumin Receptor on Hepatocyte Surface

The earliest hypothesis to explain albumin-mediated uptake was that there is an albumin-receptor on the hepatocyte cell surface (Fig. 2.5A). Oleate was one of the first ligands used to suggest this (76). When increasing [^{14}C]oleate concentration but keeping bovine albumin concentration constant, oleate uptake increased linearly relative to concentration in the perfused

rat liver. However, when increasing both oleate and albumin concentration (1:1 so the unbound oleate concentration is constant), there was a saturable process, where albumin appeared to be acting as a competitive inhibitor resulting in a plot similar to Fig. 2.6.

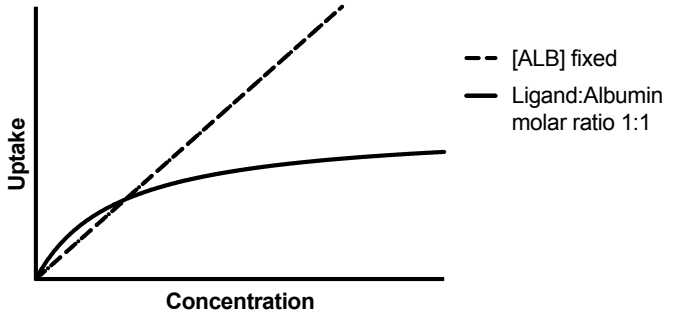

Figure 2.6: Saturation vs. linear results. An example of a saturation curve (solid line) that is seen in several studies when the concentrations of albumin and ligand are varied (at a fixed 1:1 ratio). This is in contrast to when the concentration of ligand is varied at a fixed albumin concentration and uptake is linear (dashed line). Saturation is suggested to occur for instance when free albumin is competing with the ligand-albumin complex for receptors, or when the rate limiting transport step shifts from ligand dissociation to influx or metabolism.

^{125}I-albumin was then used to evaluate the possibility of albumin binding to hepatocytes and there appeared to be a single high-affinity binding site specific for albumin. Of the wide variety of potential displacement proteins tested, including several known to have hepatocyte surface receptors, only other albumin molecules (human and rat) significantly displaced the bovine albumin (77). It was later shown that there appears to be no species specificity for the potential hepatocyte-albumin interaction (78). Based on the Stokes radius of albumin and assuming that all sites are occupied, it was estimated that somewhere between 1 to 8% of the total hepatocyte surface is occupied by the albumin-receptor complex (77), and a dissociation constant of albumin binding to hepatocytes was estimated (Table 2.1). Weisiger et al. (76) justified their hepatocyte receptor hypothesis by explaining that if only the 0.1% of free oleate accounted for uptake, the

dissociation from the oleate-albumin complex would need to be extremely rapid to explain the higher extraction, but the half-time for the dissociation of oleate from albumin is actually significantly longer than the time required for blood to pass through the liver.

An even earlier paper also suggested the potential role of an albumin receptor on the hepatocyte cell surface, but through a different mechanism. Bloomer et al. (79) saw that when the IgG fraction of goat anti-human albumin was added to a solution of [^{14}C]bilirubin and human albumin, [^{14}C]bilirubin was completely recovered in the supernatant. This suggested that bilirubin can be easily separated from albumin if albumin reacts with another macromolecule, and led to their hypothesis that if albumin receptors in the membrane interact with albumin at bilirubin binding sites, more bilirubin could be separated from albumin as it passes the hepatocyte surface, leading to higher unbound bilirubin diffusion.

While early studies suggested the possibility of a membrane protein with high affinity for albumin, others collected data that were not consistent with the hypothesis. Stremmel et al. (80) examined the binding of ^{125}I-labeled rat albumin to rat liver plasma membranes attempting to characterize the proposed hepatocyte albumin receptor. Running incubations for 30 minutes at various temperatures and various plasma membrane and albumin concentrations, there was no evidence of specific binding to the membrane. For instance, using 5 pmol of albumin and 10 mg of membrane protein, only 2.3% of the incubated albumin was recovered in the membrane pellet, and after two washes, only 0.09% remained, indicating that most of the albumin was trapped within the pellet, or loosely associated as it was easily removed with washing. Adding excess unlabeled albumin did not cause inhibition of binding, heat denaturation of the membranes caused no binding changes, and the amount of albumin binding to rat erythrocyte ghosts was the same as to the liver plasma membrane. These investigators employed additional methodologies

and used ultraviolet irradiation to prove that the failure to observe binding was not due to a rapid dissociation rate, and ran affinity chromatography with solubilized membrane proteins over albumin-agarose gels and did not find one with high albumin affinity. Stremmel et al. (80) went on to suggest that perhaps there are less specific interactions between the liver cell surface and albumin-ligand complex instead of a specific hepatocytic albumin receptor.

Similar to Stremmel et al. (80), Stollman et al. (81) did not find evidence for the interaction of albumin with a hepatocyte receptor. Perfusing rat livers with a protein-free fluorocarbon medium, Stollman et al. (81) measured the uptake of [^{3}H]bilirubin with either ^{125}I-albumin, ^{125}I-ligandin (an intracellular protein known to bind bilirubin with high affinity), or free with a [^{14}C]sucrose reference and found the same uptake across the three conditions. Furthermore, after injecting [^{3}H]bilirubin with ^{125}I-albumin and with [^{14}C]sucrose and seeing no delay in ^{125}I-albumin transit compared to that of [^{14}C]sucrose, they concluded that the off-rate of albumin from a receptor would have to be very rapid, which would be unusual.

The specific albumin receptor theory would also not be able to account for the enhanced clearance seen for ligands bound to other proteins such as β-lactoglobulin, (82, 83). Finally, Reed and Burrington (78) examined the interactions of two fragments of albumin with rat hepatocytes, and calculating similar dissociation constants in both cases, they concluded that since there does not seem to be a specific site on albumin that interacts with hepatocytes, receptor recognition seems unlikely.

Table 2.1: Estimated dissociation constants (K_d) for albumin binding to hepatocyte cell surface.

Kd (μM)	# Sites/Cell	Methodology	Source
25 ± 7	10 (± 3) x 10^6	^{125}I-labeled bovine albumin binding to rat hepatocytes (ligand free), 20°C, 30 min.	(76)
53 ± 13	10.4 (± 1.9) x 10^6	^{131}I-labeled rose bengal in perfused rats, various concentrations of BSA, fit to their kinetic model	(59)
157 ± 47		Warfarin in perfused rats, 37°C, fit to facilitated dissociation kinetic model	(61)
2.5 ± 1.7	2.2 (± 1.3) x 10^6	^{125}I-labeled monomeric albumin binding to rat hepatocytes, 4°C, 30 min.	(131)
4.4 ± 1.8	7.4 (± 2.3) x 10^6	^{125}I-labeled monomeric albumin binding to rat hepatocytes, 37°C, 30 min	(131)
1.9 ± 1.0	3.9 (± 3.0) x 10^6	^{125}I-bovine albumin binding to rat hepatocytes, 20°C	(78)
1.1 ± 0.5	2.0 (± 1.1) x 10^6	^{125}I-rat albumin binding to rat hepatocytes, 20°C	(78)

Rate-Limiting Dissociation of Ligand from the Albumin-Ligand Complex

To further explore the determinants of hepatic uptake and the possibility of an albumin receptor, Weisiger et al. (84) evaluated the role of bovine albumin on sulfobromophthalein (BSP) uptake in skates. Believing that since skates naturally lack albumin they would not have evolved an albumin receptor, the goal was to see if a different kinetic behavior occurred. Using a single-pass perfused liver model, two different steps in the uptake process were determined. For fixed albumin concentrations, as total BSP concentration increased, linear saturation kinetics were present suggesting that the rate-limiting step in these situations does not involve albumin. This was called the "intrinsic" uptake step. When the concentration of albumin and BSP were varied at a fixed molar ratio, the uptake rates did not correlate with the estimated equilibrium concentrations in the perfusate, and the saturation kinetics seen occurred at uptake velocities too small to saturate the intrinsic uptake step. The data collected from skates were similar to that from rats with oleate (76), however since skates have no reason to have an albumin receptor, an alternate explanation for the results was needed. In this case, the rate-limiting step was hypothesized to be the spontaneous dissociation of BSP from albumin, going back to the traditional assumption that clearance only occurs for free ligand (Fig. 2.5B). If free BSP clearance is faster than BSP can be replenished by dissociation from albumin, equilibrium would not actually be present in the sinusoid, and the dependence of clearance on the bound ligand concentration is explained. As the albumin concentration increases, reassociation of free BSP to albumin can start to occur instead of only BSP clearance, and when binding equilibrium is established the uptake then becomes limited by the intrinsic uptake step.

Weisiger et al. (84) explain that although similar kinetics were seen in rats, this dissociation limited model would not explain the findings since the BSP uptake rate is more

rapid in rats and exceeds the rate of spontaneous dissociation. Weisiger and Ma (60) saw that the removal rate for oleate in perfused rat liver with dilute albumin solutions is similar to the spontaneous dissociation rate measured in vitro, supporting the dissociation-limited model in rats for this ligand. If the albumin receptor model were to hold true, the removal rate could be much higher since it is not limited by the rate of spontaneous dissociation.

To further explore this, van der Sluijs et al. (85) measured dibromosulfophthalein (DBSP) uptake in rat liver perfused with native albumin vs. lactosylated albumin. After demonstrating that DBSP had similar protein binding to the lactosylated albumin as to native albumin, a 40% decrease in the hepatic uptake rate constant for the lactosylated albumin was found. These investigators also conducted rapid filtration experiments and saw that the dissociation rate constant of DBSP from lactosylated albumin was half that from albumin and concluded that the decreased off-rate could explain the decreased hepatic uptake, providing further evidence for the idea of dissociation-limited uptake.

It should be noted that these early in vitro measures of the dissociation rate constant have limitations (86). If a solid-phase acceptor is used, where it is assumed that the free ligand is diffusing and binding to the acceptor, there could be direct collisional exchange between albumin and the acceptor causing ligand transfer as well, overestimating the spontaneous dissociation rate constant. If stop-flow fluorescence is used, where the conformation change in albumin is measured, if the change is slower than the dissociation rate, the rate constant could be underestimated.

Rate-Limiting Diffusion of Ligand Through the Unstirred Water Layer

Another explanation for albumin-facilitated uptake is related to the idea of an unstirred water layer (UWL) in the space of Disse, or the space that separates sinusoidal lining cells from hepatocytes. The idea of an UWL is common with intestinal absorption where rates of highly permeable compounds are known to have an upper limit (87). Given that the space of Disse contains a matrix of fibrillar material and hepatocytes have microvilli and adherent water film (88), groups began exploring the potential role that an UWL may play in the liver.

Bass and Pond (89) created a "pseudofacilitation" model, returning to the idea that uptake occurs only from the unbound fraction of ligand. This model is reviewed in detail by Burczynski and Luxon (86). The hypothesis is that ligands undergoing cellular uptake can be rate limited by the UWL adjacent to the cell surface or can be rate limited by permeability through the membrane itself (90). For ligands with high membrane permeability that are rate limited by the UWL, a concentration gradient will develop within the UWL in the absence of protein (86). With the addition of protein, traditionally binding causes a decrease in the diffusion rate of the protein-ligand complex as compared to free ligand (90, 91). However, for highly lipophilic ligands, which have limited diffusional flux across aqueous barriers, the presence of protein promotes aqueous solubility (86, 90). The slow diffusion of unbound ligand is therefore supplemented with the diffusion of more soluble bound ligand. The albumin-ligand complex will try to replenish the depleted unbound ligand near the cell surface and restore equilibrium. As a result there is decreased diffusional distance for the unbound ligand and the unbound concentration driving uptake is increased (86). When the bound ligand concentration is much higher than that of the free ligand, the average diffusional flux of the bound ligand can be

greater than that of the free, making the flux appear to only depend on the bound concentration (90) (Fig. 2.5C).

Ichikawa et al. (88) explored the uptake of ligands with various permeabilites in perfused rat liver and isolated rat hepatocytes. Using highly-permeable diazepam and taurocholate in the perfusion study, as BSA concentrations increased and free fraction decreased, the extraction ratio did not greatly change, showing albumin-mediated transport of the compounds. Tolbutamide and salicylate, intermediate permeability compounds, also exhibited some albumin-mediated transport as their extraction ratios decreased to one-third when the free fractions were decreased to one-tenth. With cefodizime, a compound with low permeability, the extraction ratio decreased as the free fraction decreased, leading to the conclusion that albumin-mediated transport was not observed, and supporting the hypothesis.

Ichikawa et al. (88) point out that it is possible that slow dissociation from albumin could also play a role. However when investigating perfused livers vs. hepatocytes, the highly permeable compounds had a lower influx clearance in the perfused livers. It is argued that if the dissociation-limited transport were to play a large role, the influx clearances should be similar, since k_{off} should be the same in both systems. The rate-limiting diffusion theory can explain the saturation kinetics seen in earlier studies (76) as the increase in unbound clearance reaches a maximum, which is determined by the product of the effective membrane permeability and total surface area (92).

However, others believe that the UWL cannot fully explain albumin-facilitated uptake. Although the use of polyethylene sheeting has been questioned (93), Burczynski et al. (94) found that while palmitate clearance with hepatocytes was about 7 fold faster than with polyethylene, the codiffusion of bound and free palmitate to the cell surface could only account for about 20%

of the facilitated clearance observed. Furthermore, Pond et al. (92) tested the pseudofacilitation model (89) on [^{3}H]palmitic acid uptake data generated in hepatocytes finding a high dependence on parameter estimate selection. Their experimental results agree with the theoretical model predictions if a reported low equilibrium association constant was used (15 μM^{-1}); however if higher values also reported were used (62 and 94 μM^{-1}), the measured unbound clearance exceeded the model predictions.

Comparing the uptake of oleate and BSP with albumin in isolated perfused rat liver vs. hepatocyte suspensions, Nunes et al. (82) measured the same kinetics in both experiments, concluding that the facilitated uptake observed was not dependent on the intact lobule characteristics or diffusion barrier in the space of Disse present only in the perfused livers. Similarly, Blitzer and Lyons (64) still saw taurocholate facilitated uptake in rat basolateral liver plasma membrane vesicles, which were vigorously mixed during the experiments and for which the UWL effects were expected to be minimal.

Interactions with the Hepatocyte Cell Surface (not albumin receptor)

As these alternative hypotheses continued arising, more work was simultaneously conducted concerning the putative hepatocyte receptor hypothesis. As Stremmel et al. (80) suggested, instead of looking for a specific albumin receptor, the focus shifted to more general interactions that could be occurring at the liver cell surface with the albumin-ligand complex catalyzing ligand dissociation.

Conformational Change

Using rose bengal, Forker and Luxon (59) explained that while the albumin-ligand complex may interact with the cell surface, since albumin itself is not removed (95), free ligand must ultimately be what is interacting with the transport carrier, and must interact without mixing with the pool of free ligand in the extracellular fluid. They suggested that the binding of the complex to the cell surface may lead to a conformational change in albumin reducing its binding affinity for the ligand and/or presenting the ligand in a favorable location for uptake (Fig. 2.5D) (96). They also added an important corollary that the sites on the cell surface would have a similar affinity for albumin whether or not ligand is bound. This then suggests that the interaction at the cell surface is not ligand specific, and the affinity of albumin for the surface is independent of ligand concentration. Creating a kinetic model where the total rate of ligand removal is proportional to the mass of free ligand plus the mass that is bound to the cell surface as albumin-ligand complexes, they fit their perfusion data and compared the calculated values to those obtained by Weisiger et al. (76) with ligand-free albumin and hepatocytes (Table 2.1). The similar results supported their kinetic model and Forker and Luxon concluded that albumin binding to the cell surface explained how bound ligand, in this case rose bengal, in another perfusion study, taurocholate (58), and in a study using rat liver cell monolayers, palmitate (97) is available for hepatic uptake.

Facilitated-Dissociation Model

Tsao et al. (61) also suggested this hypothesis with warfarin where the interaction between the cell surface and warfarin-BSA complex (K_d = 157 μM, Table 2.1), would induce a conformational change in albumin and decrease the binding affinity of warfarin. Having

previously run perfusion studies in normal rats and analbuminemic rats and seeing albumin-mediated uptake of warfarin in both cases led to the conclusion that a specific albumin receptor on the cell surface may not be necessary for the uptake (98). A "facilitated-dissociation" kinetic model was developed to include both the uptake of unbound drug and the uptake of drug from the albumin-drug complex after a conformational change. Assuming that the dissociation of warfarin from albumin is much faster than the perfusion or hepatic uptake rate and thus, warfarin binding to albumin is at equilibrium, and assuming that the uptake of unbound warfarin is linear compared to warfarin concentration, the equation for the uptake rate (v) of drug is:

$$v = P_m \cdot f_u \cdot c_o + P_{B,influx} \cdot \lambda \cdot (1 - f_u) \cdot c_0$$

where c_0 is the total concentration of ligand, P_m and $P_{B,influx}$ are the permeability clearances for unbound ligand and unbound ligand dissociated from the drug-ligand complex respectively, while f_u is the fraction of unbound ligand in the extracellular fluid expressed as:

$$f_u = \frac{1}{1 + \frac{n[Alb]}{K_d}}$$

where n is the number of binding sites on albumin, K_d is the dissociation constant of ligand and λ is the fraction of albumin bound to the surface of hepatocytes (assuming both unbound albumin and ligand-bound albumin compete for the same binding sites on the surface).

λ is expressed as:

$$\lambda = \frac{B_{max}}{K_{d,m} + [Alb]}$$

where B_{max} is the capacity of albumin binding sites on the surface of hepatocytes and $K_{d,m}$ is the dissociation constant of bound albumin from the hepatocyte surface (61, 99).

Based on their model, Tsao et al. (61) simulated the contributions of the unbound and bound drug. At low albumin concentrations, the increase in albumin increases the albumin-bound warfarin, which facilitates the uptake of bound warfarin, but at high albumin concentrations, the increase in albumin leads to competition of free albumin and albumin-bound warfarin for the liver cell surface binding sites, and warfarin uptake is inhibited.

Twenty years later Miyauchi et al. (99) revisited the facilitated dissociation model finding it could accurately predict the uptake of two organic anion transporting polypeptide substrates, 1-anilino-8-napthalene sulfonate (ANS) in primary cultured rat hepatocytes, and pitavastatin in isolated human hepatocytes. They performed a curve-fitting exercise based on their experimental data escalating the albumin concentration in the incubation medium and upon finding the calculated line fit well, the authors concluded that the enhancement of clearance can be accurately predicted by the facilitated-dissociation model.

Acidic Microenvironment

Burczynski et al. (100) and others point out that the acidic microenvironment of the hepatocyte may also play a role since it has been shown to decrease the albumin binding of anthracyclines and long-chain fatty acids.

At physiological pH, the negatively charged groups on the hepatocyte cell surface attract positively charged ions to try to maintain electroneutrality (86). The presence of H^+ ions then lowers the pH of the environment near the hepatocyte that can modulate albumin conformation changes through the Neutral-Base and Neutral-Fast transitions where ligands can be released from the proteins.

Using absorption and electron spin resonance spectroscopy, Horie et al. (101) showed albumin undergoes conformational changes through interaction with hepatocellular membranes, as well as other membrane types, similar to those seen in the Neutral-Base and Neutral-Fast transitions of albumin. However, Foker and Ghiron (102) point out that that the nitroxide spin label used could react with the 59 free amino groups or the single available SH group of albumin, so the labeling may not be site specific and the results cannot be considered definitive.

Ionic Interactions Between the Cell Surface and Albumin-Ligand Complex

An alternative theory for the role that the hepatocyte cell surface plays in facilitated uptake is that ionic interactions can occur between the hepatocyte plasma membrane and the protein-ligand complex. This would then decrease the diffusional distance for the unbound ligand and provide more unbound ligand to the cell surface for uptake (100) (Fig. 2.5E). When this hypothesis was suggested, most studies in the field had used albumin as a binding protein

and although β-lactoglobulin was tested (83), it has a similar isoelectric point (pI) to albumin, and no difference in uptake would be expected between the two.

Burczynski et al. (100) investigated the potential of the ionic interaction first by measuring [^{3}H]-palmitate clearance for binding proteins with different pIs: AAG (pI=2.7), albumin (pI=4.9), and lysozyme (pI=11.0). The clearance with the basic lysozyme was 6.3 fold greater than with the acidic AAG and 3.2 fold greater than with albumin. This agrees with the hypothesis that the net positive charge of lysozyme would be expected to be attracted to the negatively charged groups on the membrane surface. Burczynski et al. (100) also examined the uptake with 0.23 μM albumin vs. 2.1 mM lysozyme plus 0.23 μM albumin where the unbound palmitate fraction would be expected to be lower, and found that the clearance was statistically higher with the lysozyme plus albumin, further supporting the hypothesis. In a subsequent paper they went on to chemically modify albumin (though maleylation, succinylation, and cationization) to have pIs between 2.0-8.6 to exclude the possibility of conformational and binding site differences between proteins (103). After showing that the dissociation rate constants were not statistically significant from each other, and finding that [^{3}H]-palmitate clearance significantly increased by 0.27 units with a unit increase in pI, they concluded that the ionic interactions hypothesis holds true.

$f_{u,p\text{-adjusted}}$

Specifically citing the ionic interactions hypothesis, Poulin et al. (56) hypothesized that the whole-liver f_u may be larger than $f_{u,p}$ in vivo and an adjusted f_u term, $f_{u,p\text{-adjusted}}$ should be utilized. The authors proposed using a plasma-to-whole-liver-concentration ratio (PLR) of plasma binding proteins to correct for the difference between extracellular protein binding and

liver protein binding and also built in the ionization factor, F1, mentioned previously to create the following equation:

$$f_{u,p-adjusted} = \frac{PLR \cdot f_{u,p} \cdot F1}{1 + (PLR - 1) \cdot f_{u,p} \cdot F_1}$$

Poulin et al. (56) reported this equation is applicable for HSA-bound drugs. For drugs bound to AAG, $f_{u,p\text{-adjusted}}$ is not used and only the F1 correction is employed since AAG levels are lower than HSA in plasma, and previous studies suggested that facilitated uptake is greater with HSA than with AAG (104, 105).

To estimate the PLR value for HSA, they note that the levels of HSA in the intracellular liver are negligible compared to the levels in the interstitial space and plasma, so the PLR is really a concentration ratio of the proteins in the plasma vs. interstitial space, and they assumed a homogenized distribution of HSA in accordance with the well-stirred model assumptions. For humans the PLR was estimated to be 13.3. The same value can be used for rat and monkey, but for dog, a value of 8.5 is used due to the greater volume of interstitial fluid (106).

$$CL_H = \frac{Q_H \cdot CL_{int} \cdot R_B \cdot f_{u,p-adjusted}/f_{u,inc}}{Q_H + \cdot CL_{int} \cdot R_B \cdot f_{u,p-adjusted}/f_{u,inc}}$$

Adding the new term to the well-stirred model shown above and applying it to data generated in plasma-free microsomal incubations for 25 highly bound compounds, Poulin et al. (56) found no systematic over- or underprediction, an AFE close to unity, and the best predictions for bases.

Hallifax and Houston (107) conducted a similar evaluation of methods using a larger dataset of 107 drugs, finding that the Poulin $f_{u,p\text{-adjusted}}$ method was the least biased (AFE for hepatocytes =1.3, for microsomes = 1.7) compared to the Berezhokovkiy F1 method or the conventional method with $f_{u,B}$. They raise some concerns about the method though, showing that if a hepatocytosolic pH of 7.2 instead of 7.0 had been used (given the range of 7.0-7.4 reported in the literature), or if a PLR of 133 instead of 13.3 were used, there would be overprediction for acids. Hallifax and Houston (107) ultimately conclude that the $f_{u,p\text{-adjusted}}$ method may not offer significant improvement over a simple empirical correction. However, using a simple empirical correction factor based on AFE, or using one based on a regression analysis (108, 109), requires analysis of an in vivo dataset and is dependent on compound selection in that dataset.

Poulin and coworkers have continued to validate their model showing it performs better than using an empirical correction (106) and performs well for hepatocytes (110, 111), and when combining metabolism with transporter and permeability data (112).

The PLR values mentioned earlier are for protein-free incubations, where it is assumed that protein-facilitated uptake is not occurring, and "the CL_{int} determined in vitro should represent only a measure of the hepatic uptake of the free drug moiety by contrast to the in vivo condition in liver where the bound drug moiety is also assumed to be available for uptake" (113). To apply this methodology to different experimental procedures with varied albumin concentrations, the PLR value can be changed to the actual concentration ratio of HSA in the buffer/plasma/perfusate and the organ material, and if an assay has albumin at a similar level to that in vivo, the PLR should be 1 (111). This has recently been confirmed to improve prediction accuracy for naproxen and bisphenol A in isolated perfused rat livers with different albumin concentrations (114, 115) and in the HepatoPac® system with 25 compounds (113).

Recently, the $f_{u,p\text{-adjusted}}$ model was compared to the facilitated dissociation model (116) by considering the data for ANS and pitavastatin from Miyauchi et al. (99). While specific input parameters are required for the facilitated-dissociation such as the relative interaction capacity, dissociation constant, number of binding sites, and albumin concentration, the Poulin $f_{u,p\text{-adjusted}}$ model requires less input parameters. The two models were shown to both improve IVIVE, and to be conceptually and mathematically equivalent, particularly for pitavastatin. However, for ANS, which had a lower capacity of interaction with the membrane, the $f_{u,p\text{-adjusted}}$ model overestimated the unbound CL_{int} in albumin in vivo since the model assumes each interaction between the albumin-ligand complex and cell surface would lead to facilitated uptake.

Alternative Explanations, Cells, Proteins

The theories mentioned above have gained the most traction and are frequently cited today. Over the years other possibilities have been mentioned, but often deemed less likely. One early suggestion was that there may be direct transfer of ligand from plasma albumin to hepatic intracellular binding proteins (79). For this to happen, the intracellular proteins would need to be in close proximity to the plasma albumin and have a high enough affinity for the ligand. A similar hypothesis is direct transfer where collisional exchanges (random or from ionic interactions) between the ligand-protein complex and cell membrane could cause direct transfer of the ligand to the cell without dissociation in the extracellular fluid (86, 117, 118).

Suggesting an alternative explanation for the putative albumin receptor, Reed and Burrington (78) hypothesized that there are two populations of albumin. One is a "surface" population that binds to the container surface and undergoes a conformation change that causes the molecules to have higher affinity for the hepatocyte surface, and can then transfer directly

between the container wall and cell wall. The other population is the native population, which binds with lower affinity to the cell surface.

Another hypothesis is that albumin affects the hepatocyte membrane potential and/or fluidity (61, 86). Using perfused rat livers and a microelectrode, Weisiger et al. (119) showed that depolarization of cells decreased oleate uptake, while hyperpolarization increased uptake. This could explain the increase in clearance seen in the presence of albumin for the non-protein bound antipyrine (120). Another idea that has been mentioned proposes the endocytosis of the protein-drug complex (56, 80).

No matter which is ultimately the correct mechanism, it is clear that the unbound clearance of many ligands is enhanced as the concentration of plasma protein is increased. This protein-facilitated uptake has been shown to occur in other organs and cell types besides the liver/hepatocytes including myocytes (121-125), adipocytes (124), proximal tubules (126), perfused kidney (127), brain (128), and human embryonic kidney cells overexpressing OATP1B1 and 1B3 (129), as well as inert material including polyethylene (94) and *n*-decane (90). Facilitated uptake may also be considered for nanoparticles bound to albumin as they are used to deliver drugs to tumor cells more effectively, and perhaps the complex also interacts with cells (75, 130). Facilitated uptake has been shown not only for ligands bound to albumin, but also to proteins such as β-lactoglobulin (82, 83) and ligandin (81).

Conclusions

This review explores the use of the f_u parameter in IVIVE both in terms of the traditional scale up where only unbound drug is believed to undergo uptake, and in terms of protein-facilitated uptake, where highly protein bound ligands have more efficient uptake than can be

accounted for by just their unbound concentrations. While the addition of $f_{u,inc}$ and/or F1 to the well-stirred model has sound reasoning and is commonly being implemented now, the mechanisms behind protein-facilitated uptake and how to kinetically describe this process have yet to be agreed upon. Two of the popular models, the $f_{u,p\text{-adjusted}}$ model and the FDM were recently compared and found to be complementary (116). Since $f_{u,p}$ and pK_a values can be estimated in silico, the $f_{u,p\text{-adjusted}}$ model is suitable for early stage drug discovery. (However, plasma protein binding assays must still be conducted to determine the major binding protein, and how to implement fractional binding has yet to be determined). While the FDM provides more specific results, more experimental data are needed before making it suitable for use in the later stages of drug discovery. Regardless of which mechanism or combination of mechanisms is ultimately correct, it is clear that steady state uptake of highly bound ligands is lower in the presence of proteins, but higher than predicted by traditional equilibrium binding. Additional studies and understanding of these mechanisms are needed to ultimately improve IVIVE and the drug development process.

References

(1) Goldstein A (1949) The interactions of drugs and plasma proteins. *J Pharmacol Exp Ther* **95:**102-165.

(2) Schmidt S, Gonzalez D and Derendorf H (2010) Significance of protein binding in pharmacokinetics and pharmacodynamics. *J Pharm Sci* **99:**1107-1122.

(3) Trainor GL (2007) The importance of plasma protein binding in drug discovery. *Expert Opin Drug Discov* **2:**51-64.

(4) Smith DA, Di L and Kerns EH (2010) The effect of plasma protein binding on in vivo efficacy: misconceptions in drug discovery. *Nat Rev Drug Discov* **9:**929-939.

(5) Liu X, Wright M and Hop CECA (2014) Rational use of plasma protein and tissue binding data in drug design. *J Med Chem* **57:**8238-8248.

(6) Heuberger J, Schmidt S and Derendorf H (2013) When is protein binding important? *J Pharm Sci* **102:**3458-3467.

(7) Quinlan GJ, Martin GS and Evans TW (2005) Albumin: biochemical properties and therapeutic potential. *Hepatology* **41:**1211-1219.

(8) Farrugia A (2010) Albumin usage in clinical medicine: tradition or therapeutic? *Transfus Med Rev* 24:53-63.

(9) Sudlow G, Birkett DJ and Wade DN (1975) The characterization of two specific drug binding sites on human serum albumin. *Mol Pharmacol* **11:**824-832.

(10) Wanwimolruk S and Birkett DJ (1982) The effects of N-B transition of human serum albumin on the specific drug-binding sites. *Biochim Biophys Acta* **709:**247-255.

(11) Dockal M, Carter DC and Rüker F (2000) Conformational transitions of the three recombinant domains of human serum albumin depending on pH. *J Biol Chem* **275:**3042-3050.

(12) Israili ZH and Dayton PG (2001) Human alpha-1-glycoprotein and its interactions with drugs. *Drug Metab Rev* **33:**161-235.

(13) Bohnert T and Gan LS (2013) Plasma protein binding: from discovery to development. *J Pharm Sci* **102:**2953-2994.

(14) Howard ML, Hill JJ, Galluppi GR and McLean MA (2010) Plasma protein binding in drug discovery and development. *Comb Chem High Throughput Screen* **13:**170-187.

(15) Brockman AH, Oller HR, Moreau B, Kriksciukaite K and Bilodeau MT (2015) Simple method provides resolution of albumin, lipoprotein, free fraction, and chylomicron to enhance the utility of protein binding assays. *J Med Chem* **58:**1420-1425.

(16) Nakai D, Kumamoto K, Sakikawa C, Kosaka T and Tokui T (2004) Evaluation of the protein binding ratio of drugs by a micro-scale ultracentrifugation method. *J Pharm Sci* **93:**847-854.

(17) Di L, Breen C, Chambers R, Eckley ST, Fricke R, Ghosh A, Harradine P, Kalvass JC, Ho S, Lee CA, Marathe P, Perkins EJ, Qian M, Tse S, Yan Z and Zamek-Gliszczynski MJ (2017) Industry perspective on contemporary protein-binding methodologies: considerations for regulatory drug-drug interaction and related guidelines on highly bound drugs. *J Pharm Sci* **106:**3442-3452.

(18) Parasrampuria DA, Benet LZ and Sharma A (2018) Why drugs fail in late stages of development: case study analyses from the last decade and recommendations. *AAPS J* **20:**46.

(19) Benet LZ (2010) Clearance (née Rowland) concepts: a downdate and an update. *J Pharmacokinet Pharmacodyn* **37:**529-539.

(20) Rowland M, Benet LZ and Graham GG (1973) Clearance concepts in pharmacokinetics. *J Pharmacokinet Biopharm* **1:**123-136.

(21) Wilkinson GR and Shand DG (1975) A physiological approach to hepatic drug clearance. *Clin Pharmacol Ther* **18:**377-390.

(22) Houston JB (1994) Utility of in vitro drug metabolism data in predicting in vivo metabolic clearance. *Biochem Pharmacol* **47:**1469-1479.

(23) Chao P, Uss AS and Cheng KC (2010) Use of intrinsic clearance for prediction of human hepatic clearance. *Expert Opin Drug Metab Toxicol* **6:**189-198.

(24) Rane A, Wilkinson GR and Shand DG (1977) Prediction of hepatic extraction ratio from in vitro measurement of intrinsic clearance. *J Pharmacol Exp Ther* **200:**420-424.

(25) Obach RS (1997) Nonspecific binding to microsomes: impact on scale-up of in vitro intrinsic clearance to hepatic clearance as assessed through examination of warfarin, imipramine, and propranolol. *Drug Metab Dispos* **25:**1359-1369.

(26) Obach RS (1999) Prediction of human clearance of twenty-nine drugs from hepatic microsomal intrinsic clearance data: an examination of in vitro half-life approach and nonspecific binding to microsomes. *Drug Metab Dispos* **27:**1350-1359.

(27) Hakooz N, Ito K, Rawden H, Gill H, Lemmers L, Boobis AR, Edwards RJ, Carlile DJ, Lake BG and Houston JB (2006) Determination of a human hepatic microsomal scaling factor for predicting in vivo drug clearance. *Pharm Res* **23:**533-539.

(28) Hallifax D, Foster JA and Houston JB (2010) Prediction of human metabolic clearance from in vitro systems: retrospective analysis and prospective view. *Pharm Res* **27:**2150-2161.

(29) Winkler K, Keiding S and Tygstrup N (1973) In: Paumgartner, G. & Preisig, R. (Eds.) The Liver: Quantitative Aspects of Structure and Functions. S. Karger, Basel, pp. 44-155.

(30) Roberts MS and Rowland M (1986) A dispersion model of hepatic elimination: 1. formulation of the model and bolus considerations. *J Pharmacokinet Biopharm* **14:**227-260.

(31) Chiba M, Ishii Y and Sugiyama Y (2009) Prediction of hepatic clearance in human from in vitro data for successful drug development. *AAPS J* **11:**262-276.

(32) Benet LZ, Liu S and Wolfe AR (2018) The universally unrecognized assumption in predicting drug clearance and organ extraction ratio. *Clin Pharmacol Ther* **103:**521-525.

(33) Yang J, Jamei M, Yeo KR, Rostami-Hodjegan A and Tucker GT (2007) Misuse of the well-stirred model of hepatic drug clearance. *Drug Metab Dispos* **35:**501-502.

(34) Faed EM (1981) Protein binding of drugs in plasma, interstitial fluid and tissues: effect on pharmacokinetics. *Eur J Clin Pharmacol* **21:**77-81.

(35) Obach RS (1996) The importance of nonspecific binding in in vitro matrices, its impact on enzyme kinetic studies of drug metabolism reactions, and implications for in vitro-in vivo correlations. *Drug Metab Dispos* **24:**1047-1049.

(36) Venkatakrishnan K, von Moltke LL, Obach RS and Greenblatt DJ (2000) Microsomal binding of amitriptyline: effect on estimation of enzyme kinetic parameters in vitro. *J Pharmacol Exp Ther* **293:**343-350.

(37) Ito K and Houston JB (2005) Prediction of human drug clearance from in vitro and preclinical data using physiologically based and empirical approaches. *Pharm Res* **22:**103-112.

(38) Ring BJ, Chien JY, Adkison KK, Jones HM, Rowland M, Jones RD, Yates JWT, Ku MS, Gibson CR, He H, Vuppugalla R, Marathe P, Fischer V, Dutta S, Sinha VK, Björnsoon T, Lavé T and Poulin P (2011) PhRMA CPCDC initiative on predictive models of human pharmacokinetics, part 3: comparative assessment of prediction methods of human clearance. *J Pharm Sci* **100:**4090-4110.

(39) Di L, Keefer C, Scott DO, Strelevitz TJ, Chang G, Bi YA, Lai Y, Duckworth J, Fenner K, Troutman MD and Obach RS (2012) Mechanistic insights from comparing intrinsic clearance values between human liver microsomes and hepatocytes to guide drug design. *Eur J Med Chem* **57:**441-448.

(40) Austin RP, Barton P, Mohmed S and Riley RJ (2005) The binding of drugs to hepatocytes and its relationship to physicochemical properties. *Drug Metab Dispos* **33:**419-425.

(41) Austin RP, Barton P, Cockroft SL, Wenlock MC and Riley RJ (2002) The influence of nonspecific microsomal binding on apparent intrinsic clearance, and its prediction from physicochemical properties. *Drug Metab Dispos* **30:**1497-1503.

(42) Kalvass JC, Tess DA, Giragossian C, Linhares MC and Maurer TS (2001) Influence of microsomal concentration on apparent intrinsic clearance: implications for scaling in vitro data. *Drug Metab Dispos* **29:**1332-1336.

(43) Margolis JM and Obach RS (2003) Impact of nonspecific binding to microsomes and phospholipid on the inhibition of cytochrome P4502D6: implications for relating in vitro inhibition data to in vivo drug interactions. *Drug Metab Dispos* **31:**606-611.

(44) Gertz M, Kilford PJ, Houston JB and Galetin A (2008) Drug lipophilicity and microsomal protein concentration as determinants in the prediction of the fraction unbound in microsomal incubations. *Drug Metab Dispos* **36:**535-542.

(45) Riley RJ, McGinnity DF and Austin RP (2005) A unified model for predicting human hepatic, metabolic clearance from in vitro intrinsic clearance data in hepatocytes and microsomes. *Drug Metab Dispos* **33:**1304-1311.

(46) Gao H, Steyn SJ, Chang G and Lin J (2010) Assessment of in silico models for fraction of unbound drug in human liver microsomes. *Expert Opin Drug Metab Toxicol* **6:**533-542.

(47) Zhang Y, Yao L, Lin J, Gao H, Wilson TC and Giragossian C (2010) Lack of appreciable species differences in nonspecific microsomal binding. *J Pharm Sci* **99:**3620-3627.

(48) Hallifax D and Houston JB (2006) Binding of drugs to hepatic microsomes: comment and assessment of current prediction methodology with recommendation for improvement. *Drug Metab Dispos* **34:**724-726.

(49) Kilford PJ, Gertz M, Houston, JB and Galetin A (2008) Hepatocellular binding of drugs: correction for unbound fraction in hepatocyte incubations using microsomal binding or drug lipophilicity data. *Drug Metab Dispos* **36:**1194-1197.

(50) Gao H, Yao L, Mathieu HW, Zhang Y, Maurer TS, Troutman MD, Scott DO, Ruggeri RB and Lin J (2008) In silico modeling of nonspecific binding to human liver microsomes. *Drug Metab Dispos* **36:**2130-2135.

(51) Emoto C, Murayama N, Rostami-Hodjegan A and Yamazaki H (2009) Utilization of estimated physicochemical properties as an integrated part of predicting hepatic clearance in the early drug-discovery stage: impact of plasma and microsomal binding. *Xenobiotica* **39:**227-235.

(52) Poulin P and Haddad S (2011) Microsome composition-based model as a mechanistic tool to predict nonspecific binding of drugs in liver microsomes. *J Pharm Sci* **100:**4501-4517.

(53) Fagerholm U (2007) Prediction of human pharmacokinetics—evaluation of methods for prediction of hepatic metabolic clearance. *J Pharm Pharmacol* **59:**803-828.

(54) Berezhkovskiy LM (2011) The corrected traditional equations for calculation of hepatic clearance that account for the difference in drug ionization in extracellular and intracellular tissue water and the corresponding corrected PBPK equation. *J Pharm Sci* **100:**1167-1183.

(55) Berezhovskiy LM, Liu N and Halladay JS (2012) Consistency of the novel equations for determination of hepatic clearance and drug time course in liver that account for the difference in drug ionization in extracellular and intracellular tissue water. *J Pharm Sci* **101:**516-518.

(56) Poulin P, Kenny JR, Hop CECA and Haddad S (2012) In vitro-in vivo extrapolation of clearance: modeling hepatic metabolic clearance of highly bound drugs and comparative assessment with existing calculation methods. *J Pharm Sci* **101:**838-851.

(57) Baker KJ and Bradley SE (1966) Binding of sulfobromophthalein (BSP) sodium by plasma albumin. Its role in hepatic BSP extraction. *J Clin Invest* **45:**281-287.

(58) Forker EL and Luxon BA (1981) Albumin helps mediate removal of taurocholate by rat liver. *J Clin Invest* **67:**1517-1522.

(59) Forker EL and Luxon BA (1983) Albumin-mediated transport of rose bengal by perfused rat liver. Kinetics of the reaction at the cell surface. *J Clin Invest* **72:**1764-1771.

(60) Weisiger RA and Ma WL (1987) Uptake of oleate from albumin solutions by rat liver. Failure to detect catalysis of the dissociation of oleate from albumin by an albumin receptor. *J Clin Invest* **79:**1070-1077.

(61) Tsao SC, Sugiyama Y, Sawada Y, Iga T and Hanano M (1988) Kinetic analysis of albumin-mediated uptake of warfarin by perfused rat liver. *J Pharmacokinet Biopharm* **16:**165-181.

(62) Baker M and Parton T (2007) Kinetic determinants of hepatic clearance: plasma protein binding and hepatic uptake. *Xenobiotica* **37:**1110-1134.

(63) Wood FL, Houston JB and Hallifax D (2017) Clearance prediction methodology needs fundamental improvement: trends common to rat and human hepatocytes/microsomes and implications for experimental methodology. *Drug Metab Dispos* **45:**1178-1188.

(64) Blitzer BL and Lyons L (1985) Enhancement of Na+-dependent bile acid uptake by albumin: direct demonstration in rat basolateral liver plasma membrane vesicles. *Am J Physiol* **249:**G34-38.

(65) Ludden LK, Ludden TM, Collins JM, Pentikis HS and Strong JM (1997) Effect of albumin on the estimation, in vitro, of phenytoin Vmax and Km values: implications for clinical correlation. *J Pharmacol Exp Ther* **282:**391-396.

(66) Shibata Y, Takahashi H, Chiba M and Ishii Y (2002) Prediction of hepatic clearance and availability by cryopreserved human hepatocytes: an application of serum incubation method. *Drug Metab Dispos* **30:**892-896.

(67) Blanchard N, Richert L, Notter B, Delobel F, David P, Coassolo P and Lavé T (2004) Impact of serum on clearance predictions obtained from suspensions and primary cultures of rat hepatocytes. *Eur J Pharm Sci* **23:**189-199.

(68) Blanchard N, Hewitt NJ, Silber P, Jones H, Coassolo P and Lavé T (2006) Prediction of hepatic clearance using cryopreserved human hepatocytes: a comparison of serum and serum-free incubations. *J Pharm Pharmacol* **58:**633-641.

(69) Skaggs SM, Foti RS and Fisher MB (2006) A streamlined method to predict hepatic clearance using human liver microsomes in the presence of human plasma. *J Pharmacol Toxicol Methods* **53:**284-290.

(70) Rowland A, Elliot DJ, Knights KM, Mackenzie PI and Miners JO (2008) The "albumin effect" and in vitro-in vivo extrapolation: sequestration of long-chain unsaturated fatty acids enhances phenytoin hydroxylation by human liver microsomal and recombinant cytochrome P450 2C9. *Drug Metab Dispos* **36:**870-877.

(71) Wattanachai N, Polasek TM, Heath TM, Uchaipichat V, Tassaneeyakul W, Tassaneeyakul W and Miners JO (2011) In vitro-in vivo extrapolation of CYP2C8-catalyzed paclitaxel 6α-hydroxylation: effects of albumin on in vitro kinetic parameters and assessment of interindividual variability in predicted clearance. *Eur J Clin Pharmacol* **67:**815-824.

(72) Gill KL, Houston JB and Galetin A (2012) Characterization of in vitro glucurondation clearance of a range of drugs in human kidney microsomes: comparison with liver and intestinal glucuronidation and impact of albumin. *Drug Metab Dispos* **40:**825-835.

(73) Wattanachai N, Tassaneeyakul W and Tassaneeyakul W (2015) The effects of bovine serum albumin on kinetic characterization of human liver microsomal CYP2C19 and CYP2E1 activities. *Thai J Pharmacol* **37:**27-40.

(74) Mao J, Doshi U, Wright M, Hop CECA, Li AP and Chen Y (2018) Prediction of the pharmacokinetics of pravastatin as an OATP substrate using plateable human hepatocytes with human plasma data and PBPK modeling. *CPT Pharmacometrics Syst Pharmacol* **7:**251-258.

(75) Poulin P, Burczynski FJ and Haddad S (2016) The role of extracellular binding proteins in the cellular uptake of drugs: impact on quantitative in vitro-to-in vivo extrapolations of toxicity and efficacy in physiologically based pharmacokinetic-pharmacodynamic research. *J Pharm Sci* **105:**497-508.

(76) Weisiger R, Gollan J and Ockner R (1981) Receptor for albumin on the liver cell surface may mediate uptake of fatty acids and other albumin-bound substances. *Science* **211:**1048-1051.

(77) Ockner RK, Weisiger RA and Gollan JL (1983) Hepatic uptake of albumin-bound substances: albumin receptor concept. *Am J Physiol* **245:**G13-18.

(78) Reed RG and Burrington CM (1989) The albumin receptor effect may be due to a surface-induced conformational change in albumin. *J Biol Chem* **264:**9867-9872.

(79) Bloomer JR, Berk PD, Vergalla J and Berlin NI (1973) Influence of albumin on the hepatic uptake of unconjugated bilirubin. *Clin Sci Mol Med* **45:**505-516.

(80) Stremmel W, Potter BJ and Berk PD (1983) Studies of albumin binding to rat liver plasma membranes: implications for the albumin receptor hypothesis. *Biochim Biophys Acta* **756:**20-27.

(81) Stollman YR, Gärtner U, Theilmann L, Ohmi N and Wolkoff AW (1983) Hepatic bilirubin uptake in the isolated perfused rat liver is not facilitated by albumin binding. *J Clin Invest* **72:**718-723.

(82) Nunes R, Kiang C-L, Sorrentino D and Berk PD (1988) 'Albumin-receptor' uptake kinetics do not require an intact lobular architecture and are not specific for albumin. *J Hepatol* **7:**293-304.

(83) Burczynski FJ, Moran JB, Cai Z-S and Forker EL (1990) β-Lactoglobulin enhances the uptake of free palmitate by hepatocyte monolayers: the relative importance of diffusion and facilitated dissociation. *Can J Physiol Pharmacol* **68:**201-206.

(84) Weisiger RA, Zacks CM, Smith ND and Boyer JL (1984) Effect of albumin binding on extraction of sulfobromophthalein by perfused elasmobranch liver: evidence for dissociation-limited uptake. *Hepatology* **4:**492-501.

(85) van der Sluijs P, Postema B and Meijer DKF (1987) Lactosylation of albumin reduces uptake rate of dibromosulfophthalein in perfused rat liver and dissociation rate from albumin in vitro. *Hepatology* **7:**688-695.

(86) Burczynski FJ and Luxon BA (1995) Is there facilitated uptake of fatty acids by the liver? Interpretation and analysis of experimental data. *Can J Physiol Pharmacol* **73:**409-420.

(87) Komiya I, Park JY, Kamani A, Ho NFH and Higuchi WI (1980) Quantitative mechanistic studies in simultaneous fluid flow and intestinal absorption using steroids as model solutes. *Int J Pharm* **4:**249-262.

(88) Ichikawa M, Tsao SC, Lin T-H, Miyauchi S, Sawada Y, Iga T, Hanano M and Sugiyama Y (1992) 'Albumin-mediated transport phenomenon' observed for ligands with high membrane permeability: effect of the unstirred water layer in the Disse's space of rat liver. *J Hepatol* **16:**38-49.

(89) Bass L and Pond SM (1988) The puzzle of rates of cellular uptake of protein-bound ligands. In: Pecile, A., Rescigno, A. (Eds.), Pharmacokinetics: Mathematical and Statistical Approaches to Metabolism and Distribution of Chemicals and Drugs. Plenum Press, London. pp. 241-265.

(90) Weisiger RA, Pond SM and Bass L (1989) Albumin enhances unidirectional fluxes of fatty acid across a lipid-water interface: theory and experiments. *Am J Physiol* **257:**G904-916.

(91) Amidon GE, Higuchi WI and Ho NF (1982) Theoretical and experimental studies of transport of micelle-solubilized solutes. *J Pharm Sci* **71:**77-84.

(92) Pond SM, Davis CKC, Bogoyevitch MA, Gordon RA, Weisiger RA and Bass L (1992) Uptake of palmitate by hepatocyte suspensions: facilitation by albumin? Am J Physiol **262:**G883-894.

(93) Schwab AJ and Goresky CA (1991) Free fatty acid uptake by polyethylene: what can one learn from this? *Am J Physiol* **261:**G896-906.

(94) Burczynski FJ, Cai Z-S, Moran JB, Forker EL (1989) Palmitate uptake by cultured hepatocytes: albumin binding and stagnant layer phenomena. *Am J Physiol* **257:**G584-593.

(95) Nilsson M and Berg T (1977) Uptake and degradation of formaldehyde-treated ^{125}I-labelled human serum albumin in rat liver cells in vivo and in vitro. *Biochim Biophys Acta* **497:**171-182.

(96) Forker EL, Luxon BA, Snell M and Shurmantine WO (1982) Effect of albumin binding on the hepatic transport of rose bengal: surface-mediated dissociation of limited capacity. *J Pharmacol Exp Ther* **223:**342-347.

(97) Fleischer AB, Shurmantine WO, Luxon BA and Forker EL (1986) Palmitate uptake by hepatocyte monolayers. Effect of albumin binding. *J Clin Invest* **77:**964-970.

(98) Tsao SC, Sugiyama Y, Sawada Y, Nagase S, Iga T and Hanano M (1986) Effect of albumin on hepatic uptake of warfarin in normal and analbuminemic mutant rats: analysis by multiple indicator dilution method. *J Pharmacokinet Biopharm* **14:**51-64.

(99) Miyauchi S, Masuda M, Kim S-J, Tanaka Y, Lee K-R, Iwakado S, Nemoto M, Sasaki S, Shimono K, Tanaka Y and Sugiyama Y (2018) The phenomenon of albumin-mediated hepatic uptake of organic anion transport polypeptide substrates: prediction of the in vivo uptake clearance from the in vitro uptake by isolated hepatocytes using a facilitated-dissociation model. *Drug Metab Dispos* **46:**259-267.

(100) Burczynski FJ, Wang GQ and Hnatowich M (1997) Effect of binding protein surface charge on palmitate uptake by hepatocyte suspensions. Br J Pharmacol **120:**1215-1220.

(101) Horie T, Mizuma T, Kasai S and Awazu S (1988) Conformational change in plasma albumin due to interaction with isolated rat hepatocyte. *Am J Physiol* **254:**G465-470.

(102) Forker EL and Ghiron C (1988) ESR, albumin, and the riddle of organic anion uptake by the liver. *Am J Physiol* **254:**G463-464.

(103) Burczynski FJ, Wang GQ, Elmadhoun B, She YM, Roberts MS and Standing KG (2001) Hepatocyte [3H]-palmitate uptake: effect of albumin surface charge modification. *Can J Physiol Pharmacol* **79:**868-875.

(104) Qin M, Nilsson M and Øie S (1994) Decreased elimination of drug in the presence of alpha-1-acid glycoprotein is related to a reduced hepatocyte uptake. *J Pharmacol Exp Ther* **269:**1176-1181.

(105) Bilello JA, Bilello PA, Stellrecht K, Leonard J, Norbeck DW, Kempf DJ, Robins T and Drusano GL (1996) Human serum alpha 1 acid glycoprotein reduces uptake, intracellular concentration, and antiviral activity of A-80987, an inhibitor of the human immunodeficiency virus type 1 protease. *Antimicrob Agents Chemother* **40:**1491-1497.

(106) Poulin P, Hop CECA, Ho Q, Halladay JS, Haddad S and Kenny JR (2012) Comparative assessment of in vitro-in vivo extrapolation methods used for predicting hepatic metabolic clearance of drugs. *J Pharm Sci* **101:**4308-4326.

(107) Hallifax D and Houston JB (2012) Evaluation of hepatic clearance prediction using in vitro data: emphasis on fraction unbound in plasma and drug ionisation using a database of 107 drugs. *J Pharm Sci* **101:**2645-2652.

(108) Sohlenius-Sternbeck AK, Jones C, Ferguson D, Middleton BJ, Projean D, Floby E, Bylund J and Afzelius L (2012) Practical use of the regression offset approach for the prediction of in vivo intrinsic clearance from hepatocytes. *Xenobiotica* **42:**841-853.

(109) Yamagata T, Zanelli U, Gallemann D, Perrin D, Dolgos H and Petersson C (2017) Comparison of methods for the prediction of human clearance from hepatocyte intrinsic clearance for a set of reference compounds and an external evaluation set. *Xenobiotica* **47:**741-751.

(110) Poulin P and Haddad S (2013) Toward a new paradigm for the efficient in vitro-in vivo extrapolation of metabolic clearance in humans from hepatocyte data. *J Pharm Sci* **102:**3239-3251.

(111) Poulin P and Haddad S (2015) Albumin and uptake of drugs in cells: additional validation exercises of a recently published equation that quantifies the albumin-facilitated uptake mechanism(s) in physiologically based pharmacokinetic and pharmacodynamic modeling research. *J Pharm Sci* **104:**4448-4458.

(112) Poulin P (2013) Prediction of total hepatic clearance by combining metabolism, transport, and permeability data in the in vitro-in vivo extrapolation methods: emphasis on an apparent fraction unbound in liver for drugs. J Pharm Sci **102:**2085-1095.

(113) Da-Silva F, Boulenc X, Vermet H, Compigne P, Gerbal-Chaloin S, Daujat-Chavanieu M, Klieber S and Poulin P (2018) Improving prediction of metabolic clearance using quantitative extrapolation of results obtained from human hepatic micropatterned cocultures model and by considering the impact of albumin binding. *J Pharm Sci* **107:**1957-1972.

(114) Poulin P, Bteich M and Haddad S (2017) Supplemental analysis of the prediction of hepatic clearance of binary mixtures of bisphenol A and naproxen determined in an isolated perfused rat liver model to promote the understanding of potential albumin-facilitated hepatic uptake mechanism. *J Pharm Sci* **106:**3207-3214.

(115) Bounakta S, Bteich M, Mantha M, Poulin P and Haddad S (2018) Predictions of bisphenol A hepatic clearance in the isolated perfused rat liver (IRPL): impact of albumin binding and of co-administration with naproxen. *Xenobiotica* **48:**135-147.

(116) Poulin P and Haddad S (2018) Extrapolation of the hepatic clearance of drugs in the absence of albumin in vitro to that in the presence of albumin in vivo: comparative assessment of 2 extrapolation models based on the albumin-mediated hepatic uptake theory and limitations and mechanistic insights. *J Pharm Sci* **107:**1791-1797.

(117) Wootan MG, Bernlohr DA and Storch J (1993) Mechanism of fluorescent fatty acid transfer from adipocyte fatty acid binding protein to membranes. *Biochemistry* **32:**8622-8627.

(118) Zucker SD, Goessling W and Gollan JL (1995) Kinetics of bilirubin transfer between serum albumin and membrane vesicles. Insight into the mechanism of organic anion delivery to the hepatocyte plasma membrane. *J Biol Chem* **270:**1074-1081.

(119) Weisiger RA, Fitz JG and Scharschmidt BF (1989) Hepatic oleate uptake. Electrochemical driving forces in intact rat liver. *J Clin Invest* **83:**411-420.

(120) Øie S and Fiori F (1985) Effects of albumin and alpha-1 acid glycoprotein on elimination of prasozin and antipyrine in the isolated perfused rat liver. *J Pharmacol Exp Ther* **234:**636-640.

(121) Hütter JF, Piper HM and Spieckermann PG (1984) Myocardial fatty acid oxidation: evidence for an albumin-receptor-mediated membrane transfer of fatty acids. *Basic Res Cardiol* **79:**274-282.

(122) Hütter JF, Piper HM and Spieckermann PG (1984) Kinetic analysis of myocardial fatty acid oxidation suggesting an albumin receptor mediated uptake process. *J Mol Cell Cardiol* **16:**219-226.

(123) Rauch B, Bode C, Piper HM, Hütter JF, Zimmermann R, Braunwell E, Hasselbach W and Kübler W (1987) Palmitate uptake in calcium tolerant, adult rat myocardial single cells—evidence for an albumin mediated transport across sarcolemma. *J Mol Cell Cardiol* **19:**159-166.

(124) Sorrentino D, Robinson RB, Kiang C-L and Berk PD (1989) At physiologic albumin/oleate concentrations oleate uptake by isolated hepatocytes, cardiac myocytes, and adipocytes is a saturable function of the unbound oleate concentration. Uptake kinetics are consistent with the conventional theory. *J Clin Invest* **84:**1325-1333.

(125) Elmadhoun B, Wang GQ, Kirshenbaum LA and Burczynski FJ (2001) Palmitate uptake by neonatal rat myocytes and hepatocytes. Role of extracellular protein. *Eur J Biochem* **268:**3145-3153.

(126) Besseghir K, Mosig D and Roch-Ramel F (1989) Facilitation by serum albumin of renal tubular secretion of organic anions. *Am J Physiol* **256:**F475-484.

(127) Taft DR and Sweeney KR (1995) The influence of protein binding on the elimination of acetazolamide by the isolated perfused rat kidney: evidence of albumin-mediated tubular secretion. *J Pharmacol Exp Ther* **274:**752-760.

(128) Pardridge WM, Sakiyama R and Fierer G (1983) Transport of propranolol and lidocaine through the rat blood-brain barrier. Primary role of globulin-bound drug. *J Clin Invest* **71:**900-908.

(129) Fukuchi Y, Toshimoto K, Mori T, Kakimoto K, Tobe Y, Sawada T, Asaumi R, Iwata T, Hashimoto Y, Nunoya K-I, Imawaka H, Miyauchi S and Sugiyama Y (2017) Analysis of nonlinear pharmacokinetics of a highly albumin-bound compound: contribution of albumin-mediated hepatic uptake mechanism. *J Pharm Sci* **106:**2704-2714.

(130) Saptarshi SR, Duschl A and Lopata AL (2013) Interaction of nanoparticles with proteins: relation to bio-reactivity of the nanoparticle. *J Nanotechnol* **11:**1-12.

(131) Wright TL, Lysenko N, Ockner RK and Weisiger RA (1987) Interaction of natural and synthetic albumin polymers with hepatocytes. *Hepatology* **7:**294-301.

CHAPTER 3: Hepatic Clearance Predictions from In Vitro-In Vivo Extrapolation and the Biopharmaceutics Drug Disposition Classification System*

Abstract

Predicting in vivo pharmacokinetic parameters such as clearance from in vitro data is a crucial part of the drug development process. There is a commonly cited trend that drugs that are highly protein bound and are substrates for hepatic uptake transporters often yield the worst predictions. Given this information, 11 different data sets using human microsomes and hepatocytes were evaluated to search for trends in accuracy, extent of protein binding, and drug classification based on the Biopharmaceutics Drug Disposition Classification System (BDDCS), which makes predictions about transporter effects. As previously reported, both in vitro systems (microsomes and hepatocytes) gave a large number of inaccurate results, defined as predictions falling more than 2-fold outside of in vivo values. The weighted average of the percentage of inaccuracy was 66.5%. BDDCS class 2 drugs, which are subject to transporter effects in vivo unlike class 1 compounds, had a higher percentage of inaccurate predictions and often had slightly larger bias. However, since the weighted average of the percent inaccuracy was still high in both classes (81.9% for class 2, and 62.3% for class 1), it may be currently hard to use BDDCS class to predict potential accuracy. The results of this study emphasize the need for improved IVIVE experimental methods as using physiologically based scaling is still not accurate, and BDDCS cannot currently help predict accurate results.

*Modified from the publication: Bowman CM and Benet LZ (2016) Hepatic clearance predictions from in vitro-in vivo extrapolation and the Biopharmaceutics Drug Disposition Classification System. *Drug Metab Dispos* **44:**1731-1735.

Introduction

The current drug development process is expensive, time-consuming, and inefficient due to compound attrition (1). While failures due to pharmacokinetic parameters have decreased in recent years (2), continued improvement in pharmacokinetic predictions is crucial.

Metabolic stability studies are some of the earliest in vitro studies conducted during drug development to determine the rate and extent to which a molecule is metabolized, and can be useful for rank ordering candidates. After measuring in vitro metabolic turnover, or intrinsic clearance (CL_{int}), in vivo hepatic clearance can be predicted using in vitro-in vivo extrapolation (IVIVE) methods. A common approach is to apply physiologically based scaling factors to the raw in vitro data, such as hepatocellularity for studies using hepatocytes or a factor to account for incomplete microsomal recovery for microsomes, and to then apply a model of hepatic disposition such as the well-stirred model (3). While the results are often used in the drug development process, there is perhaps an overemphasis placed on their reliability.

The first part of this study examined the overall accuracy of hepatic clearance predictions in the field at this time. Many groups have attempted IVIVE, tried to create new models to improve predictions from old in vitro values, or investigated different experimental setups. A study published 10 years ago collected and examined results from 85 compounds, concluding there was a paucity of literature data (4), however much work has been done since then.

When examining the accuracy of these values, a prediction bias has been found that is unresolved from human variability and experimental uncertainty (5). There is also a commonly cited trend that substrates for hepatic uptake transporters and highly protein bound compounds yield the poorest predictions (6). The Biopharmaceutics Drug Disposition Classification System (BDDCS), which categorizes transporter effects on drug disposition, says class 1 compounds

exhibit minimal clinically relevant transporter effects, while class 2 compounds may be governed by transporter effects in the gut and liver (7). BDDCS has become an important part of early drug discovery for predicting routes of elimination, food effects, and potential drug interactions (7). Given this trend, the main objective of this study was to determine if BDDCS classification could be a determinant of accurate IVIVE results.

Materials and Methods

A literature search was conducted for compounds previously described for which both in vitro and in vivo clearance data were available. Studies using human microsomes as well as human hepatocytes were considered, as both systems are routinely used in the pharmaceutical industry. The terms used as keywords to help in the search included "in vitro-in vivo extrapolation", "intrinsic clearance", "microsomes", "hepatocytes", or a combination of these.

All the studies considered here used the well-stirred model in their predictions, and predictions were made using physiologically based scaling factors, not empirical or regression-based factors. The data sets were examined separately, excluding re-examination of previously published data, as different experimental setups (such as the inclusion of serum in incubations) and scaling (such as the inclusion of $f_{u,B}$ and $f_{u,inc}$ vs. no binding terms) were used in each. Similarly, repeated drugs were not removed due to value differences among data sets. Overall evaluations were also tabulated. The data evaluated can be found in Appendix Table 1.

The accuracy of predictions was determined based on whether or not the predictions fell within 2-fold of the true in vivo values, as has been a standard cutoff in previous studies (8-10).

To measure bias, the average fold error (AFE) was calculated using the following equation (11):

$$AFE=10^{\frac{1}{N}\sum \log\left(\frac{observed}{predicted}\right)}$$

AFE was recorded as the whole number reciprocal if less than 1.

The precision was also calculated with the root mean squared error (RMSE) using the following equation (12):

$$RMSE=\sqrt{\frac{1}{N}\sum(predicted-observed)^2}$$

To divide the compounds based on their BDDCS classification, two publications categorizing over 900 drugs and over 175 drugs were consulted (13, 14). Five compounds were also classified here for the first time (class 1: amobarbital, bufuralol, levoprotiline, and triprolidine; class 2: tenidap). Trends in the accuracy of predictions compared to class 1 and class 2 drugs, where metabolism is the main route of elimination, were examined. Protein binding was also considered if the values used in the prediction calculations were available, as the interplay between protein binding, transporters, and enzymes is known to be important (15). Drugs with high protein binding were defined as having a free fraction less than or equal to 0.05.

Results

Seven different papers were examined that fit the criteria mentioned above (16-22). Hallifax et al. (17) compiled a large database of predictions from many of the papers also

examined here, however not all drugs from the original papers were included and often different values of $CL_{in\ vivo}$ were compared, leading the same drugs to be accurately or inaccurately predicted based on the value choices. Furthermore, while it could be argued that the more recent Hallifax et al. paper provides refined values from the original papers, looking at the percentage inaccuracy and AFE both overall and for class 1 and class 2 drugs reveals that the Hallifax et al. data often actually have comparable or higher percentage inaccuracy and AFE values compared to the original papers. All papers were therefore examined to try to obtain a fuller picture of the relationship to BDDCS. Five human microsome data sets, some with multiple scaling options, were included in this evaluation for a total of 332 values, and six human hepatocyte data sets were included also for a total of 332 values. The percentage of inaccurate predictions (more than 2-fold difference) for each data set and the AFE and RMSE are shown in Table 3.1. Every data set examined has 41.0% or greater inaccuracy and AFE values are as high as 21.7. The paper by Sohlenius-Sternbeck et al. (22) only provided individual prediction values using a regression model so further analysis could not be conducted. However, since it is the most recent paper examined, the summary statistics using the well-stirred model with protein binding that were given were still included in the table for comparison. The weighted average for the percentage of inaccurate results for microsomes is 66.8%, for hepatocytes is 66.2%, and overall is 66.5%.

The same papers and data sets were used to examine BDDCS trends. Class 1 and class 2 drugs were compiled from each set, and the inaccuracy of the predictions, AFE, and RMSE for each class were determined (Table 3.2). As expected, class 2 drugs have a higher percentage of inaccurate predictions than class 1 drugs in every case except one, where all predictions were inaccurate. The AFE was either slightly higher or almost identical for class 2 drugs compared to class 1 drugs. Considering a total of 305 class 1 drug values, the weighted average of the

percentage of inaccurate predictions is 62.3%. For a total of 155 class 2 drug values, the weighted average of the percentage of inaccuracy is 81.9%. (The total number of class 1 and 2 drugs is less than 644 since individual drugs are not enumerated in Sohlenius-Sternbeck et al. (22) and some unapproved proprietary compounds are included in other data sets.) For class 1 drugs, studies done in microsomes have a weighted average of 63.3% inaccuracy, while studies in hepatocytes are 66.2% inaccurate. For class 2 drugs, studies in microsomes have a weighted average of prediction inaccuracy of 85.6%, while studies in hepatocytes have a 78.4% average.

Table 3.1: Percentage inaccuracy, AFE, RMSE of IVIVE predictions for 11 data sets

Author	System	# Compounds Evaluated	# Inaccurate Predictions (%)	AFE	RMSE
Brown et al. (16)	hepatocytes	37	26 (70.3%)	4.5	6460.2
Hallifax et al. (17)	microsomes	68	53 (77.9%)	5.2	3708.6
	hepatocytes	89	60 (67.4%)	3.9	3137.7
Ito et al. (18)	microsomes	52	45 (86.5%)	7.9	1337.0
McGinnity et al.[a] (19)	hepatocytes	44	22 (50.0%)	1.4	94.1
Obach et al. (20)	microsomes ($f_{u,B}$ and $f_{u,inc}$)	29	13 (44.8%)	2.3	4.9
	microsomes ($f_{u,B}$)	29	22 (75.9%)	4.3	6.8
	microsomes (no binding)	29	13 (44.8%)	1.5	4.3
Riley et al.[b] (21)	microsomes	37	27 (73.0%)	3.3	2314.2
	hepatocytes	56	38 (67.9%)	3.1	1356.5
	hepatocytes (w/ serum)	14	14 (100.0%)	21.7	2124.3
Sohlenius-Sternbeck et al.[c] (22)	microsomes ($f_{u,B}$ and $f_{u,inc}$)	44	70.0%	3.8	5.8
	hepatocytes ($f_{u,B}$ and $f_{u,inc}$)	46	89.0%	5.9	8.0
	microsomes (no binding)	44	41.0%	0.5	6.1
	hepatocytes (no binding)	46	41.0%	0.8	5.4

[a]=CL_{int} data were evaluated; [b]=$CL_{int, ub, in\ vivo}$ data were evaluated; [c]=individual values for predictions with well-stirred model were not presented, only summary statistics

Table 3.2: Percentage inaccuracy, AFE, RMSE of IVIVE predictions for BDDCS class 1 and class 2 drugs

Authors	System	# Class 1 Drugs	# Inaccurate Class 1 Predictions (%)	AFE	RMSE	# Class 2 Drugs	# Inaccurate Class 2 Predictions (%)	AFE	RMSE
Brown et al.(16)	hepatocytes	24	14 (58.3%)	3.0	294.5	12	11 (91.7%)	7.4	11335.9
Hallifax et al. (17)	microsomes	42	30 (71.4%)	5.2	4521.7	22	20 (91.0%)	4.7	1834.4
	hepatocytes	55	36 (65.5%)	4.0	3976.5	30	22 (73.3%)	3.7	466.1
Ito et al. (18)	microsomes	32	27 (84.4%)	6.8	390.8	16	15 (93.8%)	11.2	2312.3
McGinnity et al. (19)	hepatocytes	32	16 (50.0%)	1.1	99.3	9	5 (55.6%)	3.0	90.9
Obach et al. (20)	microsomes ($f_{u,B}$ and $f_{u,inc}$)	20	7 (35.0%)	1.9	4.6	9	6 (66.6%)	3.2	5.4
	microsomes ($f_{u,B}$)	20	13 (65.0%)	3.7	6.9	9	9 (100.0%)	6.0	6.7
	microsomes (no binding)	20	7 (35.0%)	1.2	4.0	9	6 (66.7%)	2.5	4.8
Riley et al. (21)	microsomes	24	16 (66.7%)	2.7	2399.1	11	9 (81.8%)	6.0	2298.5
	hepatocytes	28	16 (57.1%)	2.4	175.7	22	18 (81.8%)	3.8	2125.8
	hepatocytes (serum)	8	8 (100.0%)	9.6	251.0	6	6 (100.0%)	64.2	3232.0

Finally, given that substrates of transporters and highly bound drugs often have the poorest clearance predictions (6), protein-binding differences were examined between the two BDDCS classes. First, the percentage of drugs with inaccurate predictions that are also highly protein bound in both classes was determined (Table 3.3). There are more inaccurate class 2 drugs that are highly protein bound than class 1 drugs in every case examined. The weighted average of inaccurate class 1 drugs with high protein binding is 19.8%, while the weighted average for class 2 is 67.3%. Since class 2 drugs in general are often highly protein bound (23), the numbers of highly bound drugs in both classes that have inaccurate predictions were also determined (Table 3.4). These results agree with several other conclusions that highly protein bound compounds are often poorly predicted. Class 1 highly protein bound drugs were inaccurately predicted 81.3% of the time, and class 2 highly bound drugs had an 85.7% average inaccuracy rate. In four data sets, highly bound class 2 drugs had a higher percentage of inaccuracy than class 1 drugs, in one data set the opposite was true, and in the last all highly bound drugs were inaccurate.

Looking at the bias between the high and low protein binding drugs in the two classes (Table 3.5), it is difficult to see trends between the two classes, however the bias is always higher for the high protein binding drugs, except in the case of the data from Obach et al. (20) using $f_{u,B}$ and $f_{u,inc}$, and Brown et al. (16) where there are only two class 1 high protein binding drugs and 4 class 2 low protein binding drugs perhaps skewing the results.

Table 3.3: Percentage inaccuracy of BDDCS class 1 and class 2 drugs that are highly protein bound

Author	System	# Inaccurate Class 1 Predictions	# Inaccurate Highly Protein Bound Class 1 Predictions (%)	# Inaccurate Class 2 Predictions	# Inaccurate Highly Protein Bound Class 2 Predictions (%)
Brown et al. (16)	hepatocytes	14	1 (7.1%)	11	7 (63.6%)
Hallifax et al. (17)	microsomes	30	6 (20.0%)	20	9 (45.0%)
	hepatocytes	36	9 (25.0%)	22	15 (68.2%)
Obach et al. (20)	microsomes ($f_{u,B}$ and $f_{u,inc}$)	7	1 (14.3%)	6	4 (66.6%)
	microsomes ($f_{u,B}$)	13	1 (7.7%)	9	4 (44.4%)
	microsomes (no binding)	7	2 (28.6%)	6	4 (66.7%)
Riley et al. (21)	hepatocytes	16	4 (25.0%)	18	17 (94.4%)
	hepatocytes (serum)	8	2 (25.0%)	6	6 (100.0%)

Table 3.4: Percentage of highly protein bound BDDCS class 1 and class 2 drugs that are inaccurate

Author	System	# Highly Protein Bound Class 1 Drugs	# Inaccurate Highly Protein Bound Class 1 Predictions (%)	# Highly Protein Bound Class 2 Drugs	# Inaccurate Highly Protein Bound Class 2 Predictions (%)
Brown et al. (16)	hepatocytes	2	1 (50.0%)	8	7 (87.5%)
Hallifax et al. (17)	microsomes	8	6 (75.0%)	10	9 (90.0%)
	hepatocytes	9	9 (100.0%)	20	15 (75.0%)
Obach et al. (20)	microsomes ($f_{u,B}$ and $f_{u,inc}$)	2	1 (50.0%)	4	4 (100.0%)
	microsomes ($f_{u,B}$)	2	1 (50.0%)	4	4 (100.0%)
	microsomes (no binding)	2	2 (100.0%)	4	4 (100.0%)
Riley et al. (21)	hepatocytes	5	4 (80.0%)	21	17 (81.0%)
	hepatocytes (serum)	2	2 (100.0%)	6	6 (100.0%)

Table 3.5: AFE and RMSE of high and low protein binding BDDCS class 1 and class 2 drugs

Author	System	Protein Binding	Class 1		Class 2	
			AFE	RMSE	AFE	RMSE
Brown et al. (16)	hepatocytes	high	2.0	56.4	6.3	13882.7
		low	3.1	307.1	10.3	229.6
Hallifax et al. (17)	microsomes	high	7.8	10335.3	5.3	2671.0
		low	4.8	349.9	4.2	473.3
	hepatocytes	high	12.1	9814.8	4.2	479.9
		low	3.3	242.7	2.9	437.0
Obach et al. (20)	microsomes ($f_{u,B}$ and $f_{u,inc}$)	high	1.7	0.3	4.7	3.1
		low	2.0	4.9	2.3	6.7
	microsomes ($fu_{,B}$)	high	4.7	0.4	7.3	3.1
		low	3.6	7.3	5.2	8.6
	microsomes (no binding)	high	13.7	1.5	7.7	6.8
		low	1.12	17.7	1.0	2.2
Riley et al. (21)	hepatocytes	high	3.1	175.2	3.9	2175.6
		low	2.2	173.3	2.8	136.5
	hepatocytes (serum)	high	17.0	406.3	64.2	3232.0
		low	8.0	170.2	-	-

Discussion

Being able to accurately predict pharmacokinetic parameters, especially clearance, early in the drug development process is a key part of lead optimization. However while some studies have claimed to find success in predicting in vivo clearance from in vitro data, others have questioned the reliability (24). Underpredicting in vivo clearance may result in inefficiency in the drug discovery pipeline or an ineffective therapeutic dosing regimen, while overpredicting in vivo clearance may lead to missed opportunities that were rejected early in the development process (25).

The goal of this study was to compile data to examine the accuracy of the prediction methods for in vivo clearance and relate this accuracy to BDDCS classification. For the 11 data sets considered, there is a large percentage of inaccuracy. To have a true understanding of the accuracy of in vitro methods, physiologically scaled in vitro estimations and observed in vivo clearance were directly compared, since incorporating established physiological scaling factors as well as unbound fractions in the blood and possibly in vitro matrix should in theory, give accurate predictions. This is in contrast to some groups creating linear regression equations from reference compound data and then applying an empirical scaling factor to try to further improve predictions (26). The fact that 66.5% of predictions overall are inaccurate emphasizes the idea that a mechanistic understanding of this inaccuracy still needs to be determined before IVIVE predictions can be completely trusted.

BDDCS classification and protein binding were then examined to see if they could separate accurate from inaccurate results to help determine whether predictions can be trusted in the future or not. Class 1 drugs, or those that are extensively metabolized and highly soluble, appear to overwhelm transporter effects, while class 2 drugs, also extensively metabolized but

poorly soluble, can be affected by efflux transporters in the gut, and both uptake and efflux transporters in the liver (27). Given the trend that poorly predicted compounds are often substrates for transporters (6), it was expected that class 1 drugs that have no clinically relevant transporter effects would yield better predictions than class 2 drugs. The other part of the trend is that poorly predicted compounds are also often highly protein bound, which is why protein binding was considered when data were available (28). Overall, the hypothesis was that class 2 drugs would be more poorly predicted due to the fact that they are substrates for transporters, and these poorly predicted class 2 drugs would also be highly protein bound.

As expected, class 2 drugs yielded poorer predictions in every case examined; however, there was still large inaccuracy for both class 1 and class 2 drugs. Class 2 drugs also often had a higher AFE, but not different enough (or sometimes at all) to understand bias. However, AFE provides a better measure of bias than RMSE, which is highly influenced by the marked differences in CL_{int} values from study to study. For example, the values reported by Brown et al. (16) for predicted and measured CL_{int} for propofol were 2,773 and 5,052 ml/min/kg, respectively, while for the same drug McGinnity et al. (19) reported 283 and 24 ml/min/kg. At this point in time with the current methodology, relying on BDDCS class cannot confidently provide information about whether predictions will be accurate or not. This agrees with previous findings from Poulin et al. who found that predictivity was similar between classes for a human microsome data set of 42 drugs (29). It is interesting to note that microsomes and hepatocytes gave similar prediction accuracies in both class 1 and class 2 drugs. A bigger difference between the two systems would have been expected for class 2 drugs where transporters play a role since necessary uptake transporters are not present in microsomes. This again emphasizes that there

are likely major missing determinants when trying to mimic the interplay between protein binding, uptake, and metabolism in vitro.

Poulin et al. (29) also suggested that an approach involving determination of effective fraction unbound in plasma based on albumin-facilitated hepatic uptake of acidic/neutral drugs improved the prediction accuracy and precision for 25 high protein binding drugs. Hallifax and Houston (30) examined this approach for 107 drugs studied in hepatocytes and microsomes also finding an increase in prediction accuracy, but no change in precision and reported that there was no evidence that prediction bias was associated with measured fraction unbound in plasma. These latter authors emphasized the need for further "mechanistic elucidation to improve prediction methodology rather than empirical correction of bias".

Lastly, protein binding was considered along with BDDCS. Given current trends, class 2 drugs with high protein binding would have been expected to yield the poorest results. There were more inaccurate class 2 drugs that had high protein binding than class 1, but this may be because class 2 drugs generally have higher protein binding than class 1 (23). This, coupled to the fact that there may be a slight dependency of bias on protein binding both here and as found previously with hepatocytes by Hallifax et al. (17), could explain some of the difference seen between the inaccuracies in class 1 and 2 drugs. However, on average, highly bound drugs in both classes had similar high percentages of inaccuracy, and there were no clear trends in the bias or precision of highly bound drugs between classes.

This study emphasizes the fact that the in vitro to in vivo extrapolation of hepatic clearance needs to be improved through a better understanding of clearance mechanisms as in vitro methods on their own are often not accurate, and looking at BDDCS class cannot separate out which compounds will have accurate predictions.

References

(1) Pammolli F, Magazzini L and Riccaboni M (2011) The productivity crisis in pharmaceutical R&D. *Nat Rev Drug Discov* **10:**428-438.

(2) Waring MJ, Arrowsmith J, Leach AR, Leeson PD, Mandrell S, Owen RM, Pairaudeau G, Pennie WD, Pickett SD, Wang G, Wallace O, and Weir A (2015) An analysis of the attrition of drug candidates from four major pharmaceutical companies. *Nat Rev Drug Discov* **14:**475-486.

(3) Houston JB (1994) Utility of in vitro drug metabolism data in predicting in vivo metabolic clearance. *Biochem Pharmacol* **47:**1469-1479.

(4) Nagilla R, Frank KA, Jolivette LJ and Ward KW (2006) Investigation of the utility of published in vitro intrinsic clearance data for the prediction of in vivo clearance. *J Pharmacol Toxicol Methods* **53:**106-116.

(5) Hallifax D and Houston JB (2009) Methodological uncertainty in quantitative prediction of hepatic clearance from human experimental systems. *Curr Drug Metab* **10:**307-321.

(6) Soars MG, McGinnity DF, Grime K and Riley RJ (2007) The pivotal role of hepatocytes in drug discovery. *Chem Biol Interact* **168:**2-15.

(7) Wu C-Y and Benet LZ (2005) Predicting drug disposition via application of BCS: transport/absorption/elimination interplay and development of a biopharmaceutics drug disposition classification system. *Pharm Res* **22:**11-23.

(8) Blanchard N, Hewitt NJ, Silber P, Jones H, Coassolo P and Lavé T (2006) Prediction of hepatic clearance using cryopreserved human hepatocytes: a comparison of serum and serum-free incubations. *J Pharm Pharmacol* **58:**633-641.

(9) Fagerholm U (2007) Prediction of human pharmacokinetics—improving microsome-based predictions of hepatic metabolic clearance. *J Pharm Pharmacol* **59:**1427-1431.

(10) Zuegge J, Schneider G, Coassolo P and Lavé T (2001) Prediction of hepatic metabolic clearance: comparison and assessment of prediction models. *Clin Pharmacokinet* **40:**553-63.

(11) Obach RS, Baxter JG, Liston TE, Silber BM, Jones BC, Macintyre F, Rance DJ and Wastall P (1997) The prediction of human pharmacokinetic parameters from preclinical and in vitro metabolism data. *J Pharmacol Exp Ther* **283:**46-58.

(12) Sheiner LB and Beal SL (1981) Some suggestions for measuring predictive performance. *J Pharmacokinet Biopharm* **9:**503-512.

(13) Benet LZ, Broccatelli F and Oprea TI (2011) BDDCS applied to over 900 drugs. *AAPS J* **13:**519-547.

(14) Hosey CM, Chan R and Benet LZ (2016) BDDCS predictions, self-correcting aspects of BDDCS assignments, BDDCS assignment corrections, and classification for more than 175 additional drugs. *AAPS J* **18:**251-260.

(15) Benet LZ (2009) The drug transporter-metabolism alliance: uncovering and defining the interplay. *Mol Pharm* **6:**1631-1643.

(16) Brown HS, Griffin M and Houston JB (2007) Evaluation of cryopreserved human hepatocytes as an alternative in vitro system to microsomes for the prediction of metabolic clearance. *Drug Metab Dispos* **35:**293-301.

(17) Hallifax D, Foster JA and Houston JB (2010) Prediction of human metabolic clearance from in vitro systems: retrospective analysis and prospective view. *Pharm Res* **27:**2150-2161.

(18) Ito K and Houston JB (2005) Prediction of human drug clearance from in vitro and preclinical data using physiologically based and empirical approaches. *Pharm Res* **22:**103-112.

(19) McGinnity DF, Soars MG, Urbanowicz RA and Riley RJ (2004) Evaluation of fresh and cryopreserved hepatocytes as in vitro drug metabolism tools for the prediction of metabolic clearance. *Drug Metab Dispos* **32:**1247-1253.

(20) Obach RS (1999) Prediction of human clearance of twenty-nine drugs from hepatic microsomal intrinsic clearance data: an examination of in vitro half-life approach and nonspecific binding to microsomes *Drug Metab Dispos* **27:**1350-1359.

(21) Riley RJ, McGinnity DF and Austin RP (2005) A unified model for predicting human hepatic, metabolic clearance from in vitro intrinsic clearance data in hepatocytes and microsomes. *Drug Metab Dispos* **33:**1304-1311.

(22) Sohlenius-Sternbeck AK, Afzelius L, Prusis P, Neelissen J, Hoogstraate J, Johansson J, Floby E, Bengtsson A, Gissberg O, Sternbeck J and Petersson C (2010) Evaluation of the human prediction of clearance from hepatocyte and microsome intrinsic clearance for 52 drug compounds. *Xenobiotica* **40:**637-649.

(23) Broccatelli F, Cruciani G, Benet LZ and Oprea TI (2012) BDDCS class prediction for new molecular entities. *Mol Pharm* **9:**570-580.

(24) Masimirembwa CM, Bredberg U and Andersson TB (2003) Metabolic stability for drug discovery and development. *Clin Pharmacokinet* **42:**515-528.

(25) Clarke SE and Jeffrey P (2001) Utility of metabolic stability screening: comparison of in vitro and in vivo clearance. *Xenobiotica* **31:**591-598.

(26) Sohlenius-Sternbeck AK, Jones C, Ferguson D, Middleton BJ, Projean D, Floby E, Bylund J and Afzelius L (2012) Practical use of the regression offset approach for the prediction of in vivo intrinsic clearance from hepatocytes. *Xenobiotica* **42:**841-853.

(27) Shugarts S and Benet LZ (2009) The role of transporters in the pharmacokinetics of orally administered drugs. *Pharm Res* **26:**2039-2054.

(28) Ring BJ, Chien, JY, Adkison KK, Jones HM, Rowland M, Jones RD, Yates, JWT, Ku MS, Gibson CR, He H, Vuppugalla R, Marathe P, Fischer V, Dutta S, Sinha VK, Björnsson T, Lavé T and Poulin P (2011) PhRMA CPCDC initiative on predictive models of human pharmacokinetics, part 3: comparative assessment of prediction methods of human clearance. *J Pharm Sci* **100:**4090-4110.

(29) Poulin P, Hop CE, Ho Q, Halladay JS, Haddad S and Kenny JR (2012) Comparative assessment of in vitro-in vivo extrapolation methods used for predicting hepatic metabolic clearance of drugs. *J Pharm Sci* **101:**4308-4326.

(30) Hallifax D and Houston JB (2012) Evaluation of hepatic clearance prediction using in vitro data: emphasis on fraction unbound in plasma and drug ionization using a database of 107 drugs. *J Pharm Sci* **101:**2645-2652.

CHAPTER 4: In Vitro-In Vivo Extrapolation and Hepatic Clearance Dependent Underprediction*

Abstract

Accurately predicting the hepatic clearance of compounds using in vitro to in vivo extrapolation (IVIVE) is crucial within the pharmaceutical industry. However several groups have recently highlighted the large error in the process. While empirical or regression-based scaling factors may be used to mitigate the common underprediction, they provide unsatisfying solutions since the reasoning behind the underlying error has yet to be determined. One previously noted trend was intrinsic clearance-dependent underprediction, highlighting the limitations of current in vitro systems. When applying these generated in vitro intrinsic clearance values during drug development and making first-in-human dose predictions for new chemical entities though, hepatic clearance is the parameter that must be estimated using a model of hepatic disposition such as the well-stirred model. Here we examine error across hepatic clearance ranges and find a similar hepatic clearance-dependent trend, with high clearance compounds not predicted to be so, demonstrating another gap in the field.

*Modified from the publication: Bowman CM and Benet LZ (2019) In vitro-in vivo extrapolation and hepatic clearance dependent underprediction. *J Pharm Sci* doi: 10.1016/j.xphs.2019.02.009

Introduction

Given that many drugs are primarily eliminated by metabolism, the accurate prediction of hepatic clearance (CL_H) is crucial for both evaluating and optimizing new chemical entities as well as estimating first-in-human doses. Successful predictions could help reduce the high attrition (1) associated with the current drug discovery and development process. While allometric scaling may be attempted for prediction, it is more accurate for renally cleared compounds (2,3). Alternatively, in vitro to in vivo extrapolation (IVIVE) is commonly used to predict hepatic clearance.

When implementing IVIVE, microsomes or hepatocytes can be used to determine an in vitro intrinsic clearance (CL_{int}). The in vitro value is then scaled to an in vivo CL_{int} using physiologically based parameters such as microsomal protein content/hepatocellularity and liver weight. Ultimately the scaled value is input into a model of hepatic disposition such as the well-stirred model to estimate hepatic clearance.

Several publications have examined the accuracy of IVIVE predictions with rat (4-6) and human (7-11) data and further comparisons have been made with data generated in microsomes vs. hepatocytes (12-14). One review found that on average, human microsomes underpredict clearance by 9 fold, while human hepatocytes underpredict by 3-6 fold (15). This would be expected given that hepatocytes contain transporters, both phase I and II enzymes, and the natural localization of organelles and cofactors, unlike microsomes. However, examining a larger quantity of data, groups have recently reported the error between the two systems to be more comparable (16,17).

Several hypotheses have been proposed to account for the systematic underprediction observed. Concerns with hepatocyte cryopreservation have been expressed, however studies

have shown no significant differences between cryopreserved and fresh cells (4,8,13,18). Similarly, the impact of donor variability is frequently discussed (18), however both over-and underprediction would be expected (15) and many groups now use pooled microsomes and hepatocytes**.** Other proposed reasons for the inaccuracy have included differences in liver sample viability and preparation (19), differences in the use of binding terms (7,20), inaccuracies in the measurement of fraction unbound (21,22), the presence of inhibitory long-chain unsaturated fatty acids in microsomal incubations (23,24), ignoring extra-hepatic metabolism (15,25), and simplifying the complex interplay between uptake, metabolism, biliary secretion, and efflux (26).

When exploring reasons for error, groups have also considered clearance-dependent trends. While reducing the clearance of compounds is often a goal to facilitate lower dosage requirements and longer half-lives, measuring low clearance in vitro is experimentally challenging. Stringer et al. (27) found that of compounds with an in vivo CL_{int} of 1-10 ml/min/kg, only 8% had a measurable value in microsomes and 13% in hepatocytes. Given that enzyme activity begins declining in microsomes after 1 hour of incubation, and cell viability begins decreasing in hepatocytes at 4-6 hours, a low turnover compound can have large uncertainty in its clearance and first dose estimations (28). A study examining predictions in hepatocyte preparations from four species found poorer accuracy with low clearance compounds (4). However newer methods such as the hepatocyte relay method (29,30), and hepatocyte culture systems containing flow and/or cell coculture (31,32), have been developed to try to address the error.

At the other extreme, studies have seen an increase in error with increasing in vivo CL_{int} in hepatocytes (17,33,34) and microsomes (17) in both human and rat preparations (17).

Suggested reasons for this trend include endogenous cofactor depletion, loss of enzymatic activity, permeability limitation, and rate limiting diffusion through the unstirred water layer (13,33,34,35).

While recognizing CL_{int} trends are important for determining the limitations of the cell systems currently utilized, ultimately, an accurate scaled CL_H is needed for new chemical entities and first-in-human dose predictions. Hepatic clearance is directly related to other pharmacokinetic parameters including half-life, bioavailability, and exposure, which drive the dosing regimen and efficacy/toxicity profiles of potential compounds. Here we explore the accuracy of hepatic clearance predictions across extraction ratio ranges to determine where the most improvement is needed.

Materials and Methods

The large database, including human (n=101, hepatocytes; n=83, microsomes) and rat (n=128 hepatocytes; n=71 microsomes) values, which was recently compiled by Wood et al. (17), was utilized for this analysis. Hepatic clearance was calculated using the well-stirred model as follows:

$$CL_H = \frac{Q_H \cdot \left(\frac{f_{u,B}}{f_{u,inc}}\right) \cdot CL_{int}}{Q_H + \left(\frac{f_{u,B}}{f_{u,inc}}\right) \cdot CL_{int}}$$

where Q_H is liver blood flow and $f_{u,B}$ and $f_{u,inc}$ are fraction unbound in the blood and incubation, respectively. Physiologically based scaling factors, not empirical or regression-based factors were used. Details on the values and scaling factors can be found in the original source (17).

The coefficient of determination, R^2, was used to examine the potential of clearance-dependent error. The overall bias in predictions was measured by calculating the average fold error (AFE) and precision was measured with the root mean squared error (RMSE) as follows:

$$AFE=10^{\frac{1}{N}\sum \log\left(\frac{observed}{predicted}\right)}$$

$$RMSE=\sqrt{\frac{1}{N}\sum(predicted-observed)^2}$$

Additionally, the accuracy of predictions was determined based on whether the predictions fell within 2-fold of the true in vivo values, as has been a standard cutoff in previous studies (8,12,36). As was done by Wood et al. (17), an empirical scaling factor (ESF) was calculated to determine the error associated with each prediction:

$$ESF = \frac{observed\ CL_H}{predicted\ CL_H}$$

The data were divided into difference clearance ranges: low extraction ratio (ER) (<30% of liver blood flow (LBF)), intermediate (30-70%), and high (>70%) where LBF was assumed to be 20.7 and 100 ml/min/kg for human and rat, respectively (17).

Results and Discussion

When working with new chemical entities, CL_H is the parameter that would be used for predicting first-in-human doses and deciding whether to move a compound forward. Therefore,

while a compound may have high CL_{int}, which could imply a likely error based on the CL_{int} trend (17,33,34), sizable error may not carry over for CL_H predictions. For instance, considering lorcainide and its human microsome data, its predicted CL_{int} is 449 vs. its observed value of 2559 ml/min/kg leads to a 5.7 fold difference (17). However, when actually developing this compound, its predicted CL_H would have been 16.3, a value only 1.2 fold off from its 20.0 ml/min/kg observed CL_H. Table 4.1 highlights different in vivo CL_{int} ranges and the number of these compounds in each in vivo CL_H ER range. Given that not all low CL_{int} compounds have low in vivo CL_H for instance, it is crucial to examine potential CL_H dependent trends too.

When visually examining in vivo CL_H vs. ESF in Figure 4.1, a clearance-dependent trend does not strongly appear and the R^2 values are very low. However, this is expected as any clearance dependency would be suppressed due to the blood flow limitation at higher CL. Despite the potential suppression, the AFE moderately increased from low to high ER in all cases, with the largest AFEs for the human and rat hepatocyte data (Table 4.2). The lower number of high ER drugs particularly for rats should be noted though. The larger RMSE values for the rat data could be attributed to the higher CL range for the species, and the larger RMSE values noted in every case for the high ER drugs could be due to fewer compounds in this range.

Table 4.1: Observed CL_{int} ranges and the number of compounds with observed low/intermediate/high ERs within those ranges.

	Human Hep.			Human Mic.			Rat Hep.			Rat Mic.		
CL_{int} (ml/min/kg)	**Low ER**	**Inter ER**	**High ER**	**Low ER**	**Inter ER**	**High ER**	**Low ER**	**Inter ER**	**High ER**	**Low ER**	**Inter ER**	**High ER**
<10-100	45	7	1	34	3	0	13	2	0	10	1	0
100-1000	10	19	11	7	16	11	43	23	1	25	8	1
1000->10,000	0	2	6	0	4	8	13	25	8	5	14	7

Table 4.2: The AFE and RMSE for human and rat hepatocytes and microsomes according to level of observed CL_H.

	Human Hepatocytes			Human Microsomes			Rat Hepatocytes			Rat Microsomes		
CL_H (ml/min/kg)	**AFE**	**n**	**RMSE**	**AFE**	**n**	**RMSE**	**AFE**	**n**	**RMSE**	**AFE**	**n**	**RMSE**
All	2.7	101	6.6	2.0	83	6.4	3.8	128	28	2.2	71	29
Low ER	**2.1**	**55**	**2.9**	**1.3**	**41**	**3.0**	**3.6**	**69**	**8.8**	**2.0**	**40**	**16**
Intermediate ER	**3.2**	**28**	**6.7**	**2.7**	**23**	**6.6**	**3.9**	**50**	**35**	**2.2**	**23**	**35**
High ER	**4.8**	**18**	**12**	**2.9**	**19**	**10**	**5.3**	**9**	**61**	**3.8**	**8**	**51**

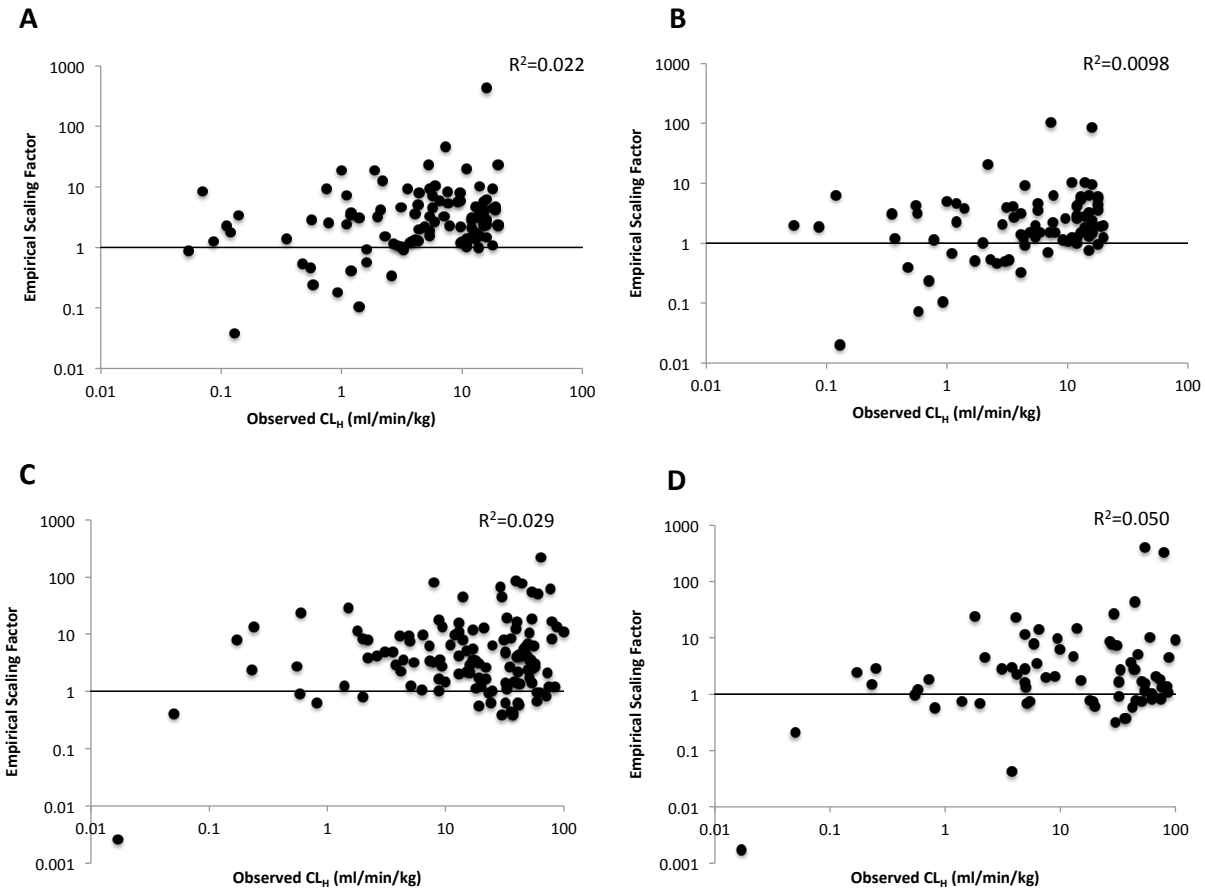

Figure 4.1: The relationship between ESF (ratio of observed to predicted hepatic clearance) and observed in vivo CL_H for hepatocytes (A and C) and microsomes (B and D) in human (A and B) and rat (C and D).

The percentage of predictions falling within two-fold of observed data was generally consistent between ranges (Fig. 4.2) and surprisingly slightly increased across ER ranges in every system except human hepatocytes (Table 4.3). There were more underpredictions than overpredictions or accurate predictions in almost every case. While there appears to be consistent percentage accuracy between ER ranges, examining human microsome data for promethazine as an example, it has an accurate (within-two fold) in vitro prediction of 9.4 vs. the observed 16, but the prediction would be deemed an intermediate, not high ER compound.

Correct determination of extraction ratio is crucial to understand if a compound will be sensitive to changes in protein binding, blood flow, and/or intrinsic clearance (37).

When examining the classification accuracy across ER ranges, similar trends were seen with both human and rat microsomes and hepatocytes (Table 4.4). The great majority of low ER drugs, >90% in all cases, were accurately predicted to be low ER drugs. However, the majority of intermediate and high ER drugs were also predicted to be low ER drugs. High ER drugs had the poorest accuracy, with ≤25% of high ER drugs predicted to have a high ER.

The predictions in Table 4.4 were made assuming the well-stirred model. Since it is generally believed that high ER drugs are better described by the dispersion and parallel tube models and it is known that for these latter models predicted ER values will always be greater than those predicted values from the well-stirred model (15), we also did the calculations for the human hepatocyte data using the parallel tube model. In essence, there is no improvement seen in Table 4.4 for human hepatocytes. One observed low ER drug is now predicted to be high ER; one observed intermediate drug is now predicted to be high ER; and two observed high ER drugs predicted to be low ER with the well-stirred model are now predicted to be intermediate ER.

Determining the mechanisms behind the likely multifactorial IVIVE error is crucial for moving the field forward and improving the efficiency of the drug discovery and development process. While several reasons have been proposed over the years and new technologies are being created to help combat extrinsic issues such cell viability and enzyme activity loss, systematic underprediction still remains. One phenomenon recently focused upon is CL_{int}-dependent underprediction, highlighting the limitations of current in vitro systems. When applying these generated in vitro values during drug development though, CL_H is the parameter that must be estimated. Here we show a similar trend of CL_H-dependent underprediction. This

underprediction could be due to the CL_{int} error previously noted, errors in protein binding measurements or the understanding of protein binding if protein-facilitated uptake is occurring (38), or yet to be discovered mechanisms. The majority of high ER drugs are not predicted to have high or even intermediate ERs, highlighting a need for improved prediction methodologies especially in this range.

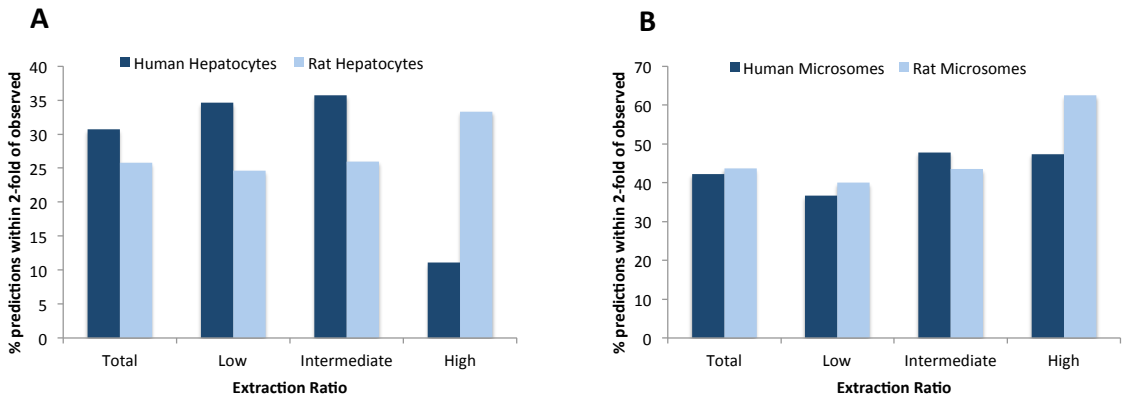

Figure 4.2: The percentage of in vitro predictions falling within two-fold of observed in vivo values grouped by extraction ratio for hepatocytes (A) and microsomes (B).

Table 4.3: The percentage of predictions falling within two-fold, below, and above for the Wood et al. (17) datasets grouped by CL_H range.

	CL_H (ml/min/kg)	All	Low ER	Intermediate ER	High ER
Human Hepatocytes	**% within 2-fold (n)**	**30.7 (31)**	**34.6 (19)**	**35.7 (10)**	**11.1 (2)**
	% below (n)	62.4 (63)	52.7 (29)	64.3 (18)	88.9 (16)
	% above (n)	6.90 (7)	12.7 (7)	0.00 (0)	0.00 (0)
Human Microsomes	**% within 2-fold (n)**	**42.2 (35)**	**36.6 (15)**	**47.8 (11)**	**47.4 (9)**
	% below (n)	48.2 (40)	43.9 (18)	52.2 (12)	52.6 (10)
	% above (n)	9.60 (8)	19.5 (8)	0.00 (0)	0.00 (0)
Rat Hepatocytes	**% within 2-fold (n)**	**25.8 (33)**	**24.6 (17)**	**26.0 (13)**	**33.3 (3)**
	% below (n)	69.5 (89)	72.5 (50)	66.0 (33)	66.7 (6)
	% above (n)	4.70 (6)	2.90 (2)	8.00 (4)	0.00 (0)
Rat Microsomes	**% within 2-fold (n)**	**43.7 (31)**	**40.0 (16)**	**43.5 (10)**	**62.5 (5)**
	% below (n)	47.9 (34)	52.5 (21)	43.5 (10)	37.5 (3)
	% above (n)	8.40 (6)	7.50 (3)	13.0 (3)	0.00 (0)

Table 4.4: The number of compounds (%) in each extraction ratio range that have correct classifications.

Human Hepatocytes		Predicted to be Low ER	Predicted to be Intermediate ER	Predicted to be High ER
Well-stirred model	**Observed Low ER**	53 (96.4%)	2 (3.6%)	0 (0.0%)
	Observed Intermediate ER	18 (64.3%)	10 (35.7%)	0 (0.0%)
	Observed High ER	12 (66.7%)	5 (27.8%)	1 (5.5%)
Parallel tube model	**Observed Low ER**	53 (96.4%)	1 (1.8%)	1 (1.8%)
	Observed Intermediate ER	17 (60.7%)	10 (35.7%)	1 (3.6%)
	Observed High ER	10 (55.6%)	7 (38.9%)	1 (5.5%)
Human Microsomes				
Well-stirred model	**Observed Low ER**	37 (90.2%)	4 (9.8%)	0 (0.0%)
	Observed Intermediate ER	14 (60.9%)	9 (39.1%)	0 (0.0%)
	Observed High ER	8 (42.1%)	8 (42.1%)	3 (15.8%)
Rat Hepatocytes				
Well-stirred model	**Observed Low ER**	67 (97.1%)	2 (2.9%)	0 (0.0%)
	Observed Intermediate ER	37 (74.0%)	7 (14.0%)	6 (12.0%)
	Observed High ER	5 (55.6%)	2 (22.2%)	2 (22.2%)
Rat Microsomes				
Well-stirred model	**Observed Low ER**	38 (95.0%)	1 (2.5%)	1 (2.5%)
	Observed Intermediate ER	10 (43.5%)	8 (34.8%)	5 (21.7%)
	Observed High ER	3 (37.5%)	3 (37.5%)	2 (25.0%)

References

(1) Hay M, Thomas DW, Craighead JL, Economides C and Rosenthal J (2014) Clinical development success rates for investigational drugs. *Nat Biotechnol* **32:**40-51.

(2) Zuegge J, Schneider G, Coassolo P and Lavé T (2001) Prediction of hepatic metabolic clearance: comparison and assessment of prediction models. *Clin Pharmacokinet* **40:**553-563.

(3) Huh Y, Smith DE and Feng MR (2011) Interspecies scaling and prediction of human clearance: comparison of small- and macro-molecule drugs. *Xenobiotica* **41:**972-987.

(4) Lau YY, Sapidou E, Cui X, White RE and Cheng K-C (2002) Development of a novel in vitro model to predict hepatic clearance using fresh, cryopreserved, and sandwich-cultured hepatocytes. *Drug Metab Dispos* **30:**1446-1454.

(5) Naritomi Y, Terashita S, Kagayama A and Sugiyama Y (2003) Utility of hepatocytes in predicting drug metabolism: comparison of hepatic intrinsic clearance in rats and humans in vivo and in vitro. *Drug Metab Dispos* **31:**580-588.

(6) Ito K and Houston JB (2004) Comparison of the use of liver models for predicting drug clearance using in vitro kinetic data from hepatic microsomes and isolated hepatocytes. *Pharm Res* **21:**785-792.

(7) Obach RS (1999) Prediction of human clearance of twenty-nine drugs from hepatic microsomal intrinsic clearance data: an examination of in vitro half-life approach and nonspecific binding to microsomes. *Drug Metab Dispos* **27:**1350-1359.

(8) McGinnity DF, Soars MG, Urbanowicz RA and Riley RJ (2004) Evaluation of fresh and cryopreserved hepatocytes as in vitro drug metabolism tools for the prediction of metabolic clearance. *Drug Metab Dispos* **32:**1247-1253.

(9) Brown HS, Griffin M and Houston JB (2007) Evaluation of cryopreserved human hepatocytes as an alternative in vitro system to microsomes for the prediction of metabolic clearance. *Drug Metab Dispos* **35:**293-301.

(10) Sohlenius-Sternbeck A-K, Afzelius L, Prusis AP, Neelissen J, Hoogstraate J, Johansson J, Floby E, Bengtsson A, Gissberg O, Sternbeck J and Petersson C (2010) Evaluation of the human prediction of clearance from hepatocyte and microsome intrinsic clearance for 52 drug compounds. *Xenobiotica* **40:**637-649.

(11) Akabane T, Gerst N, Masters JN and Tamura K (2012) A quantitative approach to hepatic clearance prediction of metabolism by aldehyde oxidase using custom pooled hepatocytes. *Xenobiotica* **42:**863-871.

(12) Houston JB and Carlile DJ (1997) Prediction of hepatic clearance from microsomes, hepatocytes, and liver slices. *Drug Metab Rev* **29:**891-922.

(13) Lu C, Li P, Gallegos R, Uttamsingh V, Xia CQ, Miwa GT, Balani SK and Gan LS (2006) Comparison of intrinsic clearance in liver microsomes and hepatocytes from rats and humans: evaluation of free fraction and uptake in hepatocytes. *Drug Metab Dispos* **34:**1600-1605.

(14) Di L, Keefer C, Scott DO, Strelevitz TJ, Chang G, Bi Y-A, Lai Y, Duckworth J, Fenner K, Troutman MD and Obach RS (2012) Mechanistic insights from comparing intrinsic clearance values between human liver microsomes and hepatocytes to guide drug design. *Eur J Med Chem* **57:**441-448.

(15) Chiba M, Ishii Y and Sugiyama Y (2009) Prediction of hepatic clearance from in vitro data for successful drug development. *AAPS J* **11:**262-276.

(16) Bowman CM and Benet LZ (2016) Hepatic clearance predictions from in vitro-in vivo extrapolation and the biopharmaceuitcs drug disposition classification system. *Drug Metab Dispos* **44:**1731-1735.

(17) Wood FL, Houston JB and Hallifax D (2017) Clearance prediction methodology needs fundamental improvement: trends common to rat and human hepatocytes/microsomes and implications for experimental methodology. *Drug Metab Dispos* **45:**1178-1188.

(18) Floby E, Johansson J, Hoogstraate J, Hewitt NJ, Hill J and Sohlenius-Sternbeck A-K (2009) Comparison of intrinsic metabolic clearance in fresh and cryopreserved human hepatocytes. *Xenobiotica* **39:**656-662.

(19) Fisher RL, Gandolfi AJ and Brendel K. (2001) Human liver quality is a dominant factor in the outcome of in vitro studies. *Cell Biol Toxicol* **17:**179-189.

(20) Riley RJ, McGinnity DF and Austin RP (2005) A unified model for predicting human hepatic metabolic clearance from in vitro intrinsic clearance data in hepatocytes and microsomes. *Drug Metab Dispos* **33:**1304-1311.

(21) Kochansky CJ, McMasters DR, Lu P, Koeplinger KA, Kerr HH, Shou M and Korzekwa KR (2008) Impact of pH on plasma protein binding in equilibrium dialysis. *Mol Pharm* **5:**438-448.

(22) Zamek-Gliszczynski MJ, Ruterbories KJ, Ajamie RT, Wickremsinhe ER, Pothuri L, Rao MVS, Basavanakatti VN, Pinjari J, Ramanathan VK and Chaudhary AK (2011). Validation of 96-well equilibrium dialysis with non-radiolabeled drug for definitive measurement of protein binding and application to clinical development of highly-bound drugs. *J Pharm Sci* **100:**2498-2507.

(23) Rowland A, Gaganis P, Elliot DJ, Mackenzie PI, Knights KM and Miners JO (2007) Binding of inhibitory fatty acids is responsible for the enhancement of UDP-glucuronosyltransferase 2B7 activity by albumin: implications for in vitro-in vivo extrapolation. *J Pharmacol Exp Ther* **321:**137-147.

(24) Rowland A, Elliot DJ, Knights KM, Mackenzie PI and Miners JO (2008) The "albumin effect": and in vitro-in vivo extrapolation: sequestration of long-chain unsaturated fatty acids enhances phenytoin hydroxylation by human liver microsomal and recombinant cytochrome P450 2C9. *Drug Metab Dispos* **36:**870-877.

(25) De Kanter R, Monshouwer M, Draaisma AL, De Jager MH, de Graaf IA, Proost JH, Meijer DK and Groothuis GM (2004) Prediction of whole-body metabolic clearance of drugs through the combined use of slices from rat liver, lung, kidney, small intestine and colon. *Xenobiotica* **34:**229-241.

(26) Camenisch G and Umehara K (2012) Predicting human hepatic clearance from in vitro drug metabolism and transport data: a scientific and pharmaceutical perspective for assessing drug-drug interactions. *Biopharm Drug Dispos* **33:**179-194.

(27) Stringer R, Nicklin PL and Houston JB (2008) Reliability of human cryopreserved hepatocytes and liver microsomes as in vitro systems to predict metabolic clearance. *Xenobiotica* **38:**1313-1329.

(28) Di L and Obach RS (2015) Addressing the challenges of low clearance in drug research. *AAPS J* **17:**352-357.

(29) Di L, Trapa P, Obach RS, Atkinson K, Bi Y-A, Wolford AC, Tan B, McDonald TS, Lai Y and Tremaine LM (2012) A novel relay method for determining low-clearance values. *Drug Metab Dispos* **40:**1860-1865.

(30) Di L, Atkinson K, Orozco CC, Funk C, Zhang H, McDonald TS, Tan B, Lin J, Chang C and Obach RS (2013) In vitro-in vivo correlation for low-clearance compounds using hepatocyte relay method. *Drug Metab Dispos* **41:**2018-2023.

(31) Novik E, Maguire TJ, Chao P, Cheng KC and Yarmush ML (2010) A microfluidic hepatic coculture platform for cell-based drug metabolism studies. *Biochem Pharmacol* **79:**1036-1044.

(32) Chan TS, Yu H, Moore A, Khetani SR and Tweedie D (2013) Meeting the challenge of predicting hepatic clearance of compounds slowly metabolized by cytochrome p450 using a novel hepatocyte model, Hepatopac. *Drug Metab Dispos* **41:**2024-2032.

(33) Hallifax D, Foster JA and Houston JB (2010). Prediction of human metabolic clearance from in vitro systems: retrospective analysis and prospective view. *Pharm Res* **27:**2150-2161.

(34) Foster JA, Houston JB and Hallifax D (2011) Comparison of intrinsic clearances in human liver microsomes and suspended hepatocytes from the same donor livers: clearance-dependent relationship and implications for prediction of in vivo clearance. *Xenobiotica* **41:**124-136.

(35) Wood FL, Houston JB and Hallifax D (2018) Importance of the unstirred water layer and hepatocyte membrane integrity in vitro for quantification of intrinsic metabolic clearance. *Drug Metab Dispos* **46:**268-278.

(36) Obach RS, Baxter JG, Liston TE, Silber BM, Jones BC, MacIntyre F, Rance, DJ and Wastall P (1997) The prediction of human pharmacokinetic parameters from preclinical and in vitro metabolism data. *J Pharmacol Exp Ther* **283:**46-58.

(37) Rowland M (1984) Protein binding and drug clearance. *Clin Pharmacokinet* **1:**10-17.

(38) Bowman CM and Benet LZ (2018) An examination of protein binding and protein-facilitated uptake relating to in vitro-in vivo extrapolation. *Eur J Pharm Sci* **123:**502-514.

CHAPTER 5: The Presence of a Transporter-Induced Protein Binding Shift: A New Explanation for Protein-Facilitated Uptake and Improvement for In Vitro-In Vivo Extrapolation*

Abstract

Accurately predicting hepatic clearance is an integral part of the drug development process, and yet current in vitro to in vivo extrapolation methods yield poor predictions, particularly for highly protein bound transporter substrates. Explanations for error include inaccuracies in protein binding measurements and the lack of recognition of protein-facilitated uptake, where both unbound and bound drug may be cleared, violating the principles of the widely accepted free drug theory. A new explanation for protein-facilitated uptake is proposed here, called a transporter-induced protein binding shift. High affinity binding to cell membrane proteins may change the equilibrium of the nonspecific binding between drugs and plasma proteins, leading to greater cellular uptake and clearance than currently predicted. The uptake of two lower protein binding OATP substrates (pravastatin and rosuvastatin) and two higher binding substrates (atorvastatin and pitavastatin) were measured in rat hepatocytes in incubations with protein-free buffer vs. 100% plasma. Decreased $K_{m,u}$ values and increased CL_{int} values were seen in the plasma incubations for the highly bound compounds, supporting the new hypothesis and mitigating the IVIVE underprediction previously seen for highly bound transporter substrates.

*Modified from the publication: Bowman CM, Okochi H and Benet LZ (2019) The presence of a transporter-induced protein binding shift: a new explanation for protein-facilitated uptake and improvement for in vitro-in vivo extrapolation. *Drug Metab Dispos* **47:**358-363.

Introduction

Accurately predicting fundamental pharmacokinetic properties such as clearance is crucial when trying to improve the lengthy and expensive drug discovery and development process (1). Hepatic clearance, which is associated with hepatic bioavailability after oral dosing, and elimination from the systemic circulation, is used both early in discovery for rank ordering compounds and later in development for determining first-in-human doses. While in vitro - in vivo extrapolation (IVIVE) for clearance predictions is commonly utilized, large errors have been found when using human or rat microsomes or hepatocytes (2, 3). Furthermore, predictions are thought to be poorest for compounds that are highly protein-bound and substrates of transporters (4).

Traditionally intrinsic clearance (CL_{int}) is measured in protein-free buffer, and after applying physiologically based scaling factors, a model of hepatic disposition such as the well-stirred model is used to predict hepatic clearance (CL_H). In vitro methods such as equilibrium dialysis, ultrafiltration, and ultracentrifugation (5) are separately used to determine the equilibrium fraction of unbound drug (f_u), which according to free drug theory (FDT) is what is available for metabolism (6) and a parameter also included in the well-stirred model. However, there is still a lack of confidence in measured f_u values as is reflected in recent drug-drug interaction guidelines stating that the lower limit should be 0.01 regardless of actual measured values (7). To try to reduce the uncertainty introduced with separately measuring f_u, groups started using plasma in incubations (8, 9).

These investigations with plasma led to decreased $K_{m,u}$ and increased CL_{int} values compared to those generated in protein-free buffer (10, 11), supporting the concept of protein-facilitated uptake, where highly bound ligands have more efficient hepatic uptake than can be

accounted for by solely their unbound concentrations (12-15). The hypotheses proposed to explain how bound concentrations may also be involved were recently reviewed (16, 17) and include the presence of a specific albumin receptor on the hepatocyte cell surface, the rate-limiting dissociation of ligand from the protein-ligand complex, the rate-limiting diffusion of ligand through the unstirred water layer, and interactions with the hepatocyte cell surface. Many of these previous hypotheses were suggested before hepatic transporters were recognized, and here a new hypothesis is proposed called a transporter-induced protein binding shift (TIPBS), a term and concept first suggested by Baik and Huang (18).

As the transporter field has evolved, exceptions to the FDT have emerged and it is now known that uptake transporters such as organic anion transporting polypeptides (OATPs) are able to control a drug's access to hepatocytes and can increase the intracellular free concentration significantly above that in plasma (19). With the TIPBS hypothesis, high affinity binding to such transporters may be able to change the equilibrium of the nonspecific binding between a drug and plasma protein. If a highly protein bound drug has a higher affinity for a transporter than for the plasma protein, the transporter may be able to strip the drug directly from the protein before the drug dissociates itself and is at binding equilibrium (Fig. 5.1B). In this case, protein binding would not be limiting the access of these compounds and utilizing f_u values measured at equilibrium in vitro would be inaccurate. Using rat hepatocytes and statins, known OATP1B1 transporter substrates, we show that there is an increase in measured affinity (decrease in unbound K_m ($K_{m,u}$)) for uptake in 100% human plasma vs. protein-free buffer incubations with highly bound drugs, and smaller changes in $K_{m,u}$ values for drugs with low binding for which the transporter-induced shift would not occur.

The TIPBS hypothesis proposed here and alternate previous hypotheses as we recently reviewed (17) have been promulgated in an attempt to explain the observed discordance of protein binding effects from the FTD. These hypotheses are proposed despite the recognition that for a simple donor compartment-receiver compartment diffusion model the permeability surface product for passive diffusion of unbound drug across the membrane should be independent of the presence or absence of plasma protein.

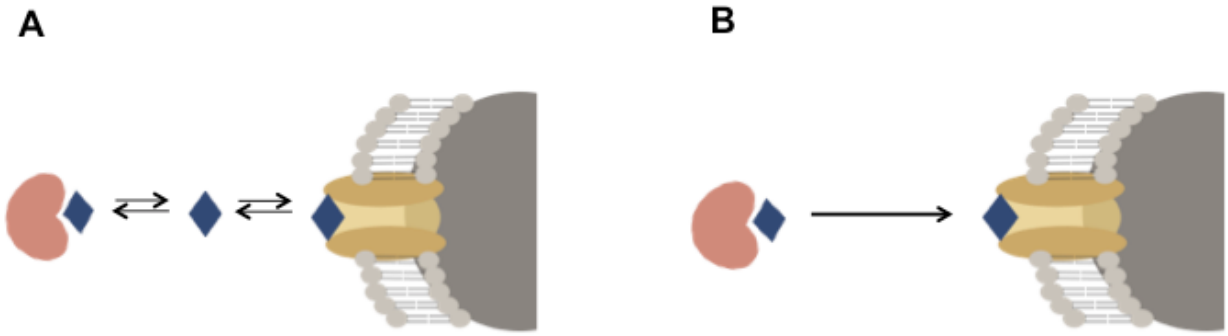

Figure 5.1: Traditional view of protein binding vs. TIPBS. The traditional view of drug dissociating from plasma proteins and being at equilibrium prior to uptake is depicted in (A). The concept of a TIPBS is depicted in (B) where high affinity binding to transporters may strip the drug directly from the proteins before equilibrium is reached.

Materials and Methods

Materials

Atorvastatin was purchased from TCI America (Portland, OR), pitavastatin was purchased from ApexBio (Houston, TX), rosuvastatin was purchased from Toronto Research Chemicals (Ontario, Canada), and [3H(G)] pravastatin sodium salt (specific activity, 5 Ci/mmol) was purchased from American Radiolabeled Compounds (St. Louis, MO). Mixed gender pooled human plasma was purchased from Biological Specialty Corporation. Male Sprague-Dawley rats (250-270 g) were purchased from Charles River Laboratories (Wilmington, MA).

Hepatocyte Isolation

Rat hepatocytes were isolated using a modified collagenase perfusion method as previously described (20, 21). Briefly, the rats were given an intraperitoneal injection of 1 ml/kg ketamine/xylazine (91 mg/ml; 9 mg/ml) before surgery. The portal vein was cannulated with an i.v. catheter (BD Biosciences, San Jose, CA) and perfused with oxygenated liver perfusion medium (Gibco/Thermo Fisher, Waltham, MA) for 10 minutes followed by perfusion with oxygenated liver perfusion medium supplemented with 1.2 U/ml collagenase (Sigma-Aldrich, St. Louis, MO) for 10 min at 20 ml/min. The digested livers were excised and broken down by gentle tapping with a glass stirring rod. Cells were washed with ice-cold hepatocyte wash medium (Gibco/Thermo Fisher), and centrifuged at 50 x g for 3 minutes. Hepatocytes were separated by 44% percoll (Sigma-Aldrich) in hepatocyte wash medium and centrifuged at 250 x g for 10 minutes at 4^{o}C. Cell viability was determined with the trypan blue exclusion method and cells with viability >90% were used for uptake studies.

Hepatocyte Uptake Studies

Hepatocyte suspensions of either protein-free Krebs-Henseleit buffer (pH 7.4) or 100% plasma were pre-incubated at 37^{o}C in 24 well plates for 10 minutes. Uptake studies were done once for each substrate and condition in triplicate and were initiated by adding various concentrations of drug solutions (1.0-100 μM for atorvastatin; 0.05-100 μM for pitavastatin; 0.1-300 μM for pravastatin; and 0.05-100 μM for rosuvastatin) to the hepatocyte suspensions. After 1 minute for atorvastatin, pitavastatin, and rosuvastatin, and 2 minutes for pravastatin (based on time course results not shown here), reactions were terminated by transferring 0.5 million hepatocytes (1 mL of the shaken mixture of 800 μL of 1 million cells/mL and 800 μL of drug

solution) into a centrifuge tube containing 300 µL of a mixture of mineral and silicone oil (density = 1.015) and centrifuging at 13,000g for 10 seconds. After removing the drug solutions and oil layers by pipetting, the pravastatin cell pellets were resuspended in 200 µL of scintillation cocktail and sonicated to ensure complete cell lysis. Intracellular concentration was measured using a scintillation counter (LS6000TA; Beckman Coulter, Fullerton, CA). For atorvastatin, pitavastatin, and rosuvastatin, cell pellets were resuspended in 200 µL of water and sonicated. Methanol and acetonitrile (ACN) containing internal standard and 3% formic acid were subsequently added to samples (1:1:2; sample:methanol:ACN) to precipitate the protein. After centrifuging at 13,000g for 10 minutes, the supernatants were transferred into HPLC vials for LC-MS/MS analysis. Measuring cold pravastatin uptake with LC-MS/MS was attempted, however two inseparable peaks appeared with the methods.

LC-MS/MS Analysis

All samples were analyzed with a Shimadzu (Carlsbad, CA) HPLC binary pump system coupled to a Sciex (Foster City, CA) API 4000 triple quadrupole tandem mass spectrometer. The TurboIonSpray voltage was set at 5500 V and operated in positive ESI mode. The LC separations were done using a Zorbax (Agilent, Santa Clara, CA) C8 column (3.5 µm, 4.6 x 50 mm) and the mobile phases consisted of water with 10 mM ammonium acetate (mobile phase A) and ACN with 10 mM ammonium acetate (mobile phase B). A gradient elution with a flow rate of 0.7 ml/min was used where 35% B increased linearly to 80% at 3 minutes, at which point it was increased to 95% until 3.75 minutes, and then decreased to 35% and equilibrated until the end of the run at 5 minutes. The following transitions were measured (Q1>Q3): atorvastatin

(559.0 > 440.2), pitavastatin (422.4 > 290.3), rosuvastatin (482.3 > 258.3), and the internal standard tolbutamide (271.1 > 172.1).

To test for potential matrix effects with atorvastatin, pitavastatin, and rosuvastatin, calibration curves were created using stock solutions spiked into protein-free buffer, and spiked into sonicated hepatocytes that had been incubated in protein-free buffer and 100% plasma. Process efficiency (comparison between spiked samples vs. neat solutions) were 95.9-107% for atorvastatin, 101-111% for pitavastatin, and 88.6-108% for rosuvastatin. The matrix effect was considered to be minimal. The lower limits of quantitation were 50 nM, 0.5 nM, and 5 nM for atorvastatin, pitavastatin, and rosuvastatin, respectively, and the average recoveries were 102±7%, 100±3%, and 98.2±7.7%, for atorvastatin, pitavastatin, and rosuvastatin, respectively.

For the calibration curves utilized, stock solutions (minimum six concentrations) were added to protein-free buffer and the same calibration curve was used for the buffer and plasma samples of each compound. The concentration range for atorvastatin was 50-4000 nM ($1/x^2$ weighting, r^2=0.99), for pitavastatin was 0.5-1500 nM ($1/x^2$ weighting, r^2=0.99), and for rosuvastatin was 5-1500 nM (1/x weighting, r^2=0.99). Inter-day precision (percent coefficient variation) were between 5.31% and 10.7% for atorvastatin, between 3.4% and 10.0% for pitavastatin and between 2.41% and 15.3% for rosuvastatin, and inter-day accuracies (percent relative error) were between -4.00% and 2.00% for atorvastatin, between -2.90% and 2.40% for pitavastatin and between -1.20% and 0.67% for rosuvastatin.

Data Analysis

Data analyses were done using GraphPad Prism version 7 (GraphPad Software, La Jolla, CA). The total drug dosing concentrations were corrected to unbound drug concentrations. For

the protein-free buffer incubations, the fraction unbound ($f_{u,p}$) was assumed to be 1 so the unbound concentration was the same as total dosing concentration. For the plasma incubations, $f_{u,p}$ values in the FDA labels were used that were 0.020 for atorvastatin (22); 0.010 for pitavastatin (23); 0.50 for pravastatin (24); 0.12 for rosuvastatin (25).

The kinetic parameters for uptake were estimated by fitting the intracellular concentrations to following equation: $v = (V_{max} \times S)/(K_m + S) + P_{dif} \times S$, where v is the rate of uptake (pmol/min/10^6 cells), V_{max} is the maximum uptake rate (pmol/min/10^6 cells), S is the substrate concentration (μM), K_m is the Michaelis-Menten constant (μM), and P_{dif} is the nonsaturable diffusion constant (μl/min/10^6 cells). The linear portion of the total uptake curve represents the passive diffusion, and the difference between the total uptake and passive diffusion represents the active transport.

Results

The uptake curves for the four known OATP substrates in both incubation conditions are shown in Figure 5.2. As expected, all compounds exhibited both passive diffusion and active uptake. The calculated $K_{m,u}$, V_{max}, $P_{dif,u}$, and CL_{int} values are reported in Table 5.1. The $K_{m,u}$ values generated in the protein-free buffer aligned well with previously reported values in the literature. The values generated in the plasma incubations were similar to those in the buffer for the lower protein binding compounds (9.66 vs. 16.5 μM for pravastatin and 0.995 vs. 4.00 for rosuvastatin). There were much larger $K_{m,u}$ differences for the highly bound compounds where the apparent values were 31.4 and 107 fold lower in the plasma incubations for atorvastatin and pitavastatin, respectively (Fig. 5.3A).

The V_{max} values showed a similar, but less marked trend (Fig. 5.3B). Values generated in the two incubations were similar for pravastatin (2.12 fold different) and rosuvastatin (0.953 fold different), while there were larger decreases in apparent V_{max} in the plasma for atorvastatin (6.07 fold lower) and pitavastatin (15.0 fold lower). These decreases in V_{max} were less than the decreases in $K_{m,u}$, so when CL_{int} ($V_{max}/K_{m,u}$) was examined, there were increases for the higher binding compounds. Figure 3C depicts that as the fraction unbound decreases, the difference in CL_{int} (plasma/buffer) increases.

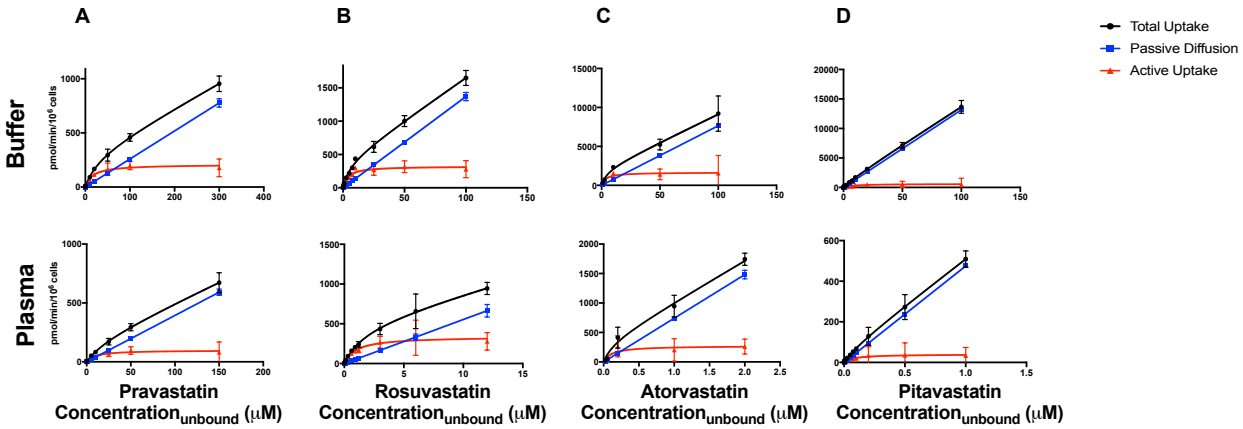

Figure 5.2: Uptake curves for pravastatin (A), rosuvastatin (B), atorvastatin (C), and pitavastatin (D). Total uptake is depicted in circles, passive diffusion is depicted in squares, and active uptake is depicted in triangles. The error bars represent the standard deviation of the triplicate**.**

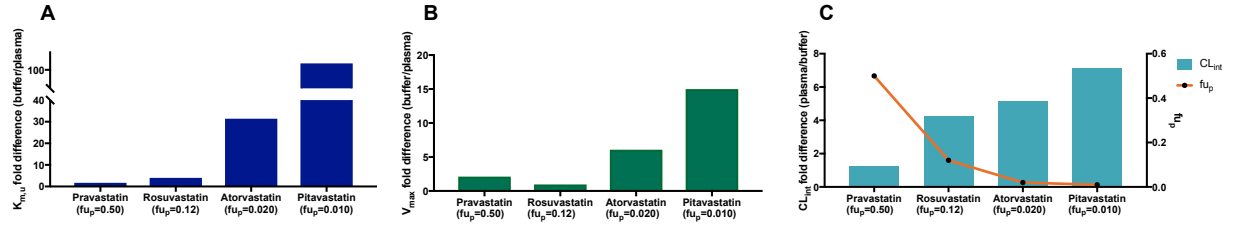

Figure 5.3: The fold difference in $K_{m,u}$ values (buffer/plasma) (A), V_{max} values (buffer/plasma) (B), and CL_{int} values (plasma/buffer) (C) between the two incubations.

Table 5.1: $K_{m,u}$, V_{max}, $P_{dif,u}$, and CL_{int} values generated for each compound in buffer and plasma incubations.

Compound	Incubation	$K_{m,u}$ (µM)	V_{max} (pmol/ min/10^6 cells)	$P_{dif,u}$ (µL/min/10^6 cells)	CL_{int} (µL/min/10^6 cells)	$K_{m,u}$ (µM) Reported in Lit.
Pravastatin	Buffer	16.5 ± 4.43	208 ± 14.3	2.59 ± 0.128	12.6 ± 3.50	16.5[a], 29.1[b], 30.5[c]
	Plasma	9.66 ± 3.27	97.9 ± 8.84	3.94 ± 0.180	10.1 ± 3.55	
	Fold difference	1.71	2.12	0.657	1.25	
Rosuvastatin	Buffer	4.00 ± 0.962	323 ± 20.2	13.7 ± 0.620	80.8 ± 20.1	6.05[c], 9.17[a]
	Plasma	0.995 ± 0.148	339 ± 15.6	55.4 ± 6.60	341 ± 53.0	
	Fold difference	4.02	0.953	0.265	4.22	
Atorvastatin	Buffer	3.61 ± 1.96	1650 ± 203	76.5 ± 1.99	458 ± 254	4.03[c]
	Plasma	0.115 ± 0.116	272 ± 65.5	741 ± 37.1	2370 ± 2450	
	Fold difference	31.4	6.07	0.103	5.16	
Pitavastatin	Buffer	8.71 ± 2.12	600 ± 47.0	132 ± 0.481	68.9 ± 17.6	6.30[c], 26.0[d]
	Plasma	0.0812 ± 0.0157	39.9 ± 2.45	475 ± 1.53	491 ± 99.7	
	Fold difference	107	15.0	0.278	7.13	

[a]Nezasa et al. (50); [b]Yamazaki et al. (51); [c]Yabe et al. (52); [d]Shimada et al. (53)

Discussion

Obtaining accurate in vitro data is crucial for CL_H predictions; however there are often larger errors for compounds that are substrates of transporters (4). A previous study examining the active uptake of seven OATP substrates with sandwich culture human hepatocytes in protein-free incubations found that predictions were poorest for highly protein-bound substrates, while pravastatin and rosuvastatin, compounds with the lowest protein-binding, gave more accurate predictions (26).

Considering this trend, we propose the idea of a transporter-induced protein binding shift, where high affinity binding to transporters may strip ligands directly from plasma proteins before they dissociate. For OATP substrates with lower protein binding such as pravastatin and rosuvastatin, where there is already free drug near the uptake transporters, such a shift may not occur, and current methodologies may yield accurate IVIVE predictions. However for transporter substrates with high binding such as pitavastatin and atorvastatin where TIPBS would occur, current equilibrium protein binding measurements may be driving the high IVIVE error.

Here, the uptake of four statins, known to be OATP substrates (27), were measured in rat hepatocytes with protein-free buffer and 100% human plasma. Given the well-known human $f_{u,p}$ values for these compounds, 100% human plasma was utilized. With the frequent similarity between human and rat $f_{u,p}$ values (28, 29), similar results would be expected if 100% rat plasma were utilized. For the low binding compounds, pravastatin and rosuvastatin, $K_{m,u}$ values were similar between the two incubations (1.71 and 4.02 fold different respectively), while the difference in the values increased with increased protein binding for atorvastatin and pitavastatin (31.4 and 107 fold different respectively). If protein-binding is not limiting the uptake of atorvastatin and pitavastatin, a lower apparent $K_{m,u}$ value (or increased affinity) would be

expected when adding plasma to hepatocyte incubations as compared to using protein-free buffer. TIPBS can be viewed mechanistically, perhaps considering the competing processes as competitive inhibition (Fig. 5.4). The traditional enzyme, substrate, and inhibitor (Fig. 5.4A) are swapped out for drug, transporter, and protein (Fig. 5.4B), where according to FDT, the protein would be "inhibiting" the access of the drug to the transporter. With TIPBS and the non-inhibitory protein, a larger k_1 is expected, resulting in decreased $K_{m,u}$ values.

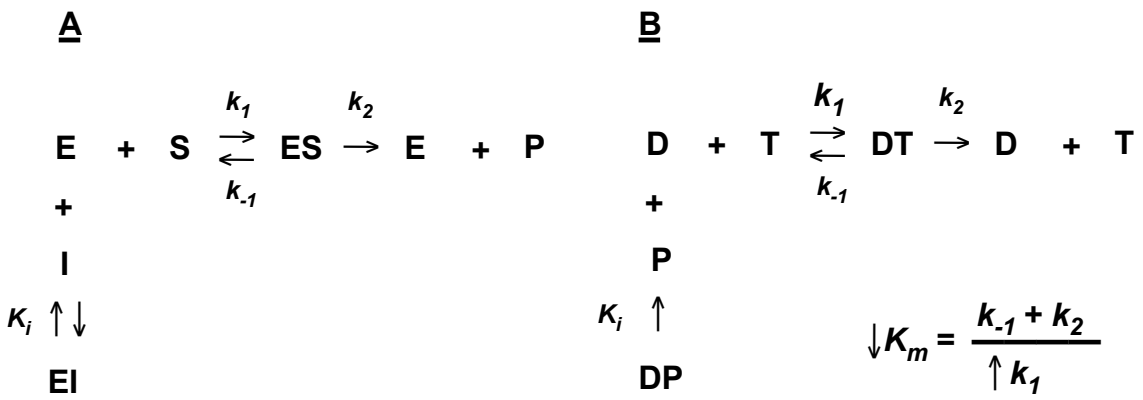

Figure 5.4: TIPBS and competitive inhibition. A traditional schematic of competitive inhibition with enzyme (E), inhibitor (I), substrate (S), and product (P) is shown in (A). A modified version where protein (P) is acting as an inhibitor for drug (D) to access the transporter (T) is shown in (B). With a TIPBS, the transporter will strip the drug from the DP complex, leading to a larger k_1 and lower K_m.

This study also noted greater decreases in V_{max} values for the highly bound compounds. Pravastatin and rosuvastatin had 2.12 and 0.953 fold differences in plasma compared to buffer, while atorvastatin and pitavastatin had 6.07 and 15.0 differences. Despite these larger decreases, $K_{m,u}$ decreases were larger, leading to increased CL_{int} values for atorvastatin and pitavastatin. The TIPBS hypothesis and these larger generated CL_{int} values can explain and mitigate the IVIVE underprediction seen for highly bound transporter substrates. A larger CL_{int} increase would have been expected for atorvastatin given that the 5.16 fold increase is only marginally

larger than the 4.22 fold increase seen with the lower binding rosuvastatin. However, since atorvastatin is the most lipophilic of the four compounds, perhaps the active uptake process is not as crucial and TIPBS should have less of an impact.

Similar protein-facilitated uptake has been previously noted, however alternative hypotheses are frequently cited. The potential role of the hepatocyte cell surface is often considered, in contrast to the role of high affinity transporters described here. One such previous proposal was that ionic interactions between the albumin-drug complex and the hepatocyte plasma membrane may decrease the diffusional distance for unbound ligand (30), while another proposal stated that binding of the albumin-drug complex to the cell surface may lead to a conformational change in albumin enhancing the dissociation of drug (15). However despite citing these alternative hypotheses, recent data in the literature agree with the idea of TIPBS.

Miyauchi et al. (31) examined the uptake of 1-anilino-8-naphthalene sufonate (ANS) in rat hepatocytes with bovine serum albumin and the uptake of pitavastatin in human hepatocytes with HSA. While the addition of protein led to increases in unbound uptake clearances for both compounds, the difference was greater for pitavastatin, which is known to have high affinity for OATP, while ANS has a relatively lower affinity for Oatp. Kim et al. (32) examined the uptake of 11 OATP substrates with varying concentrations of HSA. Similar to the results presented here, there was no change in pravastatin uptake with the addition of HSA, and using their previously proposed facilitated-dissociation kinetic model, the uptake of rosuvastatin with 5% HSA was estimated to increase 2.48 fold. The uptake of the remaining compounds, all with high protein binding, was estimated to increase to a greater extent, up to 63.8 fold with valsartan, with the exception of pitavastatin (a 2.44 fold increase was predicted). Their model predicts the

contribution of albumin-mediated uptake to be similar for both pitavastatin and rosuvastatin (56.9 and 54.4% respectively).

Both papers stated, "the higher the affinity for the transporter, the more effective is the albumin-mediated enhancement," agreeing with the concept of TIPBS. Additional previous support for TIPBS was seen when measuring the uptake of a highly bound new chemical entity, shown to be an OATP1B3 substrate. The CL_{int} increased with increased HSA concentration in transfected HEK293 cells where the mechanisms hypothesized with the hepatocyte cell surface may not be present, but overexpression of the OATP transporter is present (33).

Examining the pitavastatin data, Miyauchi et al. (31) calculated the dissociation constant (K_d) of bound albumin from the hepatocyte cell surface to be 199 ± 61 μM with the facilitated-dissociation model (15) and 275 ± 131 μM with a kinetic model proposed by Forker and Luxon (13). Simultaneously fitting data from 10 OATP substrates including pitavastatin, Kim et al. (32) calculated the value to be 45.2 ± 13.0 μM. Using fluorescence quenching, Shi et al. (34) measured the binding constant of pitavastatin to bovine serum albumin as 0.56 $x10^4$ M^{-1} at 310K and inverting this, the dissociation constant would be 179 μM. Although not directly comparable as K_d is a thermodynamic constant while K_m is a kinetic constant, in this study the measured $K_{m.u}$ values for the interaction between pitavastatin and active uptake transporters were 17.3 μM in buffer and 0.0688 μM in plasma, which are significantly lower than the K_d values for binding to the hepatocyte surface or to protein.

The yet to be explained decrease in V_{max} values in plasma incubations for highly bound compounds has been previously noted. Based on the idea of competitive inhibition with TIPBS (Fig. 5.4B), the V_{max} values were expected to remain the same across incubations and across f_u ranges. As described by Poulin et al. (35) and Bounakta et al. (36), the clearance of bisphenol A

and naproxen were measured using isolated perfused rat livers with and without albumin. Bisphenol A, the higher binding compound had an 83.8 fold decrease in its apparent $K_{m,u}$ value with the albumin addition (compared to the 4.73 fold decrease for the lower binding naproxen) and the V_{max} value of bisphenol A decreased 6.2 fold with albumin (while decreasing 1.3 fold for naproxen) (Table 5.2). A potential explanation could be that a weaker attraction mentioned earlier between the protein-drug complex and the hepatocyte cell surface brings more bound drug near the cell, and once the complex is oriented correctly, the transporter with higher affinity can strip the drug directly from the protein. The additional larger protein-drug complexes near the surface may limit access of both bound and free drug to transporters, decreasing the maximum velocity of substrate transport compared to protein-free incubations.

Table 5.2: Data from Poulin et al. (35) and Bounakta et al. (36) also supporting the trends seen with a TIPBS.

Compound	**$f_{u,p}$**	**K_m (µM) [ALB] = 0 g/L**	**K_m (µM) [ALB] = 30 g/L**	**$K_{m,u} = K_m \cdot f_{u,p}$ [ALB]= 30 g/L**	**$K_{m,u}$ Fold Dif**	**V_{max} (nmol/min/mg) [ALB]= 0 g/L**	**V_{max} (nmol/min/mg) [ALB]= 30 g/L**	**V_{max} Fold Dif**
Bisphenol A	0.045	13.4	3.5	0.16	83.8	8.0	1.3	6.2
Naproxen	0.12	98.9	174.4	20.9	4.73	2.9	2.2	1.3

In summary, the $K_{m,u}$ decrease and $CL_{int,}$ increase for the highly protein bound statins support the idea of a transporter-induced protein binding shift and suggest that plasma should be used in hepatocyte incubations for highly bound transporter substrates. TIPBS can also explain some of the large IVIVE error seen for highly bound compounds. If protein binding is not restricting the access of highly bound transporter substrates, perhaps total concentration, not unbound concentration should be used in clearance predictions, an idea previously applied for

alternate reasons (37, 38). To further support this hypothesis, additional studies are needed to determine the off rate of drug dissociating from plasma protein vs. the on rate of drug associating with the membrane transporters under the two incubation conditions, and studies to differentiate transporter-mediated uptake vs. transporter binding are necessary.

It is important to note that the proposed shift may occur with any type of plasma protein, and may occur anywhere in the body where there is interplay between plasma proteins, cells, and transporters including the intestine and brain. That is, the shift is not specific to only albumin and only hepatocytes. Previous studies have found facilitated uptake with β-lactoglobulin (39, 40) and ligandin (41), as well as with myocytes (42-46), adipocytes (45), proximal tubules (47), perfused kidney (48), and brain (49).

References

(1) Thomas DW, Burns J, Audette J, Carroll A, Dow-Hygelund C and Hay M (2016) Clinical development success rates 2006–2015. *BIO Industry Analysis* 1–16.

(2) Bowman CM and Benet LZ (2016) Hepatic clearance predictions from in vitro-in vivo extrapolation and the Biopharmaceutics Drug Disposition Classification System. *Drug Metab Dispos* **44**:1731-1735.

(3) Wood FL, Houston JB and Hallifax D (2017) Clearance prediction methodology needs fundamental improvement: trends common to rat and human hepatocytes/microsomes and implications for experimental methodology. *Drug Metab Dispos* **45**:1178-1188.

(4) Soars MG, McGinnity DF, Grime K and Riley RJ (2007) The pivotal role of hepatocytes in drug discovery. *Chemico-Biological Interact* **168:**2-15.

(5) Bohnert T and Gan LS (2013) Plasma protein binding: from discovery to development. *J Pharm Sci* **102:**2953-2994.

(6) Trainor GL (2007) The importance of plasma protein binding in drug discovery. *Expert Opin Drug Discov* **2:**51-64.

(7) Di L, Breen C, Chambers R, Eckley ST, Fricke R, Ghosh A, Harradine P, Kalvass JC, Ho S, Lee CA, Marathe P, Perkins EJ, Qian M, Tse S, Yan Z, and Zamek-Gliszczynski MJ (2017) Industry perspective on contemporary protein-binding methodologies: considerations for regulatory drug-drug interaction and related guidelines on highly bound drugs. *J Pharm Sci* **106:**3442-3452.

(8) Shibata Y, Takahashi H and Ishii Y (2000) A convenient in vitro screening method for predicting in vivo drug metabolic clearance using isolated hepatocytes suspended in serum. *Drug Metab Dispos* **28:**1518-1523.

(9) Shibata Y, Takahashi H, Chiba M and Ishii Y (2002) Prediction of hepatic clearance and availability by cryopreserved human hepatocytes: an application of serum incubation method. *Drug Metab Dispos* **30:**892-896.

(10) Blanchard N, Richert L, Notter B, Delobel F, David P, Coassolo P and Lavé T (2004) Impact of serum on clearance predictions obtained from suspensions and primary cultures of rat hepatocytes. *Eur J Pharm Sci* **23:**189-199.

(11) Blanchard N, Hewitt NJ, Silber P, Jones H, Coassolo P and Lavé T (2006) Prediction of hepatic clearance using cryopreserved human hepatocytes: a comparison of serum and serum-free incubations. *J Pharm Pharmacol* **58:**633-641.

(12) Forker EL and Luxon BA (1981) Albumin helps mediate removal of taurocholate by rat liver. *J Clin Invest* **67:**1517-1522.

(13) Forker EL and Luxon BA (1983) Albumin-mediated transport of rose bengal by perfused rat liver. Kinetics of the reaction at the cell surface. *J Clin Invest* **72:**1764-1771.

(14) Weisiger RA and Ma WL (1987) Uptake of oleate from albumin solutions by rat liver. Failure to detect catalysis of the dissociation of oleate from albumin by an albumin receptor. *J Clin Invest* **79:**1070-1077.

(15) Tsao SC, Sugiyama Y, Sawada Y, Iga T and Hanano M (1988) Kinetic analysis of albumin-mediated uptake of warfarin by perfused rat liver. *J Pharmacokinet Biopharm* **16:**165-181.

(16) Poulin P, Burczynski FJ and Haddad S (2016) The role of extracellular binding proteins in the cellular uptake of drugs: impact on quantitative in vitro-to-in vivo extrapolations of toxicity and efficacy in physiologically based pharmacokinetic-pharmacodynamic research. *J Pharm Sci* **105:**497-508.

(17) Bowman CM and Benet LZ (2018) An examination of protein-binding and protein-facilitated uptake relating to in vitro-in vivo extrapolation. *Eur J Pharm Sci* **123:**502-514.

(18) Baik J and Huang Y (2015) Transporter-induced protein binding shift (TIPBS) hypothesis and modeling. *20th North American ISSX Meeting:* abstract

(19) Giacomini KM, Huang SM, Tweedie DJ, Benet LZ, Brouwer KL, Chu X, Dahlin A, Evers R, Fischer V, Hillgren KM, Hoffmaster KA, Ishikawa T, Keppler D, Kim RB, Lee CA, Niemi M, Polli JW, Sugiyama Y, Swaan PW, Ware JA, Wright SH, Yee SW, Zamek-Gliszczynski MJ, and Zhang, L (2010) Membrane transporters in drug development. *Nat Rev Drug Discov* **9:**215-236.

(20) Lam JL and Benet LZ (2004) Hepatic microsome studies are insufficient to characterize in vivo hepatic metabolic clearance and metabolic drug-drug interactions: studies of digoxin metabolism in primary rat hepatocytes versus microsomes. *Drug Metab Dispos* **32:**1311-1316.

(21) Lam JL, Shugarts SB, Okochi H and Benet LZ (2006) Elucidating the effect of final-day dosing of rifampin in induction studies on hepatic drug disposition and metabolism. *J Pharmacol Exp Ther* **319:**864-870.

(22) Lipitor (atorvastatin calcium). [Package insert]. New York, NY: Pfizer; 1996.

(23) Livalo (pitavastatin). [Package insert]. Montgomery, AL: Kowa Pharmaceuticals America, Inc; 2009.

(24) Pravachol (pravastatin sodium). [Package insert]. New York, NY: Bristol-Myers Squibb; 1991.

(25) Crestor (rosuvastatin calcium). [Package insert]. Wilmington, DE: AstraZeneca Pharmaceuticals LP; 2003.

(26) Jones HM, Barton HA, Lai Y, Bi Y, Kimoto E, Kempshall S, Tate SC, El-Kattan A, Houston JB, Galetin A and Fenner KS (2012) Mechanistic pharmacokinetic modeling for the prediction of transporter-mediated disposition in humans from sandwich culture human hepatocyte data. *Drug Metab Dispos* **40:**1007-1017.

(27) Kalliokoski A and Niemi M (2009) Impact of OATP transporters on pharmacokinetics. *Br J Pharmacol* **158:**693-705.

(28) Hosea NA, Collard WT, Cole S, Maurer TS, Fang RX, Jones H, Kakar SM, Nakai Y, Smith BJ, Webster R and Beaumont K (2009) Prediction of human pharmacokinetics from preclinical information: comparative accuracy of quantitative prediction approaches. *J Clin Pharmacol* **49:**513-533.

(29) Colclough N, Ruston L, Wood JM and MacFaul PA (2014) Species differences in drug plasma protein binding. *Med Chem Comm* **5:**963.

(30) Burczynski FJ, Wang GQ, and Hnatowich M (1997) Effect of binding protein surface charge on palmitate uptake by hepatocyte suspensions. *Br J Pharmacol* **120:**1215-1220.

(31) Miyauchi S, Masuda M, Kim S-J, Tanaka Y, Lee K-R, Iwakado S, Nemoto M, Sasaki S, Shimono K, Tanaka Y and Sugiyama Y (2018) The phenomenon of albumin-mediated hepatic uptake of organic anion transport polypeptide substrates: prediction of the in vivo uptake clearance from the in vitro uptake by isolated hepatocytes using a facilitated-dissociation model. *Drug Metab Dispos* **46:**259-267.

(32) Kim S-J, Lee K-R, Miyauchi S and Sugiyama Y (2019) Extrapolation of in vivo hepatic clearance from in vitro uptake clearance by suspended human hepatocytes for anionic drugs with high binding to human albumin: improvement of in vitro-to-in vivo extrapolation by considering the "albumin-mediated" hepatic uptake mechanism on the basis of the 'facilitated-dissociation model". *Drug Metab Dispos* **47:**94-103.

(33) Fukuchi Y, Toshimoto K, Mori T, Kakimoto K, Tobe Y, Sawada T, Asaumi R, Iwata T, Hashimoto Y, Nunoya K-I, Imawaka H, Miyauchi S and Sugiyama Y (2017) Analysis of nonlinear pharmacokinetics of a highly albumin-bound compound: contribution of albumin-mediated hepatic uptake mechanism. *J Pharm Sci* **106:**2704-2714.

(34) Shi JH, Wang Q, Pana DQ, Liu TT and Jiang M (2017) Characterization of interactions of simvastatin, pravastatin, fluvastatin, and pitavastatin with bovine serum albumin: multiple spectroscopic and molecular docking. *J Biomol Struct Dyn* **35:** 1529-1546.

(35) Poulin P, Bteich M and Haddad S (2017) Supplemental analysis of the prediction of hepatic clearance of binary mixtures of bisphenol A and naproxen determined in an isolated perfused rat liver model to promote the understanding of potential albumin-facilitated hepatic uptake mechanism. *J Pharm Sci* **106:**3207-3214.

(36) Bounakta S, Bteich M, Mantha M, Poulin P, and Haddad S (2018) Predictions of bisphenol A hepatic clearance in the isolated perfused rat liver (IRPL): impact of albumin binding and of co-administration with naproxen. *Xenobiotica* **48:**135-147.

(37) Obach RS (1999) Prediction of human clearance of twenty-nine drugs from hepatic microsomal intrinsic clearance data: an examination of in vitro half-life approach and nonspecific binding to microsomes. *Drug Metab Dispos* **27:**1350-1359.

(38) Poulin P, Hop CECA, Ho Q, Halladay JS, Haddad S and Kenny JR (2012) Comparative assessment of in vitro-in vivo extrapolation methods used for predicting hepatic metabolic clearance of drugs. *J Pharm Sci* **101:**4308-4326.

(39) Nunes R, Kiang C-L, Sorrentino D and Berk PD (1988) 'Albumin-receptor' uptake kinetics do not require an intact lobular architecture and are not specific for albumin. *J Hepatol* **7:**293-304.

(40) Burczynski FJ, Moran JB, Cai Z-S, and Forker EL (1990) β-Lactoglobulin enhances the uptake of free palmitate by hepatocyte monolayers: the relative importance of diffusion and facilitated dissociation. *Can J Physiol Pharmacol* **68:**201-206.

(41) Stollman YR, Gärtner U, Theilmann L, Ohmi N and Wolkoff AW (1983) Hepatic bilirubin uptake in the isolated perfused rat liver is not facilitated by albumin binding. *J Clin Invest* **72:**718-723.

(42) Hütter JF, Piper HM and Spieckermann PG (1984) Myocardial fatty acid oxidation: evidence for an albumin-receptor-mediated membrane transfer of fatty acids. *Basic Res Cardiol* **79:**274-282.

(43) Hütter JF, Piper HM and Spieckermann PG (1984) Kinetic analysis of myocardial fatty acid oxidation suggesting an albumin receptor mediated uptake process. *J Mol Cell Cardiol* **16:**219-226.

(44) Rauch B, Bode C, Piper HM, Hütter JF, Zimmermann R, Braunwell E, Hasselbach W and Kübler W (1987) Palmitate uptake in calcium tolerant, adult rat myocardial single cells—evidence for an albumin mediated transport across sarcolemma. *J Mol Cell Cardiol* **19:**159-166.

(45) Sorrentino D, Robinson RB, Kiang C-L and Berk PD (1989) At physiologic albumin/oleate concentrations oleate uptake by isolated hepatocytes, cardiac myocytes, and adipocytes is a saturable function of the unbound oleate concentration. Uptake kinetics are consistent with the conventional theory. *J Clin Invest* **84:**1325-1333.

(46) Elmadhoun B, Wang GQ, Kirshenbaum LA, and Burczynski FJ (2001) Palmitate uptake by neonatal rat myocytes and hepatocytes. Role of extracellular protein. *Eur J Biochem* **268:**3145-3153.

(47) Besseghir K, Mosig D, and Roch-Ramel F (1989) Facilitation by serum albumin of renal tubular secretion of organic anions. *Am J Physiol* **256:**F475-484.

(48) Taft DR and Sweeney KR (1995) The influence of protein binding on the elimination of acetazolamide by the isolated perfused rat kidney: evidence of albumin-mediated tubular secretion. *J Pharmacol Exp Ther* **274:**752-760.

(49) Pardridge WM, Sakiyama R and Fierer G (1983) Transport of propranolol and lidocaine through the rat blood-brain barrier. Primary role of globulin-bound drug. *J Clin Invest* **71:**900-908.

(50) Nezasa K, Higaki K, Takeuchi M, Nakano M and Koike M (2003) Uptake of rosuvastatin by isolated rat hepatocytes: comparison with pravastatin. *Xenobiotica* **33:** 379-388.

(51) Yamazaki M, Suzuki H, Hanano M, Tokui T Komai T, and Sugiyama Y (1993) Na(+)-independent multispecific anion transporter mediates active transport of pravastatin into rat liver. *Am J Physiol* **264:**G36-G44.

(52) Yabe Y, Galetin A and Houston JB (2011) Kinetic characterization of rat hepatic uptake of 16 actively transported drugs. *Drug Metab Dispos* **39:**1808-1814.

(53) Shimada S, Fujino H, Morikawa T, Moriyasu M and Kojima J (2003) Uptake mechanism of pitavastatin, a new inhibitor of HMG-CoA reductase, in rat hepatocytes. *Drug Metab Pharmacokinet* **18:**245-251.

CHAPTER 6: Organic Anion Transporting Polypeptide (OATP) Uptake Predictions in HEK293 Overexpressing Cells In the Presence and Absence of Human Plasma*

Abstract

Generating accurate in vitro data is crucial for in vitro to in vivo extrapolation and pharmacokinetic predictions. The use of HEK293 cells overexpressing OATP1B1 and OATP1B3 in protein-free buffer and 100% human plasma incubations was explored for the uptake of four OATP substrates, pravastatin, rosuvastatin, repaglinide and pitavastatin. Differences were observed for each parameter ($K_{m,u}$, V_{max}, CL_{int}, and $P_{dif,u}$) obtained from the buffer and human plasma incubations in both cells, and in general, the fold differences increased as plasma protein binding increased. The fold change in $K_{m,u}$ values ranged from 2.03-1020, while the fold change in V_{max} values ranged from 1.22-97.4. As a result, the CL_{int} values generated in the plasma incubations were 1.66-51.9 fold higher than the values generated in protein-free buffer in both cells. The unbound passive diffusion was also consistently higher in the human plasma incubations for all four compounds, with a fold difference range of 2.06-38.4. These shifts in the presence and absence of human plasma suggest that plasma proteins may play a role in both the active uptake and passive diffusion processes. The results also support the idea of a transporter-induced protein binding shift, where high protein binding may not limit the uptake of compounds that have high affinity for transporters. The addition of plasma to incubations leading to higher CL_{int} values for transporter substrates helps mitigate the underprediction commonly noted with in vitro to in vivo extrapolation.

* Modified from: Bowman CM, Chen E, Chen L, Liang X, Wright M, Chen Y and Mao J. Organic anion transporting polypeptide (OATP) uptake predictions in HEK293 overexpressing cells in the presence and absence of human plasma. *Manuscript in preparation.*

Introduction

Membrane transporters are known to play a key role in the absorption, distribution, and elimination of drugs as well as be determinants of their safety and efficacy profiles (1). Two such transporters, Organic Anion Transporting Polypeptide (OATP) 1B1 and OATP1B3, are expressed on the sinusoidal membrane of hepatocytes and mediate the uptake of both endogenous substrates as well as numerous drugs, including statins (2).

During the drug discovery and development process, accurate in vitro kinetic characterization of compounds is crucial for predictions of pharmacokinetic behavior using the physiologically based pharmacokinetic (PBPK) approach (3). However, limited understanding of in vitro to in vivo extrapolation (IVIVE) has brought challenges for such predictions with uptake transporter substrates. There are gaps in the field including: 1) how to incorporate the in vitro data generated in various systems (hepatocytes vs. cell lines), 2) how to incorporate different types of in vitro data generated (intrinsic clearance (CL_{int}) from substrate depletion studies (where the loss of compound from the incubation media into microsomes/hepatocytes is measured) vs. V_{max}/K_m from more robust uptake experiments), 3) how to incorporate the transporter expression levels measured in various in vitro systems, and 4) determination if the in vitro systems used are physiologically relevant.

While traditional uptake experiments are conducted in protein-free buffer and there is the assumption that only free drug is available for uptake, in the 1980's several single-pass liver perfusion studies found that highly bound ligands had more efficient hepatic uptake than could be accounted for by just their unbound concentrations (4-7). The hypotheses proposed to explain this protein-facilitated uptake phenomenon were recently reviewed (8, 9) and include the rate-limiting dissociation of ligand from the protein-ligand complex, rate-limiting diffusion of ligand

through the unstirred water layer, interactions with the hepatocyte cell surface, and a transporter-induced protein binding shift. In vitro investigations have also found more accurate predictions when using plasma in incubations to account for protein-facilitated uptake (10-12). In a recent study, incorporating kinetic uptake data generated using plateable human hepatocytes with human plasma for the OATP substrate pravastatin enabled the PBPK model to simulate the intravenous and oral pharmacokinetic (PK) profiles of the drug successfully without incorporating a scaling factor (12). This demonstrated an approach to translate in vitro OATP uptake transporter data to in vivo, with a hope of utilizing future in vitro data for accurate human PK predictions.

As a continuing effort to understand the translation of in vitro data to in vivo and the plasma effect with uptake transporters, the use of human embryonic kidney (HEK) 293 cells transfected with OATP1B1 and OATP1B3 was explored in the current investigation. These cells were chosen for two reasons: 1) While HEK293 cells are the typical cell lines used in the drug discovery stage serving as an economical option to qualitatively address if a new chemical entity is a substrate for OATPs, there is an IVIVE gap for quantitative translation. 2) Given that any protein-facilitated uptake noted with HEK293 cells could not be due to interactions with the hepatocyte cell surface, the system serves a tool to assess the various hypotheses mentioned above. The objective of this study was to evaluate the uptake of known OATP substrates, with both low and high protein binding, in HEK293 cells transfected with OATP1B1 and OATP1B3 in buffer and human plasma incubations.

Materials and Methods

Materials

Pitavastatin calcium and repaglinide were purchased from Abcam (Cambridge, UK); pravastatin sodium was purchased from TCI America (Portland, OR); and rosuvastatin was purchased from BioVision Inc. (Milpitas, CA). Corning TransportoCells™ Cryopreserved SLC Transporter Cells (human OATP1B1*1a (lot 6034125), OATP1B3 (lot 5278015), and control cells (lot 6075312) were purchased (Corning, NY) and used for uptake studies. Human Plasma Medium-A (100% human plasma) (HPZ-A™) and Hepatocyte Rinse Medium (HRM™) were purchased from In Vitro ADMET Laboratories, Inc. (IVAL, Columbia, MD). Poly-D-lysine coated 96 well plates were purchased from Greiner Bio-One (Monroe, NC). Fetal bovine serum was purchased from VWR (Radnor, PA) and all other cell culture reagents were purchased from Thermo Fisher Scientific (Waltham, MA).

Uptake in OATP1B1-and OATP1B3-Overexpressing Cells

Uptake studies were performed in triplicate following the TransportoCells™ manual. Briefly, after thawing, cells were seeded onto poly-D-lysine coated 96-well plates with a seeding density of 100,000 cells per well in plating media consisting of DMEM (high glucose) with MEM non-essential amino acid solution (100X) and fetal bovine serum. After incubation in a humidified atmosphere with 5% CO_2 at 37^{o}C for 3 hours, the cells were re-fed with plating media supplemented with 2mM sodium butyrate. Uptake experiments were initiated 24 hours after plating.

To begin uptake experiments, plating media was removed from the cells, and cells were washed once with either HBSS buffer (with 10 mM HEPES, pH 7.4) or human plasma. Drug

solutions of either protein-free HBSS buffer or human plasma were added for one minute. The incubation time of one minute was selected based on time course experiment results for both medium conditions (results not shown). For studies in buffer, uptake was terminated by removing the dosing solution and washing cells twice with ice-cold PBS. For studies in plasma, uptake was terminated similarly, but by washing three times with ice-cold Hepatocyte Rinse Medium. The following concentrations were tested in both cells with buffer and plasma: 200, 100, 50, 25, 12.5, 6.25, 3.13 μM for pravastatin; 1.25, 0.625, 0.3125, 0.156, 0.0781, 0.0391 μM for repaglinide; and 50, 25, 12.5, 6.25, 3.13, 1.56, 0.781 for rosuvastatin. For pitavastatin, 10, 5, 2.5, 1.25, 0.625, 0.313, 0.156, 0.0781 μM concentrations were tested under both conditions, however biphasic kinetics were seen after 2.5 μM in plasma, so calculations were based on 2.5, 1.25, 0.625, 0.313, 0.156, 0.0781 μM concentrations for the plasma incubations.

The viability of the cells in buffer and human plasma was determined with a Nexcelom GigaCyte Cellometer Hepatometer. The amount of protein in each well was determined using the Pierce™ BCA® Protein Assay Kit (Thermo Fisher Scientific, Waltham, MA).

Bioanalyical Method

To measure the analyte concentrations, incubation samples were mixed with 80:20 acetonitrile:water containing propranolol as an internal standard, sonicated and then centrifuged. The supernatant was mixed with 50% water and bioanalytical assays were developed to obtain analyte concentrations.

All samples were analyzed with a Shimadzu Nexera X2 (LC-30AD) (Kyoto, Japan) coupled to a Sciex 6500 QTRAP mass spectrometer (Foster City, CA). Pitavastatin, repaglinide, and rosuvastatin were analyzed in positive ion mode with propranolol (260.0/116.1) as an

internal standard, and pravastatin was analyzed in negative ion mode with probenecid (284.0/139.0) as an internal standard. The LC separations were performed using a Kinetex C18 column (2.6 µm, 30 x 2.1mm) (Phenomenex, Torrance, CA). The mobile phases consisted of water with 0.1% formic acid (mobile phase A) and acetonitrile with 0.1% formic acid (mobile phase B). Additional details about the methods can be found in Table 6.1.

Table 6.1: LC-MS/MS methods for the four OATP substrates and the internal standards used

Analyte	ESI	Q1/Q3 Transition (m/z ratio)	Gradient Profile (min[%B]) Flow Rate (1.0 mL/min)	Declustering Potential	Collision Energy	Collision Cell Exit Potential	Lower and Upper Limits of Quantification
Pitavastatin	+	422.2 / 274.2	Gradient: 0.10[5%]-0.40[5%]-1.30[85%]-1.60[85%]-1.61[5%]-2.00[5%]	88.0	65.0	12.0	0.376nM, 114 nM
Repaglinide	+	453.2 / 230.2	Gradient: 0.10[5%]-0.40[5%]-1.30[85%]-1.60[85%]-1.61[5%]-2.00[5%]	66.0	35.0	18.0	0.0610nM, 250nM
Rosuvastatin	+	482.3 / 258.3	Gradient: 0.40[10%]-1.19[90%]-1.60[90%]-1.61[10%]-2.00[10%]	125	45.0	10.0	0.977nM, 1000nM
Pravastatin	-	423.1 / 303.0	Gradient: 0.10[10%]-1.00[80%]-1.40[80%]-1.41[10%]-1.80[10%]	-175	-22.0	-17.0	1.95nM, 1000nM

Modeling of the Active Hepatic Uptake Transporter Kinetic Parameters and Passive Diffusion

Data analysis was done using GraphPad Prism version 7 (GraphPad Software, La Jolla, CA). Nominal concentrations were used for the plots. Uptake curves from the control cells, representing passive diffusion only, were fit linearly to determine the unbound passive diffusion ($P_{dif,u} = P_{dif,} \bullet f_{u,p}$). The difference between uptake in the transfected cells (active + passive uptake) and uptake the control cells (passive uptake) was plotted, representing the active uptake alone and this curve was used to obtain the unbound K_m ($K_{m,u} = K_m \bullet f_{u,p}$) and V_{max} values assuming Michaelis-Menten kinetics. For the protein-free buffer incubations, the fraction unbound ($f_{u,p}$) was assumed to be 1 and for the plasma incubations, $f_{u,p}$ values in the literature were used which were 0.485 for pravastatin (Simcyp V17 compound profile, 3, 13, 14), 0.107 for rosuvastatin (Simcyp V17 compound profile, 15, 16), 0.0188 for repaglinide (Simcyp V17 compound profile, 16-18), and 0.00450 for pitavastatin (19). While there can be variability in reported literature $f_{u,p}$ values, leading to shifts in the exact fold differences between buffer vs. plasma incubation values, the overall trends still hold.

Results

First the morphology and viability of the cells were tested in 100% human plasma vs. protein-free buffer. While cellular clumping visually appeared to occur during the plasma incubations (Fig. 6.1), the viability of both OATP1B1 and 1B3 cells were high and comparable between the two incubations (Table 6.2).

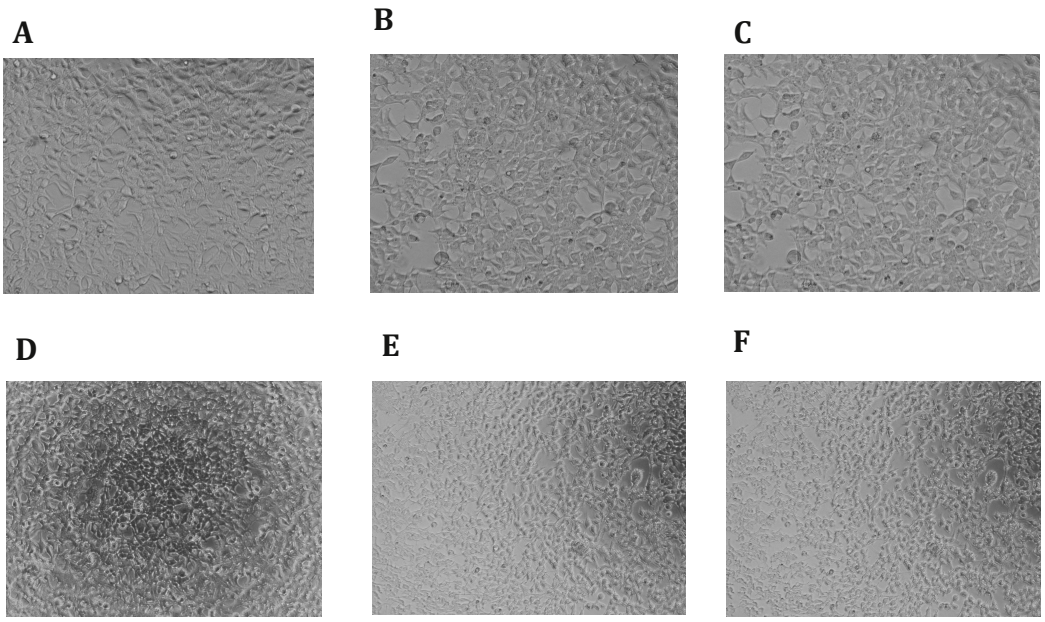

Figure 6.1: The morphology of OATP1B1 overexpressing cells in plating media 24 hours after plating (A, D); after 1 minute in buffer (B) and plasma (E); and after 2 minutes in buffer (C) and plasma (F)

Table 6.2: The viability of the OATP1B1 and OATP1B3 cells in protein-free buffer and 100% human plasma

Time in Buffer (min)	OATP1B1 Viability	OATP1B3 Viability	Time in Plasma (min)	OATP1B1 Viability	OATP1B3 Viability
1	81.3%	90.4%	1	91.1%	85.9%
2	85.2%	90.1%	2	88.6%	88.2%
3	89.6%	88.0%	3	89.3%	82.2%

The uptake curves for four known OATP substrates in both incubation conditions are shown in Figure 6.2. Active uptake was observed for pitavastatin, pravastatin and rosuvastatin in both OATP1B1 and OATP1B3 cells in the buffer and plasma incubations. For repaglinide, active uptake was observed in the OATP1B1 cells, and the uptake in the OATP1B3 cells overlapped with the uptake in control cells, demonstrating that the drug is not an OATP1B3 substrate in the concentration range tested.

The calculated $K_{m,u}$, V_{max}, and $P_{dif,u}$ values are shown in Table 6.3. The $K_{m,u}$ values generated in the buffer aligned well with reported values in the literature. When examining the difference in $K_{m,u}$ values generated in buffer vs. plasma incubations, there were large differences for the highly protein bound compounds. For instance, examining the OATP1B1 cell data, pravastatin with the lowest protein binding ($f_{u,p}$=0.485) had a $K_{m,u}$ fold difference of 2.03 between the two incubations (84.9 vs. 41.9 μM) while rosuvastatin ($f_{u,p}$=0.107) had 16.1 (22.2 vs. 1.38 μM), repaglinide ($f_{u,p}$=0.0188) had 127 (1.07 vs. 0.00840 μM), and pitavastatin ($f_{u,p}$=0.00450) had 1120 (5.29 vs. 0.00520 μM) fold differences. For the OATP1B3 cell data, a similar trend was observed. The $K_{m,u}$ values were 2.15, 7.56, and 923 fold different for the pravastatin, rosuvastatin, and pitavastatin incubations respectively. The V_{max} also decreased for the highly bound compounds. Focusing on OATP1B1, the difference was 1.22 fold for pravastatin compared to 2.64, 21.7, 19.5 fold for rosuvastatin, repaglinide, and pitavastatin, respectively. Similar trends were seen with the OATP1B3 cells with 1.23, 4.20, and 97.4 fold differences with pravastatin, rosuvastatin, and pitavastatin.

The CL_{int} ($V_{max}/K_{m,u}$) was determined for each compound and the fold differences between the values in plasma and buffer were calculated (Fig. 6.3). Again, the difference in CL_{int} became greater as the free fraction decreased. For the lowest binding pravastatin, the

differences in CL_{int} values were 1.66 fold in OATP1B1 cells and 1.74 fold in OATP1B3, while for the highest binding pitavastatin, the fold differences were 51.9 and 9.46 respectively. The percentage of active uptake ($CL_{int}/(CL_{int} + P_{dif,u})$) was examined between the incubations as well (Table 6.4). The values are similar for pravastatin, rosuvastatin and pitavastatin between the two incubation conditions for OATP1B1 cells. Repaglinide, the compound with the highest passive diffusion, had the largest increase in percentage of active uptake with the use of plasma (45.2 vs. 70.2%) in the OATP1B1 cells.

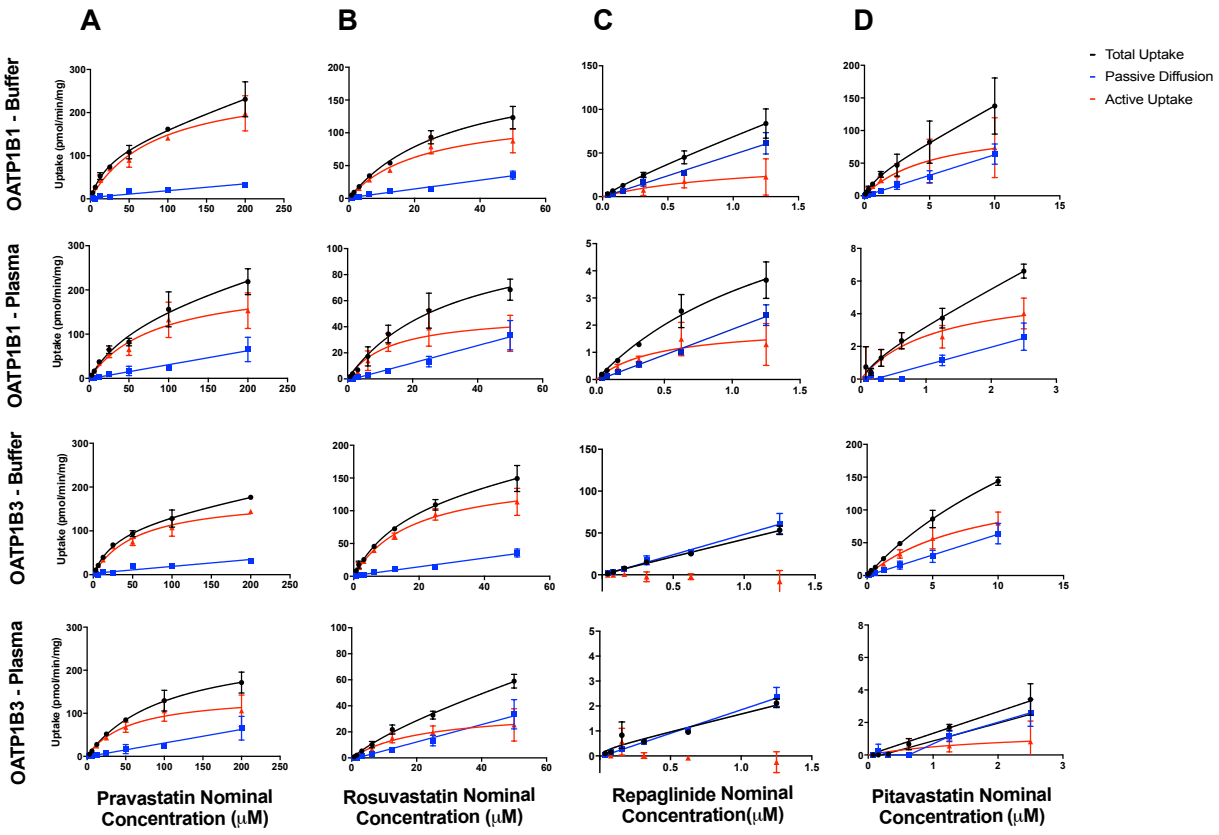

Figure 6.2: The rate of the uptake vs. the concentration of pravastatin (A), rosuvastatin (B), repaglinide (C), and pitavastatin (D) in OATP1B1- and OATP1B3-overexpressing cells in buffer and human plasma. Total uptake (overexpressed cells) is depicted in circles, passive diffusion (control cells) is depicted in squares, and active uptake (the difference) is depicted in triangles.

Table 6.3: $K_{m,u}$, V_{max}, and $P_{dif,u}$ values generated for pravastatin, rosuvastatin, repaglinide, and pitavastatin in OATP1B1 and OATP1B3 overexpressing cells in buffer and human plasma.

Drug	Transporter	Incubation	$K_{m,u}$ (µM)	V_{max} (pmol/ min/mg)	$P_{dif,u}$ (µL/ min/mg)	$K_{m,u}$ (µM) Reported in Lit.
Pravastatin	**OATP1B1**	Buffer	84.9 ± 19.8	274 ± 29.1	0.159 ± 0.0143	85.7[a], 104[b], 109[c]
		Plasma	41.9 ± 6.54	224 ± 16.1	0.652 ± 0.0445	
		Fold difference (Buffer/Plasma)	2.03	1.22	0.244	
	OATP1B3	Buffer	57.5 ± 11.5	179 ± 14.5	0.159 ± 0.0143	228[b]
		Plasma	26.8 ± 3.58	145 ± 7.71	0.652 ± 0.0445	
		Fold difference (Buffer/Plasma)	2.15	1.23	0.244	
Rosuvastatin	**OATP1B1**	Buffer	22.2 ± 5.25	132 ± 14.5	0.667 ± 0.0407	9.31[d], 13.0[e], 13.1[f]
		Plasma	1.38 ± 0.324	50.0 ± 4.59	6.24 ± 0.273	
		Fold difference (Buffer/Plasma)	16.1	2.64	0.107	
	OATP1B3	Buffer	18.0 ± 1.74	156 ± 6.57	0.667 ± 0.0407	14.2[g], 16.5[e]
		Plasma	2.38 ± 0.269	37.1 ± 1.95	6.24 ± 0.273	
		Fold difference (Buffer/Plasma)	7.56	4.20	0.107	

Drug	Transporter	Incubation	$K_{m,u}$ (µM)	V_{max} (pmol/ min/mg)	$P_{dif,u}$ (µL/ min/mg)	$K_{m,u}$ (µM) Reported in Lit.
Repaglinide	**OATP1B1**	Buffer	1.07 ± 0.414	42.9 ± 9.50	48.6 ± 1.78	1.36[d]
		Plasma	0.00840 ± 0.00263	1.98 ± 0.268	100 ± 3.21	
		Fold difference (Buffer/Plasma)	127	21.7	0.486	
	OATP1B3	Buffer	N/A	N/A	48.6 ± 1.78	N/A
		Plasma	N/A	N/A	100 ± 3.21	
		Fold difference (Buffer/Plasma)			0.486	
Pitavastatin	**OATP1B1**	Buffer	5.29 ± 0.984	111 ± 10.1	6.33 ± 0.109	1.30[h], 2.48[d], 3.00[i]
		Plasma	0.00520 ± 0.00134	5.69 ± 0.689	243 ± 31.1	
		Fold difference (Buffer/Plasma)	1020	19.5	0.0260	
	OATP1B3	Buffer	8.80 ± 2.77	152 ± 27.7	6.33 ± 0.109	2.60[j], 3.25[i]
		Plasma	0.00953 ± 0.00877	1.56 ± 0.822	243 ± 31.1	
		Fold difference (Buffer/Plasma)	923	97.4	0.0260	

[a]Kameyama et al. (39); [b]Kindla et al. (40); [c]Furihata et al. (41); [d]Izumi et al. (42); [e]Bosgra et al. (43); [f]van de Steeg et al. (44); [g]Kitamura et al. (45); [h]Sharma et al. (46); [i]Hirano et al. (47); [j]Vildhede et al. (48)

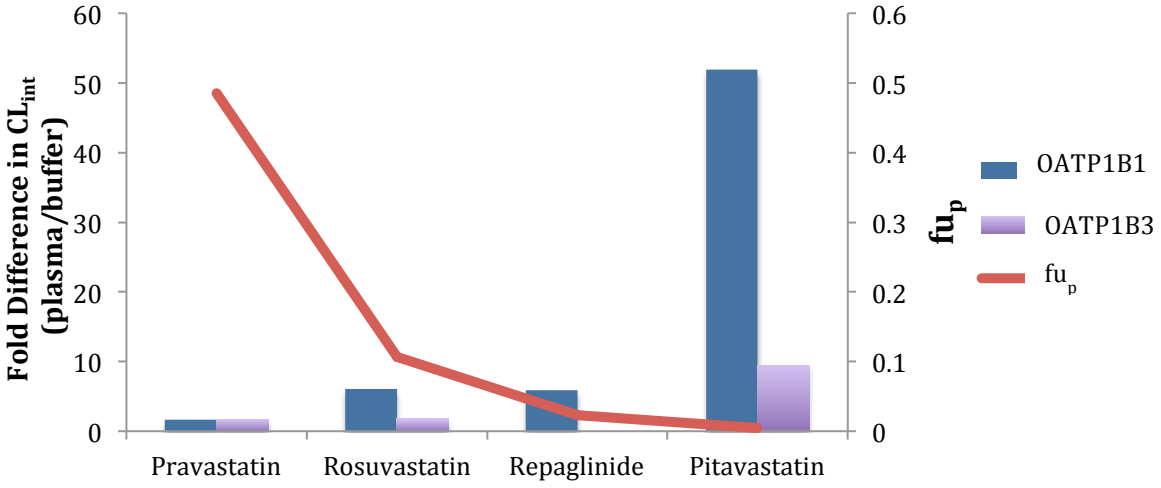

Figure 6.3: The plasma protein binding vs. the fold difference in CL_{int} of pravastatin, rosuvastatin, repaglinide, and pitavastatin generated in buffer and human plasma for OATP1B1 and OATP1B3.

Table 6.4: The intrinsic clearance and percentage of active uptake of pravastatin, rosuvastatin, repaglinide, and pitavastatin in OATP1B1 and OATP1B3-overexpressing cells in buffer and human plasma.

		Pravastatin ($f_{u,p}$=0.485)		**Rosuvastatin** ($f_{u,p}$=0.107)		**Repaglinide** ($f_{u,p}$=0.0188)		**Pitavastatin** ($f_{u,p}$=0.00450)	
		Buffer	Plasma	Buffer	Plasma	Buffer	Plasma	Buffer	Plasma
OATP 1B1	$CL_{int,}$(μL/min/mg)	3.22 ± 0.827	5.34 ± 0.919	5.94 ± 1.55	36.2 ± 9.13	40.1 ± 17.9	236 ± 80.4	21.0 ± 4.35	1090 ± 312
	Fold dif. (Plasma/Buffer)	1.66		6.09		5.89		51.9	
	$P_{dif,u}$ (μL/min/mg)	0.159 ± 0.0143	0.652 ± 0.0445	0.667 ± 0.0407	6.24 ± 0.273	48.6 ± 1.78	100 ± 3.21	6.33 ± 0.109	243 ± 31.1
	Fold dif. (Plasma/Buffer)	4.10		9.36		2.06		38.4	
	% Active	**95.3**	**89.1**	**89.8**	**85.3**	**45.2**	**70.2**	**76.8**	**81.8**
OATP 1B3	CL_{int} (μL/min/mg)	3.11 ± 0.672	5.41 ± 0.778	8.67 ± 0.914	15.6 ± 1.94	N/A	N/A	17.3 ± 6.28	164 ± 173
	Fold dif. (Plasma/Buffer)	1.74		1.80		N/A		9.46	
	$P_{dif,u}$ (μL/min/mg)	0.159 ± 0.0143	0.652 ± 0.0445	0.667 ± 0.0407	6.24 ± 0.273	48.6 ± 1.78	100 ± 3.21	6.33 ± 0.109	243 ± 31.1
	Fold dif. (Plasma/Buffer)	4.10		9.36		2.06		38.4	
	% Active	**95.1**	**89.2**	**92.9**	**71.4**	**N/A**	**N/A**	**73.2**	**40.3**

$CL_{int} = V_{max}/K_{m,u}$

Discussion

Obtaining accurate in vitro data is crucial for predicting pharmacokinetic parameters such as clearance with IVIVE, as well as for generating reliable concentration profiles with PBPK modeling. There is often a disconnect with current IVIVE methods particularly for compounds that are substrates of transporters (20). In vivo clearance for seven OATP substrates was previously underpredicted using human hepatocytes in protein-free incubations, and predictions were poorest for those substrates that were highly protein-bound (16).

Here we evaluated HEK293 cells overexpressing OATP1B1 and OATP1B3 in protein-free buffer and 100% plasma incubations as an alternative system. Groups have recently begun adding protein to incubations with overexpressing cell lines using 2% human serum albumin (HSA) (21) or 10% fetal bovine serum (22) for instance. In this investigation, using 100% human plasma with HEK293 cells was also demonstrated to be a reasonable option as the cells maintained high viability throughout the study.

Four known substrates of OATP with a range of protein binding values were chosen to evaluate. Pravastatin, pitavastatin, and rosuvastatin were all substrates of OATP1B1 and OATP1B3 agreeing with previously reported in vitro studies (Table 6.3) and in vivo studies (23-25). Repaglinide was found to be a substrate of OATP1B1 in the concentration range tested agreeing with previous in vitro and in vivo studies (26). While in vitro studies have found repaglinide to be an inhibitor of OATP1B3 (27), it was not demonstrated to be a substrate here. However, a recent study found repaglinide to be an OATP1B3 substrate using longer incubation times (28).

Differences were observed with each parameter ($K_{m,u}$, V_{max}, CL_{int}, and $P_{dif,u}$) obtained from the buffer and human plasma incubations in both cells. As has been previously noted with

the use of plasma in hepatocyte incubations (29), the $K_{m,u}$ values decreased in the plasma as protein binding increased (with fold changes ranging from 2.03-1020). The V_{max} also decreased in the plasma for the higher binding compounds in particular (the fold changes ranged from 1.22-97.4). It is interesting to note the decreases in both $K_{m,u}$ and V_{max}, and the more dramatic differences in $K_{m,u}$ values led to consistently higher CL_{int} ($V_{max}/K_{m,u}$) values in the human plasma incubations for all four compounds. The fold difference (plasma/buffer) was largest for the highest protein bound pitavastatin (51.9 and 9.46 for OATP1B1 and OATP1B3, respectively) compared to the differences with the other three compounds (1.66-6.09 and 1.74-1.80 for OATP1B1 and OATP1B3, respectively) (Figure 6.3). This suggests that plasma proteins may play a role in the active uptake process. The unbound passive diffusion was also consistently higher in the human plasma incubations for all four compounds. The fold difference again was higher for pitavastatin (38.4) compared to the other three compounds (2.06-9.36), suggesting that plasma proteins may play a role in the passive diffusion process too. This was previously seen, but to a lesser extent with hepatocytes (29), and the mechanism remains unknown. However, since there was also an increase in $CL_{int,}$ when examining the percentage of active uptake shifts, generally for the three statin compounds the differences did not have an effect. For compounds with high plasma protein binding that are not substrates for active uptake (but predominately metabolized, for example), the results from protein-free incubations may be underestimated due to the inaccurate intracellular concentrations.

These $K_{m,u}/V_{max}/CL_{int}$ values shifted in the same way as those for a highly protein bound new chemical entity in HEK293 overexpressing cells with HSA (21) where $K_{m,u}$ decreased, V_{max} decreased, and CL_{int} increased with increasing concentrations of HSA. Many groups have also seen decreased $K_{m,u}$ and higher CL_{int} values when using plasma in hepatocyte incubations (11,

30) An early idea of including plasma was to eliminate the uncertainty in prediction introduced with separately measuring plasma protein binding, which improved clearance predictions (10, 31). Having plasma or proteins present also can account for potential protein-facilitated uptake (32, 33). For pravastatin, the $K_{m,u}$ measured in the OATP1B1 and OATP1B3 overexpressed cell lines in plasma were 41.9 and 26.8 μM, which were quite comparable to the reported $K_{m,u}$ of 37 uM generated with plated human hepatocytes in plasma (12).

According to the free drug theory, hepatic uptake of drug is solely dependent on the unbound concentration available at the hepatocyte surface; however, several studies have unexpectedly found uptake to be greater than the unbound concentration (8, 9). While the presence of a specific albumin receptor on the hepatocyte cell surface was originally proposed, numerous studies and negative results from affinity chromatography have deemed the hypothesis less likely (34). The idea of more general interactions of the albumin-drug complex with the hepatocyte cell surface are discussed frequently instead (35). For instance, binding of the albumin-drug complex to the cell surface may lead to a conformational change in albumin reducing its binding affinity for the drug (7) or ionic interactions between the protein-drug complex and the hepatocyte plasma membrane may decrease the diffusional distance for unbound ligand (36). These hypotheses focus on hepatocytes specifically though and protein-facilitated uptake has been shown to occur in other cell types including myocytes (36), adipocytes (37), and here, in HEK293 cells overexpressing transporters.

These data support a recent hypothesis called a transporter-induced protein binding shift (TIPBS) (9, 29). The idea is that if a highly protein bound drug has a higher affinity for a transporter than for albumin (or the suggested hepatocyte cell surface), the transporter may be able to strip the drug from the protein before the drug dissociates itself and is at binding

equilibrium. In these cases, protein binding would not be restricting the access of the compounds. While the alternative hypotheses may have been able to explain the trends seen in hepatocytes in the past, the TIPBS explanation agrees with data from hepatocytes as well as from HEK293 cells, where overexpressed transporters, not a hepatocyte cell surface, would be driving the $K_{m,u}$ and CL_{int} shifts seen. Interesting results were found for repaglinide. Although it has the second highest protein binding of the four compounds evaluated ($f_{u,p}$=0.0188), compared to rosuvastatin with lower binding ($f_{u,p}$=0.107), repaglinide did not have as large of a CL_{int} shift. One simple explanation could be that the other compounds examined were statins and they can be more directly compared to each other than to repaglinide. In addition, an explanation related to a TIPBS could also explain the difference. Repaglinde had the largest percentage of passive diffusion of the four compounds in the overexpressed OATP1B1 cell line (Table 6.4). Given the lesser involvement of transporters and active uptake, a transporter-induced protein binding shift would also be expected to be less. The addition of plasma did increase the percentage of active uptake for repaglinide, but it was still less than that of the other three compounds.

In summary, this work demonstrates that using HEK293 cells overexpressing transporters in plasma incubations is a viable option for assessing the kinetic uptake of OATP1B1 and OATP1B3 substrates. Overall, the CL_{int} values generated in the plasma incubations were higher than the values generated in protein-free buffer in both cells, addressing the underprediction related to OATP substrates reported previously. The results also support the recent hypothesis of a transporter-induced protein binding shift for compounds with high protein binding and high affinity for transporters. PBPK modeling work is on-going to provide a systematic understanding of the in vitro to in vivo translation of data from overexpressed cell lines in the presence and absence of human plasma.

References

(1) Giacomini KM, Huang SM, Tweedie DJ, Benet LZ, Brouwer KL, Chu X, Dahlin A, Evers R, Fischer V, Hillgren KM, Hoffmaster KA, Ishikawa T, Keppler D, Kim RB, Lee CA, Niemi M, Polli JW, Sugiyama Y, Swaan PW, Ware JA, Wright SH, Yee SW, Zamek-Gliszczynski MJ, and Zhang, L (2010) Membrane transporters in drug development. *Nat Rev Drug Discov* **9:**215-236.

(2) Kalliokoski A and Niemi M (2009) Impact of OATP transporters on pharmacokinetics. *Br J Pharmacol* **158:**693-705.

(3) Watanabe T, Kusuhara H, Maeda K, Shitara Y, and Sugiyama Y (2009) Physiologically based pharmacokinetic modeling to predict transporter-mediated clearance and distribution of pravastatin in humans. *J Pharmacol Exp Ther* **328:**652-662.

(4) Forker EL and Luxon BA (1981) Albumin helps mediate removal of taurocholate by rat liver. *J Clin Invest* **67:**1517-1522.

(5) Forker EL and Luxon BA (1983) Albumin-mediated transport of rose bengal by perfused rat liver. Kinetics of the reaction at the cell surface. *J Clin Invest* **72:**1764-1771.

(6) Weisiger RA and Ma WL (1987) Uptake of oleate from albumin solutions by rat liver. Failure to detect catalysis of the dissociation of oleate from albumin by an albumin receptor. *J Clin Invest* **79:**1070-1077.

(7) Tsao SC, Sugiyama Y, Sawada Y, Iga T, and Hanano M (1988) Kinetic analysis of albumin-mediated uptake of warfarin by perfused rat liver. *J Pharmacokinet Biopharm* **16:**165-181.

(8) Poulin P, Burczynski FJ, and Haddad S (2016) The role of extracellular binding proteins in the cellular uptake of drugs: impact on quantitative in vitro-to-in vivo extrapolations of toxicity and efficacy in physiologically based pharmacokinetic-pharmacodynamic research. *J Pharm Sci* **105:**497-508.

(9) Bowman CM and Benet LZ (2018) An examination of protein-binding and protein-facilitated uptake relating to in vitro-in vivo extrapolation. *Eur J Pharm Sci* **123:**502-514.

(10) Shibata Y, Takahashi H, Chiba M, and Ishii Y (2002) Prediction of hepatic clearance and availability by cryopreserved human hepatocytes: an application of serum incubation method. *Drug Metab Dispos* **30:**892-896.

(11) Blanchard N, Richert L, Notter B, Delobel F, David P, Coassolo P, Lavé T (2004) Impact of serum on clearance predictions obtained from suspensions and primary cultures of rat hepatocytes. *Eur J Pharm Sci* **23:**189-199.

(12) Mao J, Doshi U, Wright M, Hop CECA, Li AP, and Chen Y (2018) Prediction of the pharmacokinetics of pravastatin as an OATP substrate using plateable human hepatocytes with human plasma data and PBPK modeling. *CPT Pharmacometrics Syst Pharmacol* **7:**251-258.

(13) Pan HY, DeVault AR, Swites BJ, Whigan D, Ivashkiv E, Willard DA, and Brescia D (1990) Pharmacokinetics and pharmacodynamics of pravastatin alone and with cholestyramine in hypercholesterolemia. *Clin Pharmacol Ther* **48:**201-207.

(14) Lennernäs H and Fager G (1997) Pharmacodynamics and pharmacokinetics of the HMG-CoA reductase inhibitors. Similarities and differences. *Clin Pharmacokinet* **32:**403-425.

(15) Martin PD, Warwick MJ, Dane AL, Brindley C, and Short T (2003) Absolute oral bioavailability of rosuvastatin in healthy white adult male volunteers. *Clin Ther* **25:**2553-2563.

(16) Jones HM, Barton HA, Lai Y, Bi Y, Kimoto E, Kempshall S, Tate SC, El-Kattan A, Houston JB, Galetin A, and Fenner KS (2012) Mechanistic pharmacokinetic modeling for the prediction of transporter-mediated disposition in humans from sandwich culture human hepatocyte data. *Drug Metab Dispos* **40:**1007-1017.

(17) Hatorp V, Walther KH, Christensen MS, and Haug-Pihale G (2000) Single-dose pharmacokinetics of repaglinide in subjects with chronic liver disease. *J Clin Pharmacol* **40:**142-152.

(18) Plum A, Müller LK, and Jansen JA (2000) The effects of selected drugs on the in vitro protein binding of repaglinide in human plasma. *Methods Find Exp Clin Pharmacol* **22:**139-143.

(19) Fujino H, Yamada I, Kohima J, Hirano M, Matsumoto H, and Yoneda M (1999) Studies on the metabolic fate of NK-104, a new inhibitor of HMG-CoA reductase (5): in vitro metabolism and plasma protein binding in animals and humans. *Drug Metab Pharmacokinet* **14:**415-424.

(20) Soars, MG, McGinnity, DF, Grime, K, and Riley RJ (2007) The pivotal role of hepatocytes in drug discovery. *Chemico-Biological Interact* **168:**2-15.

(21) Fukuchi Y, Toshimoto K, Mori T, Kakimoto K, Tobe Y, Sawada T, Asaumi R, Iwata T, Hashimoto Y, Nunoya K, Imawaka H, Miyauchi S, and Sugiyama Y (2017) Analysis of nonlinear pharmacokinetics of a highly albumin-bound compound: contribution of albumin-mediated hepatic uptake mechanism. *J Pharm Sci* **106:**2704-2714.

(22) Oh Y, Jeong Y-S, Kim M-S, Min JS, Ryoo G, Park JE, Jun Y, Song Y-K, Chun S-E, Han S, Bae SK, Chung S-J, and Lee W (2018) Inhibition of organic anion transporting polypeptide 1B1 and 1B3 by betulinic acid: effects of preincubation and albumin in the media. *J Pharm Sci* **107:**1713-1723.

(23) Choi JH, Lee MG, Cho JY, Lee JE, Kim KH, and Park K (2008) Influence of OATP1B1 genotype on the pharmacokinetics of rosuvastatin in Koreans. *Clin Pharmacol Ther* **83:**251-257.

(24) Deng JW, Song IS, Shin HJ, Yeo CW, Cho DY, Shon JH, and Shin JG (2008) The effect of SLCO1B1*15 on the disposition of pravastatin and pitavastatin is substrate dependent: the contribution of transporting activity changes by SLCO1B1*15. *Pharmacogenet Genomics* **18:**424-433.

(25) Alam K, Crowe A, Wang X, Zhang P, Ding K, Li L, and Yue W (2018) Regulation of organic anion transporting polypeptides (OATP) 1B1- and OATP1B3-mediated transport: an updated review in the context of OATP-mediated drug-drug interactions. *Int J Mol Sci* doi: 10.3390/ijms19030855.

(26) Kalliokoski A, Neuvonen M, Neuvonen PJ, and Niemi M (2008) The effect of SLCO1B1 polymorphism on repaglinide pharmacokinetics persists over a wide dose range. *Br J Clin Pharmacol* **66:**818-825.

(27) Bachmakov I, Glaeser H, Fromm MF, and König J (2008) Interaction of oral antidiabetic drugs with hepatic uptake transporters: focus on organic anion transporting polypeptides and organic cation transporter 1. *Diabetes* **57:**1463-1469.

(28) Fujino R, Hashizume K, Aoyama S, Maeda K, Ito K, Toshimoto K, Lee W, Ninomiya S, Sugiyama Y (2018) Strategies to improve the prediction accuracy of hepatic intrinsic clearance of three antidiabetic drugs: application of the extended clearance concept and consideration of the effect of albumin on CYP2C metabolism and OATP1B-mediated uptake. *Eur J Pharm Sci* **125:**181-192.

(29) Bowman CM, Okochi H, and Benet LZ (2019) The presence of a transporter-induced protein binding shift: a new explanation for protein-facilitated uptake and improvement for in vitro-in vivo extrapolation. *Drug Metab Dispos* doi:118.085779

(30) Blanchard N, Hewitt NJ, Silber P, Jones H, Coassolo P, Lavé T (2006) Prediction of hepatic clearance using cryopreserved human hepatocytes: a comparison of serum and serum-free incubations. *J Pharm Pharmacol* **58:**633-641.

(31) Shibata Y, Takahashi H, and Ishii Y (2000) A convenient in vitro screening method for predicting in vivo drug metabolic clearance using isolated hepatocytes suspended in serum. *Drug Metab Dispos* **28:**1518-1523.

(32) Miyauchi S, Masuda M, Kim S-J, Tanaka Y, Lee KR, Iwakado S, Nemoto M, Sasaki S, Shimono K, Tanaka Y, and Sigiyama Y (2018) The phenomenon of albumin-mediated hepatic uptake of organic anion transport polypeptide substrate: prediction of the in vivo uptake clearance from the in vitro uptake by isolated hepatocytes using a facilitated-dissociation model. *Drug Metab Dispos* **46:**259-267.

(33) Kim S-J, Lee K-R, Miyauchi S and Sugiyama Y (2019) Extrapolation of in vivo hepatic clearance from in vitro uptake clearance by suspended human hepatocytes for anionic drugs with high binding to human albumin: improvement of in vitro-to-in vivo extrapolation by considering the "albumin-mediated" hepatic uptake mechanism on the basis of the 'facilitated-dissociation model". *Drug Metab Dispos* **47:**94-103.

(34) Stremmel W, Potter BJ, and Berk PD (1983) Studies of albumin binding to rat liver plasma membranes: implications for the albumin receptor hypothesis. *Biochim Biophys Acta* **756:**20-27.

(35) Poulin P and Haddad S (2018) Extrapolation of the hepatic clearance of drugs in the absence of albumin in vitro to that in the presence of albumin in vivo: comparative assessment of 2 extrapolation models based on the albumin-mediated hepatic uptake theory and limitations and mechanistic insights. *J Pharm Sci* doi: 10.1016/j.xphs.2018.03.012.

(36) Burczynski FJ, Wang GQ, and Hnatowich M (1997) Effect of binding protein surface charge on palmitate uptake by hepatocyte suspensions. *Br J Pharmacol* **120:**1215-1220.

(37) Hütter JF, Piper HM and Spieckermann PG (1984) Myocardial fatty acid oxidation: evidence for an albumin-receptor-mediated membrane transfer of fatty acids. *Basic Res Cardiol* **79:**274-282.

(38) Sorrentino D, Robinson RB, Kiang C-L, and Berk PD (1989) At physiologic albumin/oleate concentrations oleate uptake by isolated hepatocytes, cardiac myocytes, and adipocytes is a saturable function of the unbound oleate concentration. Uptake kinetics are consistent with the conventional theory. *J Clin Invest* **84:**1325-1333.

(39) Kameyama Y, Yamashita K, Kobayashi K, Hosokawa M, and Chiba K (2005) Functional characterization of SLCO1B1 (OATP-C) variants, SCLO1B1*5, SLCO1B1*15 and SLCO1B1*15+C1007G, by using transient expression systems of HeLa and HEK293 cells. *Pharmacogenetic Genomics* **15:**513-522.

(40) Kindla J, Müller F, Mieth M, Fromm MF, and König J (2011) Influence of non-steroidal anti-inflammatory drugs on organic anion transporting polypeptide (OATP) 1B1- and OATP1B3-mediated drug transport. *Drug Metab Dispos* **39:**1047-1053.

(41) Furihata T, Satoh N, Ohishi T, Ugajin M, Kameyama Y, Morimoto K, Matsumoto S, Yamashita K, Kobayashi K, and Chiba K (2009) Functional analysis of a mutation in the SLCO1B1 gene (c.1628T>G) identified in a Japanese patient with pravastatin-induced myopathy. *Pharmacogenomics J* **9:**185-193.

(42) Izumi S, Nozaki Y, Maeda K, Komori T, Takenaka O, Kusuhara H, and Sugiyama Y (2015) Investigation of the impact of substrate selection on in vitro organic anion transporting polypeptide 1B1 inhibition profiles for the prediction of drug-drug interactions. *Drug Metab Dispos* **43:**235-247.

(43) Bosgra S, van de Steeg E, Vlaming ML, Verhoeckx KC, Huisman MT, Verwei M, and Wortelboer HM (2014) Predicting carrier-mediated hepatic disposition of rosuvastatin in man by scaling from individual transfected cell-lines in vitro using absolute transporter protein quantification and PBPK modeling. *Eur J Pharm Sci* **65:**156-166.

(44) van de Steeg E, Greupink R, Schreurs M, Nooijen IHG, Verhoeckx KCM, Hanemaaijer R, Ripken D, Monshouwer M, Vlaming MLH, DeFroot J, Verwei M, Russel FGM, Huisman MT, and Wortelboer HM (2013) Drug-drug interactions between rosvuastatin and oral antidiabetic drugs occurring at the level of OATP1B1. *Drug Metab Dispos* **41:**592-601.

(45) Kitamura S, Maeda K, Wang Y, and Sugiyama Y (2008) Involvement of multiple transporters in the hepatobiliary transport of rosuvastatin. *Drug Metab Dispos* **36:**2014-2023.

(46) Sharma P, Butters CJ, Smith V, Elsby R and Surry D (2012) Prediction of the in vivo OATP1B1-mediated drug-drug interaction potential of an investigational drug against a range of statins. *Eur J Pharm Sci* **47:**244-255.

(47) Hirano M, Maeda K, Shitara Y and Sugiyama Y (2004) Contribution of OATP2 (OATP1B1) and OATP8 (OATP1B3) to the hepatic uptake of pitavastatin in humans. *J Pharmacol Exp Ther* **311:**139-146.

(48) Vildhede A, Mateus A, Khan EK, Lai Y, Karlgren M, Artursson P, and Kjellsson MC (2016) Mechanistic modeling of pitavastatin disposition in sandwich-cultured human hepatocytes: a proteomics-informed bottom-up approach. *Drug Metab Dispos* **44:**505-516.

CHAPTER 7: Interlaboratory Variability in Human Hepatocyte Intrinsic Clearance Values and Trends with Physicochemical Properties*

Abstract

Purpose: To examine the interlaboratory variability in CL_{int} values generated with human hepatocytes and determine trends in variability and clearance prediction accuracy using physicochemical and pharmacokinetic parameters.

Methods: Data for 50 compounds from 14 papers were compiled with physicochemical and pharmacokinetic parameter values taken from various sources.

Results: Coefficients of variation were as high as 99.8% for individual compounds and variation was not dependent on the number of prediction values included in the analysis. When examining median values, it appeared that compounds with a lower number of rotatable bonds had more variability. When examining prediction uniformity, those compounds with uniform in vivo underpredictions had higher $CL_{int, in\ vivo}$ values, while those with non-uniform predictions typically had lower $CL_{int, in\ vivo}$ values. Of the compounds with uniform predictions, only a small number were uniformly predicted accurately. Based on this limited dataset, less lipophilic, lower intrinsic clearance, and lower protein binding compounds yield more accurate clearance predictions.

Conclusions: Caution should be taken when compiling in vitro CL_{int} values from different laboratories as variations in experimental procedures (such as extent of shaking during incubation) may yield different predictions for the same compound. The majority of compounds with uniform in vitro values had predictions that were inaccurate, emphasizing the need for a

*Modified from the publication: Bowman CM and Benet LZ (2019) Interlaboratory variability in human hepatocyte intrinsic clearance values and trends with physicochemical properties. *Pharm Res* **31:**113.

better mechanistic understanding of IVIVE. The non-uniform predictions, often with low turnover compounds, reaffirmed the experimental challenges for drugs in this clearance range. Separating new chemical entities by lipophilicity, intrinsic clearance, and protein binding may help instill more confidence in IVIVE predictions.

Introduction

Clearance is one of the most fundamental pharmacokinetic parameters, and its accurate in vivo prediction is necessary for compound prioritization and first-in-human estimates. However, the surprising inaccuracy in predictions from in vitro to in vivo extrapolation (IVIVE) has recently been reviewed (1, 2).

The typical IVIVE process involves measuring an intrinsic clearance (CL_{int}) in microsomes or hepatocytes and applying biological scaling factors and a model of hepatic disposition to estimate an in vivo hepatic clearance (CL_H). In an attempt to eliminate the systematic error with IVIVE, groups have begun applying regression or empirical based scaling factors (3).

When examining the widespread IVIVE error, significant interlaboratory in vitro variability has been noted (1, 4, 5). While variability may result from interdonor differences, pooled lots are now commonly used to reduce lot-to-lot variation, or may result from differences in the biological scaling factors applied, efforts have been directed toward reaching a consensus (6, 7). There could also be variation due to the use of fresh vs. cryopreserved hepatocytes, however previous studies have not found significant differences (8, 9).

When collating in vivo hepatic clearance values from intravenous studies, Stringer et al. (5) found low variability; however, upon examining in vitro hepatocyte CL_{int} values, the authors found large coefficients of variation (CVs), which increased with increasing CL_{int}. Nagilla et al. (4) noted the paucity and variability of in vitro literature data, explaining that CL_{int} values should be taken from a consistent assay rather than arbitrarily chosen from different literature sources. Now that more data have been generated, we reexamine the interlaboratory variability, and

search for trends with variability and physicochemical and pharmacokinetic parameters. We also examine trends in prediction accuracy for compounds with uniform in vitro values.

Methods

A total of 14 papers were examined (Table 7.1) and overlapping values were found for 50 compounds with data generated in human hepatocytes (Table 7.2). All in vitro CL_{int} values were scaled to a predicted $CL_{int,in\ vivo}$ using consistent scaling factors of 120 x 10^6 hepatocytes/g liver and 21.4 g liver/kg body weight, and the fraction unbound in the hepatocyte incubation ($f_{u,hep}$) values taken from the Wood et al. (2) database:

$$Predicted\ CL_{int,in\ vivo} = \frac{CL_{int,in\ vitro}}{fu_{hep}} \cdot 120 \cdot 21.4$$

Coefficients of variation (CV) were determined as standard deviation divided by the average.

Values for hepatic clearance ($CL_{H,in\ vivo}$) (ml/min/kg), fraction unbound in the blood and plasma ($f_{u,B}$, $f_{u,p}$), and intrinsic clearance ($CL_{int,\ in\ vivo}$) (ml/min/kg) were taken from Wood et al. (2). $CL_{int,\ in\ vivo}$ values were calculated using the well-stirred model (since the difference in bias between the well-stirred and parallel tube model, the two extremes for models of hepatic disposition, was determined to be minimal) (2).

The ChEMBL database (https://www.ebi.ac.uk/chembl) (10) was used to obtain values for molecular weight (MW), logP, logD, polar surface area (PSA), number of hydrogen bond donors

(HBD), number of hydrogen bond acceptors (HBA), number of rotatable bonds, and number of aromatic rings.

Values for the steady state volume of distribution (VD_{ss}) (l/kg) and mean residence time (MRT) (hr) were found for 45 compounds in Obach et al. (11).

Classification within the Biopharmaceuticals Drug Disposition Classification System (BDDCS) was determined using Benet et al. (12) and Hosey et al. (13).

Main metabolizing enzyme information was found for 33 compounds in El-Kattan et al. (14)

The relationship between variability and the properties was evaluated by examining the coefficient of correlation R^2.

The accuracy of predictions was determined based on whether the predicted CL_{int} values fell within two fold of the observed CL_{int} values:

$$0.5 \leq \frac{observed\ CL_{int}}{predicted\ CL_{int}} \leq 2$$

Table 7.1: Human hepatocyte data examined for this evaluation

Source	Human Hepatocytes	Donors
Akabane et al. (26)	Cryopreserved	Individual, 9-11 donors
Blanchard et al. (27)	Cryopreserved	Individual, 2 donors
Floby et al. (9)	Fresh	Individual, 7 donors
Hallifax et al. (8)	Fresh	Individual, 5 donors
Hallifax et al. (28)	Cryopreserved	Individual, 5 donors
Jacobson et al. (29)	Cryopreserved	Pooled, 2 donors
Lau et al. (30)	Cryopreserved	Pooled, 5+ donors
Lu et al. (31)	Cryopreserved	Pooled, 4 donors
McGinnity et al. (17)	Fresh	Individual, 1-90 donors
Naritomi et al. (32)	Cryopreserved	Individual, 5-7 donors
Riley et al. (33)	Not Reported	Individual, 3+ donors
Soars et al. (34)	Cryopreserved	Individual, 3 donors
Sohlenius-Sternbeck et al. (35)	Cryopreserved	Pooled, 2-5 donors
Sohlenius-Sternbeck et al. (3)	Cryopreserved	Pooled, 5 donors

Table 7.2: The variability of reported CL_{int} values generated in human hepatocytes

Drug	CL_{int} values	References	CV (%)	n	Largest fold difference
Acetaminophen	3.59; 2.14; 2.76	3; 32; 35	25.7	3	1.68
Alprazolam	0.263; 1.82	8; 28		2	6.92
Caffeine	3.21; 8.83; 3.75	3; 17; 30	58.9	3	2.75
Carvedilol	297; 237; 196;	3; 17; 35	21.0	3	1.52
Chlorpheniramine	10.9; 3.89	17; 35		2	2.80
Chlorpromazine	684; 415; 642	3; 30; 35	24.9	3	1.65
Cimetidine	3.24; 35.1	17; 35		2	10.8
Clozapine	28.2; 22.0; 11.0; 27.9	3; 17; 29; 35	36.1	4	2.57
Codeine	63.5; 33.1	17; 34		2	1.92
Desipramine	62.6; 48.2; 177; 53.0	3; 17; 30; 35	72.0	4	3.67
Diazepam	5.71; 3.02; 24.3; 1.43; 9.57; 6.66; 6.38; 7.13	3; 8; 9; 17; 28; 30; 32; 35	87.6	8	17.0
Diclofenac	89.3; 49.2; 128; 296; 410; 51.9	3; 9; 17; 26; 33; 35	86.9	6	8.33
Diltiazem	52.8; 64.2; 34.2; 33.5; 167; 64.2; 48.5	3; 17; 29; 30; 32; 33; 35	69.7	7	4.99
Diphenhydramine	22.3; 7.44	17; 35		2	3.00
Fenoprofen	19.5; 11.4	3; 35		2	1.71
Flunitrazepam	1.05; 4.80	8; 28		2	4.55
Gemfibrozil	84.8; 66.3; 177; 3.50; 44.2	3; 17; 26; 34; 35	85.9	5	50.7

Drug	**CL_{int} values**	**References**	**CV (%)**	**n**	**Largest fold difference**
Glipizide	2.41; 2.68	3; 35		2	1.11
Granisetron	7.38; 26.6; 8.56	3; 17; 35	75.9	3	3.60
Ibuprofen	21.9; 11.5; 65.8; 18.3	3; 30; 33; 35	84.1	4	5.74
Imipramine	104; 114; 104; 117; 94.2	3; 17; 29; 30; 35	8.53	5	1.24
Irbesartan	39.1; 17.5; 22.7	3; 29; 35	42.7	3	2.23
Ketoprofen	6.15; 10.7; 9.90	3; 17; 35	27.2	3	1.74
Lorazepam	3.02; 0.816	17; 30		2	3.70
Methylprednisolone	5.61; 28.6; 6.50	3; 30; 35	96.1	3	5.11
Metoprolol	17.7; 20.0; 12.3; 20.0; 3.99	3; 17; 29; 33; 35	46.0	5	5.00
Midazolam	44.7; 11.1; 27.4; 39.1; 35.3; 153; 19.5; 16.9; 39.1	3; 8; 9; 17; 27; 28; 30; 31; 35	99.8	9	13.8
Naloxone	105; 596; 167; 220; 77.3; 589; 69.0	3; 17; 26; 27; 30; 34; 35	89.5	7	8.64
Naproxen	14.1; 5.64	17; 35		2	2.50
Nifedipine	18.2; 25.0; 42.3	17; 30; 35	43.5	3	2.32
Omeprazole	11.2; 5.02; 8.86	3; 17; 35	37.4	3	2.24
Ondansetron	5.25; 4.09; 2.92	3; 17; 35	28.6	3	1.80
Oxaprozin	4.37; 5.74	3; 35		2	1.31
Oxazepam	9.74; 5.90; 9.45	3; 30; 35	25.5	3	1.65

Drug	**CL_{int} values**	**References**	**CV (%)**	**n**	**Largest fold difference**
Phenacetin	13.8; 26.2; 5.75; 17.8	9; 29, 31; 35	53.6	4	4.57
Pindolol	5.93; 7.90; 5.64	3; 17; 35	19.0	3	1.40
Prazosin	13.4; 6.28; 8.20; 11.7	3; 17; 29; 35	32.7	4	2.13
Prednisolone	4.75; 27.1; 13.7	3; 30; 35	74.1	3	5.71
Propranolol	81.1; 40.8; 44.8; 40.8; 15.9; 40.8; 31.8	3; 17; 29; 30; 31; 33; 35	46.6	7	5.12
Quinidine	12.8; 18.1	3; 35		2	1.41
Ranitidine	3.78; 2.70; 4.33	3; 17; 35	22.9	3	1.60
Ritonavir	21.1; 13.8	3; 17		2	1.52
Sildenafil	37.4; 14.5; 22.6	3; 30; 35	46.7	3	2.58
Tenoxicam	6.96; 2.68	30; 35		2	2.60
Theophylline	2.68; 1.39	3; 30		2	1.92
Timolol	7.99; 11.7	3; 35		2	1.46
Tolbutamide	2.17; 4.95; 7.42; 3.40	3; 30; 33; 35	50.5	4	3.43
Triazolam	1.34; 2.82; 10.3	8; 17; 27	99.4	3	7.64
Verapamil	114; 88.9; 54.3; 79.0; 237; 64.2	3; 17; 29; 30; 33; 35	66.4	6	4.36
Zolpidem	9.85; 8.36	3; 35		2	1.18

Results

Coefficients of Variation and Physicochemical Parameters

Data for 50 compounds were evaluated and each compound had values from 2-9 sources. Of the 50 compounds, 17 had n=2, preventing a statistically relevant CV from being calculated. For the remaining 33 compounds, the CVs ranged from 8.53-99.8%. The potential for CV dependence on the number of values (n) was examined first. Pindolol with the second lowest CV of 19.0% had data from three sources, and triazolam with the second highest CV of 99.4% similarly had data from three sources. Imipramine, with n=5 had the lowest CV of 8.53%. Therefore, a high value of n did not necessarily cause high CV values as shown in Figure 7.1A. The fold difference between the highest and lowest predictions for each compound was also examined and there did not appear to be a dependence on n (Fig. 7.1B).

Sixteen physiochemical and pharmacokinetic properties were examined in relation to CV (Fig. 7.2) and there were no direct correlations here as the highest R^2 value was only 0.071. The 5 largest correlations are reported in Table 7.3. The data were then divided into a lower CV group (CV<50%) and higher CV group (CV≥50%) and median parameter values were examined (Table 7.3). The largest relative difference was seen with $f_{u,B}$ and $f_{u,p}$ values, followed by the number of rotatable bonds. In the lower CV half, 29% of compounds had ≥ 7 rotatable bonds compared to 6.3% of compounds with higher CV.

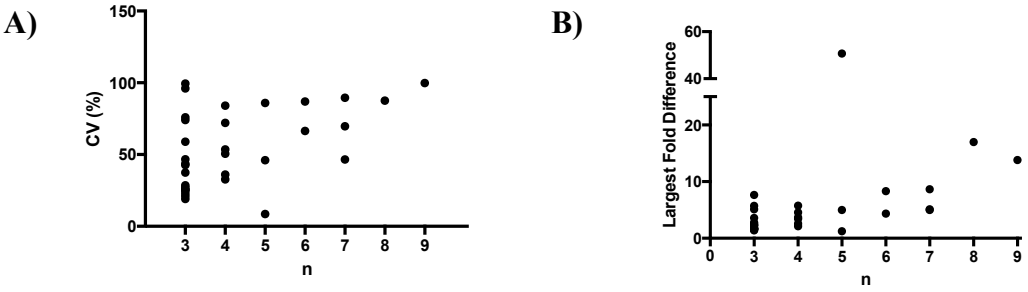

Figure 7.1: The dependence of CV (A) and the largest fold difference (B) on n

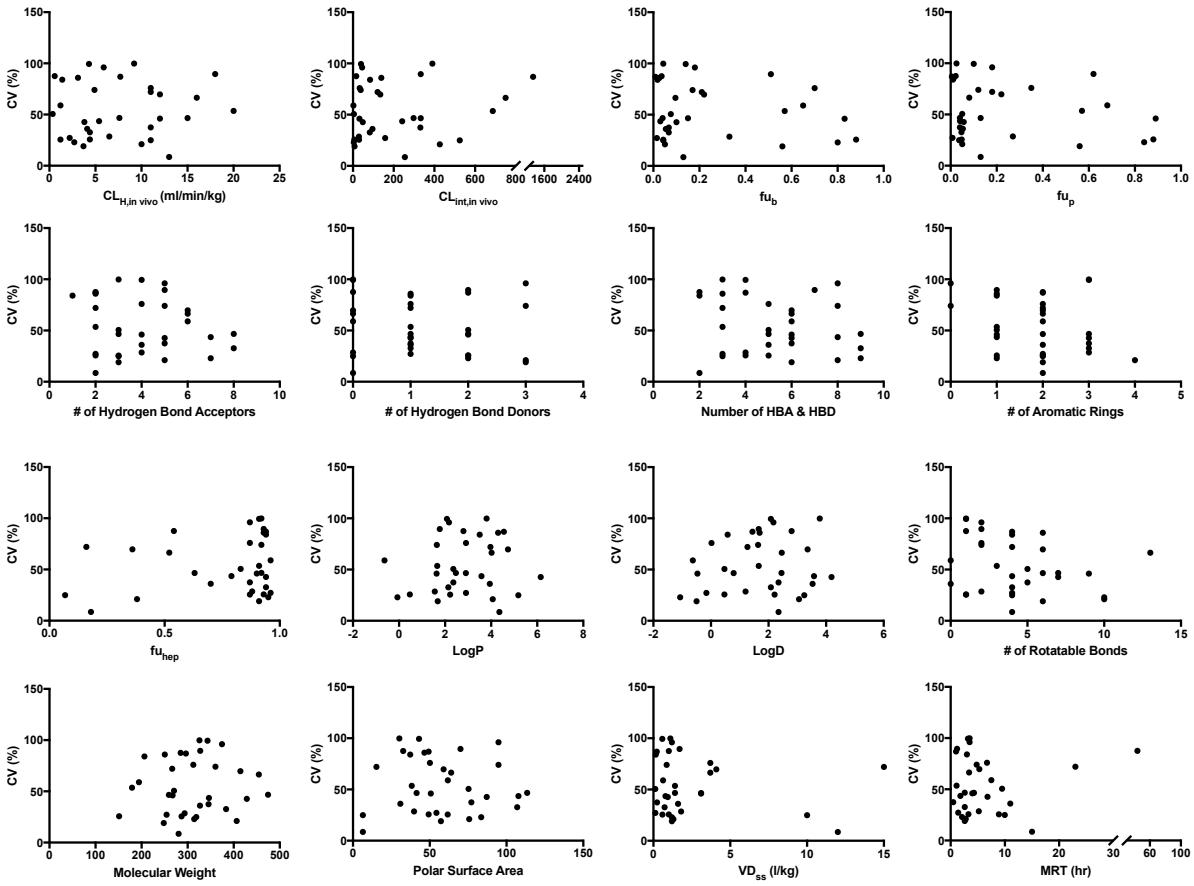

Figure 7.2: Trends between various physicochemical and pharmacokinetic properties and CV.

Table 7.3: Highest correlations, R^2, of CV with parameters.

	#Rot Bonds	#Aromatic Rings	$f_{u,hep}$	$f_{u,p}$	#HBD & HBA
CV	0.071	0.059	0.037	0.031	0.027

Table 7.4: Median parameter values for compounds with lower vs. higher CV values with (n).

CV	$f_{u,B}$	$f_{u,p}$	# Rot Bonds	HBA & HBD	LogD	$CL_{H,\ in\ vivo}$	LogP	PSA	HBA	VD_{ss}	$CL_{int,\ in\ vivo}$	MRT	$f_{u,hep}$	MW	# Aromatic Rings	HBD
<50%	0.067 (17)	0.053 (17)	4.0 (17)	6.0 (17)	2.2 (17)	5.4 (17)	2.5 (17)	57 (17)	4.0 (17)	1.2 (17)	96 (17)	3.3 (17)	0.88 (17)	314 (17)	2.0 (17)	1.0 (17)
≥50%	0.16 (16)	0.11 (16)	2.5 (16)	4.5 (16)	1.7 (16)	6.8 (16)	2.9 (16)	50 (16)	3.5 (16)	1.1 (15)	103 (16)	3.5 (15)	0.91 (16)	304 (16)	2.0 (16)	1.0 (16)

BDDCS class, molecular species, and main metabolizing enzymes were also examined. BDDCS Class 1 drugs appeared to have a wider range of CV values than Class 2 drugs (Fig. 7.3A). When examining molecular species, neutral drugs had the highest CV values (Fig. 7.3B). Looking at main metabolizing enzymes, compounds metabolized by CYP3A4 appeared to have the highest CV values (Fig. 7.3C). For CYP3A4 substrates, 38% had a CV > 90%, while no CYP2D6, CYP1A2, CYP2C, and UGT substrates had CVs > 90%.

Given the difference seen between BDDCS classes, the data were also split by class 1 and class 2 compounds (n=21 and 11 respectively). Examining the same physiochemical properties with CV for both classes, there were no correlations for BDDCS class 1 compounds (every R^2 value was less than 0.10). For BDDCS class 2 though, there were potential trends (Fig. 7.4A). The number of HBA and HBD and number of aromatic rings had the largest correlations, however the smaller number of compounds should be noted. The lack of correlation with BDDCS class 1 compounds is shown in Fig. 7.4B for comparison.

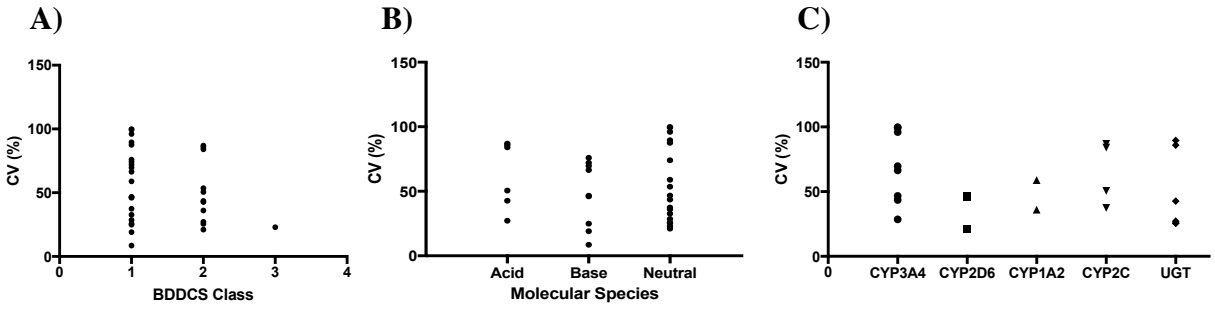

Figure 7.3: Trends between CV and BDDCS class (A), molecular species (B), and main metabolizing enzyme (C).

A)

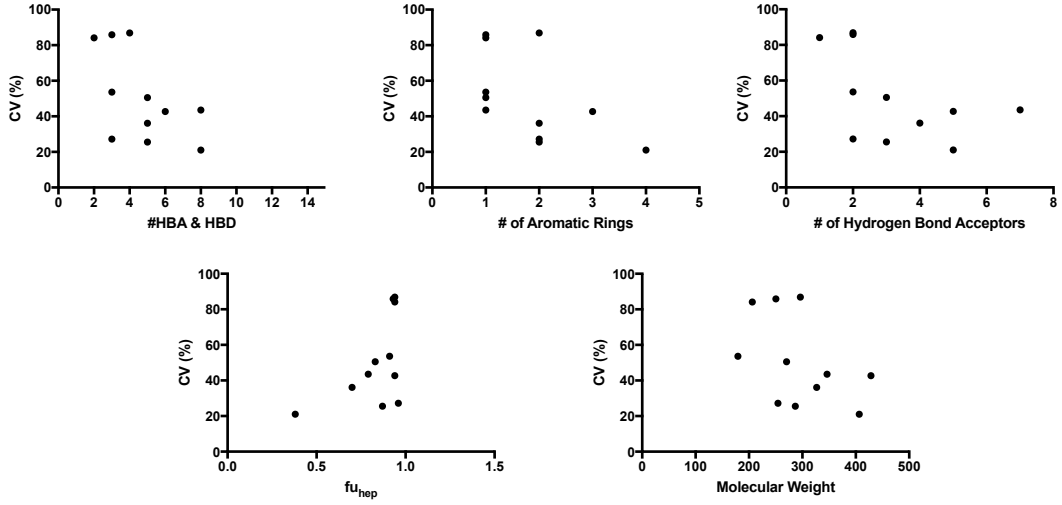

R^2	#HBA & HBD	#Aromatic Rings	#HBA	$f_{u,hep}$	MW
CV	0.33	0.30	0.29	0.27	0.22

B)

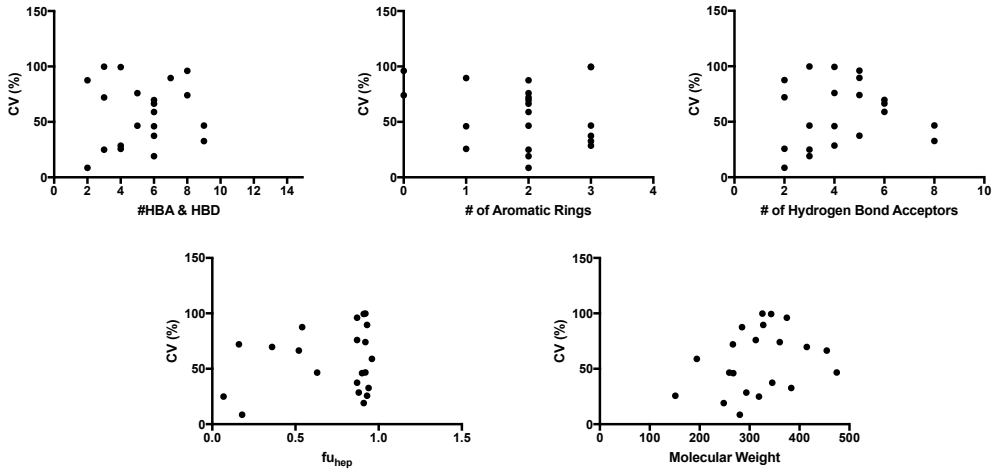

R^2	#HBA & HBD	#Aromatic Rings	#HBA	$f_{u,hep}$	MW
CV	0.0031	0.036	0.0063	0.038	0.082

Figure 7.4: The highest correlations of CV with physicochemical properties for BDDCS class 2 compounds (A) and the lack of correlation for BDDCS class 1 compounds (B).

Uniformity of Predictions and Physicochemical Parameters

Next the variability relating to the accuracy of predictions was examined. Accurate predictions are typically defined as predictions that fall within two fold of observed values (15, 16, 17). Here, if a compound had predictions all falling either within two-fold or outside two-fold, it was categorized as "uniform". If a compound had some predictions falling within two-fold, and some falling outside two-fold, it was categorized as "non-uniform". The same properties were then examined to determine if any drive the difference between the two categories.

Returning to the 50 compiled compounds, there were 31 uniform compounds and 19 non-uniform compounds. Of the uniform predictions, 6 (19%) were accurate predictions, and 25 (81%) were inaccurate underpredictions. The most distinct difference between the uniform and non-uniform categories was seen with $CL_{int,\ in\ vivo}$. Compounds with uniform predictions typically had higher $CL_{int,in\ vivo}$ values (Fig. 7.5). Furthermore, 37% of non-uniform predictions had $CL_{int,\ in\ vivo}$ values <10 ml/min/kg compared to 10% of uniform predictions.

Accuracy of predictions and physicochemical parameters

Finally, all 31 compounds with uniform predictions were further examined. It is expected that new understandings of mechanisms will help reduce the current IVIVE underprediction, but for now, it is important to know which new compounds may yield results that will be accurate, and which may not. Here only 6 compounds had accurate predictions, limiting the power of the evaluation. Despite this, there were accuracy distinctions when considering logD, $CL_{int,\ in\ vivo}$, and $f_{u,p}$ (Table 7.4). Of the accurate predictions, 83% had a logD of <1.0 compared to 28% of inaccurate predictions. 42% of compounds with logD of <1.0 had

accurate predictions and 5.0% of compounds with logD ≥1.0 had accurate predictions. For $CL_{int, in\ vivo}$, 31% of compounds with $CL_{int, in\ vivo}$ <100 ml/min/kg had accurate predictions compared to 6.7% with $CL_{int, in\ vivo} \geq 100$. Finally, for $f_{u,p}$, 11% of predictions with $f_{u,p} < 0.1$ were accurate compared to 33% of predictions with $f_{u,p} \geq 0.1$.

Table 7.5: Properties of compounds with accurate, uniform predictions.

Parameter	#Accurate	#Inaccurate	%Accurate
LogD			
<1.0	5	7	41.7%
≥ 1.0	1	18	5.26%
$CL_{int, in\ vivo}$			
<100	5	11	31.3%
≥ 100	1	14	6.67%
$f_{u,p}$			
<0.1	2	17	10.5%
≥ 0.1	4	8	33.3%

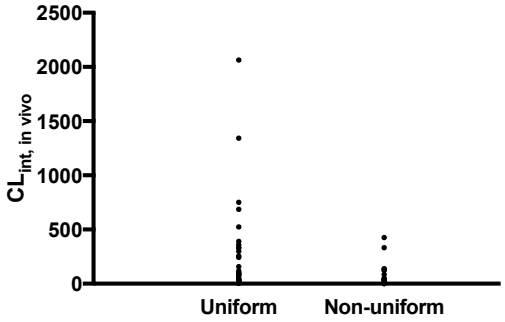

Figure 7.5: Relationship between compounds with uniform vs. non-uniform predictions and $CL_{int, in\ vivo}$

Discussion

Variability in the in vitro data generated and used for IVIVE can significantly affect clearance predictions. This compilation found varying reported data for 50 compounds. Of these, 33 had $n \geq 3$, and CV values for the same compound were as high as 99.8%. Trends were sought in hopes of determining in the future which new compounds may yield more reliable predictions than others. However, after confirming that variability was not dependent on n, no direct trends appeared with the physicochemical properties examined.

Upon more generally splitting the compounds into low and high CV groups though there appeared to be marked relative differences in the median values for $f_{u,B}$ and $f_{u,p}$ and the average number of rotatable bonds. After further examining the binding values though, an obvious trend did not appear. For $f_{u,B}$, 35% of the low CV group had high protein binding ($f_u \leq 0.05$) and 31% of the high CV group also had high binding. A similar result was seen with $f_{u,p}$ where 47% of the low CV group had high protein binding and 38% of the high CV group did also. A difference did hold for rotatable bonds where in the lower CV half, 29% of compounds had ≥ 7 rotatable bonds compared to 6.3% of compounds with higher CV. It has previously been shown that decreasing rotatable bond count is paralleled by increasing permeation rate (18), and here this may lead to larger variability. Wood et al. (19) previously examined the importance of the unstirred water layer (UWL) on clearance predictions with hepatocytes. Given that the UWL has been shown to reduce the apparent permeability of highly permeable compounds, the authors showed that shaking of incubations can lead to 3 to 5-fold higher CL_{int} values (19). Perhaps the increase in variability noted with lower rotatable bond counts (and thus higher permeability) could be related to experimental differences for incubation shaking among laboratories and moving forward, this factor should be considered for new chemical entities.

Interestingly BDDCS class 1 drugs had a larger CV range than BDDCS class 2 drugs and neutral drugs had more variation than acidic or basic. Although the number of drugs with main metabolizing enzyme information was more limited, CYP3A4 substrates had higher CV values, perhaps due to the potential of extrahepatic metabolism. When examining R^2 values with class 2 drugs and different properties, the number of HBA and HBD stood out, which has also been shown to be related to permeation rate (18, 20). As more data are generated and shared, it would be useful to reevaluate these potential trends and their statistical significance with a larger sample size.

Some compounds had large CV values, however upon further examination, no matter which value was used, the predictions would have fallen outside of two-fold of the observed value and been considered inaccurate. For instance for triazolam that had a CV of 99.9%, data from three sources underpredicted by 3.8, 14, and 29 fold. For these cases, the compounds were deemed to have "uniform" predictions. The main difference noted between uniform and non-uniform compounds was that uniform compounds had higher $CL_{int,\ in\ vivo}$ values. The majority of the uniform compounds were uniformly inaccurate (80%), and all of these inaccurate compounds were underpredicted. This is not unexpected given the high inaccuracy previously reported (1, 2) and emphasizes the need to find a mechanistic reason for the underprediction. It has been noted that compounds with high $CL_{int,in\ vivo}$ commonly have large error (2, 21, 22), which explains why these compounds would have uniform inaccurate predictions. More low clearance ($CL_{int,\ in\ vivo}$<10 ml/min/kg) compounds fell in the non-uniform category, confirming the experimental challenges for low turnover compounds (5, 23).

Finally, trends in accuracy for the 31 compounds with uniform predictions were examined. More or less confidence could theoretically be placed in a new compound's

extrapolation results if any trends exist and accordingly more or less experiments may be needed. Of the 50 drugs examined, only 6 compounds had uniform accurate predictions, limiting the power of the evaluation. Of the accurate compounds, there were 5 accurate BDDCS class 1 and 0 accurate class 2 compounds (the 6th accurate compound was class 3) supporting the hypothesis that class 1 drugs would have more accurate predictions (1). Based on this dataset it appears that less lipophilic, lower intrinsic clearance, and lower protein binding compounds have more accurate predictions. The intrinsic clearance finding agrees with the idea of CL_{int} dependent underprediction mentioned earlier, and the protein binding finding agrees with previous studies concluding that highly bound compounds have more inaccuracy (24, 25). It will be useful to reevaluate these trends as more uniform, accurate data are generated for compounds.

Conclusions

This investigation highlights the interlaboratory variability in generated CL_{int} values and the need for consistent and improved methodologies. Compounds with lower rotatable bond counts and therefore higher permeability had more variability, perhaps due to experimental differences in incubation shaking and the role of the unstirred water layer. Compounds with uniform predictions typically had higher $CL_{int,\ in\ vivo}$ values and uniform underpredictions, confirming a lack of mechanistic understanding with IVIVE; while compounds with non-uniform predictions typically had lower $CL_{int,\ in\ vivo}$ values, reaffirming the current experimental challenges for compounds falling within this clearance range. While only a limited number of uniform predictions were accurate, lipophilicity, intrinsic clearance, and protein binding may be determinants of accurate IVIVE.

References

(1) Bowman CM and Benet LZ (2016) Hepatic clearance predictions from in vitro-in vivo extrapolation and the biopharmaceuitcs drug disposition classification system. *Drug Metab Dispos* **44:**1731-1735.

(2) Wood FL, Houston JB and Hallifax D (2017) Clearance prediction methodology needs fundamental improvement: trends common to rat and human hepatocytes/microsomes and implications for experimental methodology. *Drug Metab Dispos* **45:**1178-1188.

(3) Sohlenius-Sternbeck AK, Jones C, Ferguson D, Middleton BJ, Projean D, Floby E, Bylund J and Afzelius L (2012) Practical use of the regression offset approach for the prediction of in vivo intrinsic clearance from hepatocytes. *Xenobiotica* **42:**841-853.

(4) Nagilla R, Frank KA, Jolivette LJ and Ward KW (2006) Investigation of the utility of published in vitro intrinsic clearance data for prediction of in vivo clearance. *J Pharmacol Toxicol Methods* **53:**106-116.

(5) Stringer R, Nicklin PL and Houston JB (2008) Reliability of human cryopreserved hepatocytes and liver microsomes as in vitro systems to predict metabolic clearance. *Xenobiotica* **38:**1313-1329.

(6) Hakooz N, Ito K, Rawden H, Gill H, Lemmers L, Boobis AR, Edwards RJ, Carlile DJ, Lake BG and Houston JB (2006) Determination of a human hepatic microsomal scaling factor for predicting in vivo drug clearance. *Pharm Res* **23:**533-539.

(7) Barter ZE, Bayliss MK, Beaune PH, Boobis AR, Carlile DJ, Edwards RJ, Houston JB, Lake BG, Lipscomb JC, Pelkonen OR, Tucker GT and Rostami-Hodjegan, A (2007) Scaling factors for the extrapolation of in vivo metabolic drug clearance from in vitro data: reaching a consensus on values of human microsomal protein and hepatocellularity per gram liver. Curr Drug Metab **8:**33-45.

(8) Hallifax D, Galetin A and Houston JB (2008) Prediction of metabolic clearance using fresh human hepatocytes: comparison with cryopreserved hepatocytes and hepatic microsomes for five benzodiazepines. *Xenobiotica* **38:**353-367.

(9) Floby E, Johansson J, Hoogstraate J, Hewitt NJ, Hill J and Sohlenius-Sternbeck A-K (2009) Comparison of intrinsic metabolic clearance in fresh and cryopreserved human hepatocytes. *Xenobiotica* **39:**656-662.

(10) Gaulton A, Hersey A, Nowotka M, Bento AP, Chambers J, Mendez D, Mutowo P, Atkinson F, Bellis LJ, Cibrián-Uhalte E, Davies M, Dedman N, Karlsson A, Magariños MP, Overington JP, Papadatos G, Smit I and Leach AR (2017) The ChEMBL database in 2017. *Nucleic Acids Res* **45:**D945-D954.

(11) Obach RS, Lombardo F and Waters NJ (2018) Trend analysis of a database of intravenous pharmacokinetic parameters in humans for 670 drug compounds. Drug Metab Dispos **36:**1385-1405.

(12) Benet LZ, Broccatelli F, Oprea TI (2011) BDDCS applied to over 900 drugs. *AAPS J* **13:**519-547.

(13) Hosey CM, Chan R, Benet LZ (2016) BDDCS predictions, self-correcting aspects of BDDCS assignments, BDDCS assignment corrections, and classification for more than 175 additional drugs. *AAPS J* **18:**251-260.

(14) El-Kattan AF, Varma MV, Steyn SJ, Scott DO, Maurer TS and Bergman A (2016) Projecting ADME behavior and drug-drug interactions in early discovery and development: application of the extended clearance classification system. *Pharm Res* **33:**3021-3033.

(15) Houston JB and Carlile DJ (1997) Prediction of hepatic clearance from microsomes, hepatocytes, and liver slices. *Drug Metab Rev* **29:**891-922.

(16) Obach RS, Baxter JG, Liston TE, Silber BM, Jones BC, MacIntyre F, Rance, DJ and Wastall P (1997) The prediction of human pharmacokinetic parameters from preclinical and in vitro metabolism data. *J Pharmacol Exp Ther* **283:**46-58.

(17) McGinnity DF, Soars MG, Urbanowicz RA and Riley RJ (2004) Evaluation of fresh and cryopreserved hepatocytes as in vitro drug metabolism tools for the prediction of metabolic clearance. *Drug Metab Dispos* **32:**1247-1253.

(18) Verber DF, Johnson SR Cheng H-Y, Smith BR Ward KW and Kopple KD (2002) Molecular properties that influence the oral bioavailability of drug candidates. *J Med Chem* **45:**2615-2623.

(19) Wood FL, Houston JB and Hallifax D (2018) Importance of the unstirred water layer and hepatocyte membrane integrity in vitro for quantification of intrinsic metabolic clearance. *Drug Metab Dispos* **46:**268-278.

(20) Clark DE (1999) Rapid calculation of polar molecular surface area and its application to the prediction of transport phenomena. 1. Prediction of intestinal absorption. *J Pharm Sci* **88:**807-814.

(21) Hallifax D, Foster JA and Houston JB (2010) Prediction of human metabolic clearance from in vitro systems: retrospective analysis and prospective view. *Pharm Res* **27:**2150-2161.

(22) Foster JA, Houston JB and Hallifax D (2011) Comparison of intrinsic clearances in human liver microsomes and suspended hepatocytes from the same donor livers: clearance-dependent relationship and implications for prediction of in vivo clearance. *Xenobiotica* **41:**124-136.

(23) Di L and Obach RS (2015) Addressing the challenges of low clearance in drug research. *AAPS J* **17:**352-357.

(24) Baker M and Parton T (2007) Kinetic determinants of hepatic clearance: plasma protein binding and hepatic uptake. *Xenobiotica* **37:**1110-1134.

(25) Soars MG, McGinnity DF, Grime K and Riley RJ (2007) The pivotal role of hepatocytes in drug discovery. *Chem Biol Interact* **168:**2-15.

(26) Akabane T, Gerst N, Naritomi Y, Masters JN and Tamura K (2012) A practical and direct comparison of intrinsic metabolic clearance of several non-CYP enzyme substrates in freshly isolated and cryopreserved hepatocytes. *Drug Metab Pharmacokinet* **27:**181-191.

(27) Blanchard N, Alexandre E, Abadie C, Lavé T, Heyd B, Mantion G, Jaeck D, Richert L and Coassolo P (2005) Comparison of clearance predictions using primary cultures and suspensions of human hepatocytes. *Xenobiotica* **35:**1-15.

(28) Hallifax D, Rawden HC, Hakooz N and Houston JB (2005) Prediction of metabolic clearance using cryopreserved human hepatocytes: kinetic characteristics for five benzodiazepines. *Drug Metab Dispos* **33:**1852-1858.

(29) Jacobson L, Middleton B, Holmgren J, Eirefelt S, Fröjd M, Blomgren A and Gustavsson L (2007) An optimized automated assay for determination of metabolic stability using hepatocytes: assay validation, variance component analysis, and in vivo relevance. *Assay Drug Dev Technol* **5:**403-415.

(30) Lau YY, Sapidou E, Cui X, White RE and Cheng K-C (2002) Development of a novel in vitro model to predict hepatic clearance using fresh, cryopreserved, and sandwich-cultured hepatocytes. *Drug Metab Dispos* **30:**1446-1454.

(31) Lu C, Li P, Gallegos R, Uttamsingh V, Xia CQ, Miwa GT, Balani SK and Gan L-S (2006) Comparison of intrinsic clearance in liver microsomes and hepatocytes from rats and humans: evaluation of free fraction and uptake in hepatocytes. *Drug Metab Dispos* **34:**1600-1605.

(32) Naritomi Y, Terashita S, Kagayama A and Sugiyama Y (2003) Utility of hepatocytes in predicting drug metabolism: comparison of hepatic intrinsic clearance in rats and humans in vivo and in vitro. *Drug Metab Dispos* **31:**580-588.

(33) Riley RJ, McGinnity DF and Austin RP (2005) A unified model for predicting human hepatic, metabolic clearance from in vitro intrinsic clearance data in hepatocytes and microsomes. *Drug Metab Dispos* **33:**1304-1311.

(34) Soars MG, Burchell B and Riley RJ (2002) In vitro analysis of human drug glucuronidation and prediction of in vivo metabolic clearance. *J Pharmacol Exp Ther* **301:**382-390.

(35) Sohlenius-Sternbeck A-K, Afzelius L, Prusis P, Neelissen J, Hoogstraate J, Johansson J, Floby E, Bengtsson A, Gissberg O, Sternbeck J and Petersson C (2010) Evaluation of the human prediction of clearance from hepatocyte and microsome intrinsic clearance for 52 drug compounds. *Xenobiotica* **40:**637-649.

CHAPTER 8: Conclusions

Clearance is a crucial pharmacokinetic parameter that is further linked to drug exposure, half life, and dosing regimen. Accurately predicting the hepatic clearance of compounds is necessary to reduce the cost and time associated with the current drug discovery and development process, and is commonly done using IVIVE. However as discovered in this dissertation research, there is high error surrounding these IVIVE predictions and new mechanisms are needed to more fully understand the clearance process.

In Chapter 3 we found high percentages of prediction inaccuracies (based on whether predictions fell more than two fold outside of their observed clearance values), with human microsome data having 66.8% inaccuracy and human hepatocyte data having 66.5% inaccuracy. Since compounds with poor IVIVE are typically substrates for transporters, we hypothesized that BDDCS class 1 drugs that appear to overwhelm transporter effects, would have more accurate predictions than BDDCS class 2 drugs. While this was true with class 1 drugs being 62.3% inaccurate and class 2 drugs being 81.9% inaccurate, there was still high inaccuracy in both cases. We also found that highly protein bound drugs in both classes had high inaccuracy (81.3% of highly protein bound class 1 drugs and 85.7% of highly protein bound class 2 drugs were inaccurate). These results highlighted that IVIVE must be improved through a better understanding of clearance mechanisms since traditional in vitro methods often yield inaccurate predictions and utilizing BDDCS class currently cannot distinguish between accurate and inaccurate predictions.

As discussed in Chapter 4, groups have also suggested that IVIVE error increases with increasing in vivo CL_{int} due to endogenous cofactor depletion or permeability limitation for example. While this trend is important for understanding the limitations of in vitro systems, CL_H

is the parameter that must be estimated for first-in-human dose predictions and we found a similar trend of CL_H-dependent underprediction. The majority of high extraction ratio drugs were not predicted to have high or even intermediate extraction ratios. This study again highlighted a need for improved prediction methodologies as the underprediction could be due to CL_{int} error, errors in protein binding measurements or the understanding of protein-facilitated uptake, or yet to be determined mechanisms.

In Chapter 5 we propose an innovative hypothesis called a transporter-induced protein-binding shift to help mitigate IVIVE error and provide a new explanation for protein-facilitated uptake. In Chapter 2 we discussed previous explanations of protein-facilitated uptake that included a specific albumin receptor on the hepatocyte surface, the rate-limiting dissociation of ligand from the albumin-ligand complex, the rate-limiting diffusion of ligand through the unstirred water layer, and more general interactions with the hepatocyte cell surface. None of these hypotheses considered the role of hepatic uptake transporters. With the TIPBS hypothesis, high affinity binding to these transporters, such as OATPs, may change the equilibrium of the nonspecific binding between drugs and plasma proteins, leading to higher clearance than currently predicted as depicted in Figure 8.1. Using rat hepatocytes in incubations with protein-free buffer and 100% plasma, the uptake of two lower protein binding OATP substrates, pravastatin and rosuvastatin, and two higher protein binding OATP substrates, atorvastatin and pitavastatin was measured. Decreased $K_{m,u}$ values and increased CL_{int} values were seen in the plasma incubations for the highly bound compounds, while more similar values were found between incubations for the lower binding compounds. These results supported our new hypothesis and help mitigate the IVIVE underprediction previously seen for highly bound transporter substrates.

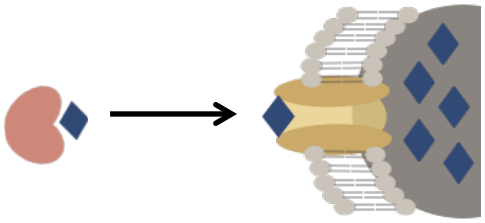

Figure 8.1: A transporter-induced protein-binding shift may lead to greater uptake, and therefore greater clearance, than currently predicted.

We hypothesize that a TIPBS can occur with any type of plasma protein and anywhere in the body where there is interplay between proteins, cells, and transporters. In Chapter 6 we used HEK293 cells overexpressing OATP1B1 and OATP1B3 in protein-free buffer and 100% human plasma incubations to explore the uptake of four OATP substrates (pravastatin, rosuvastatin, repaglinide and pitavastatin). Here any shifts that occur would be due to the overexpression of transporters, not the hepatocyte cell surface. We again saw decreased $K_{m,u}$ values and increased CL_{int} values as plasma protein binding increased, also supporting the idea of a transporter-induced protein binding shift, where high protein binding may not limit the uptake of compounds that have high affinity for transporters.

Finally, in Chapter 7 we examined trends in clearance prediction accuracy using physiochemical and pharmacokinetic parameters. When trying to determine which drugs have accurate IVIVE results and which do not, it was noted that there can be large variability in the predictions for the same drug. Data for 50 compounds were compiled and coefficients of variation were as high as 99.8% for individual compounds. Examining median values, compounds with a lower number of rotatable bonds had more variability, suggesting that perhaps differences in experimental procedures (such as the amount of shaking during incubation) could yield different results. Prediction uniformity was also examined and compounds with uniform underpredictions had higher $CL_{int,\ in\ vivo}$ values, while those with non-uniform predictions

typically had lower $CL_{int, in\ vivo}$ values, highlighting the experimental challenges with low turnover compounds. Finally, based on the small number of compounds that were uniformly predicted accurately, less lipophilic, lower intrinsic clearance, and lower protein binding compounds yielded more accurate clearance predictions (Figure 8.2), which may provide confidence in IVIVE predictions for new compounds with these characteristics.

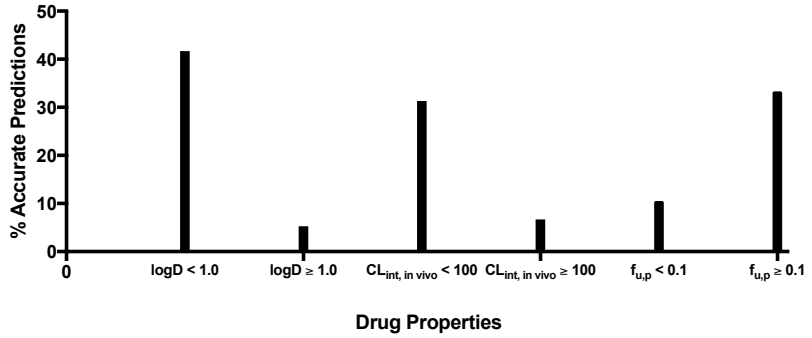

Figure 8.2: Compounds with lower lipophilicity (logD <1.0), lower intrinsic clearance ($CL_{int, in\ vivo}$ <100), and lower protein binding ($f_{u,p} \geq 0.1$) have more accurate predictions.

This thesis sheds light on the current errors seen with IVIVE. Highly protein-bound drugs and those with high extraction ratios in particular were found to have high prediction errors. There was also often high inter-laboratory variability in the predictions for the same drug. We propose the concept of a transporter-induced protein binding shift, which reevaluates the role of protein-binding in IVIVE. Based on our findings, we suggest that when evaluating highly protein bound substrates of transporters, assays should be conducted with 100% plasma to more accurately capture the true in vivo clearance. We also found that compounds with higher lipophilicty, higher intrinsic clearance, or higher protein binding may need additional experiements beyond the traditional IVIVE to accurately estimate clearance. These ideas as well as additional novel hypotheses are needed to continue to improve hepatic clearance predictions.

Appendix Table 1: Compiled IVIVE predictions and BDDCS classifications

Author (System)	Drug	CL Predicted	CL Observed	Fold Dif	BDDCS Class	$f_{u,B}$
Brown et al. (16)						
(Hepatocytes)						
	Furosemide	0.91	162	178.02	4	0.022
	Ketoprofen	4.7	129	27.45	2	0.018
	Mephenytoin	3.6	64	17.78	2	0.714
	Timolol	4.4	77	17.50	1	0.476
	Metoprolol	4.3	75	17.44	1	0.788
	Lorazepam	0.95	14	14.74	1	0.090
	Tolbutamide	0.38	4.9	12.89	2	0.067
	Gemfibrozil	5.5	67	12.18	2	0.055
	Propranolol	39	454	11.64	1	0.157
	Terfenadine	4136	43333	10.48	2	0.030
	Dextromethorphan	172	1482	8.62	1	0.284
	Naproxen	1.4	11	7.86	2	0.018
	Imipramine	49	380	7.76	1	0.094
	Lidocaine	21	157	7.48	1	0.337
	Ibuprofen	12	80	6.67	2	0.018
	Diltiazem	19	125	6.58	1	0.220
	Triazolam	11	66	6.00	1	0.132
	Diclofenac	98	561	5.72	2	0.018
	Oxazepam	6.9	34	4.93	2	0.045
	Flunitrazepam	4.5	20	4.44	1	0.282
	Nifedipine	146	597	4.09	2	0.068
	Quinidine	18	61	3.39	1	0.149
	S-Warfarin	1.9	6.1	3.21	2	0.018
	Diazepam	6.6	18	2.73	1	0.040
	Desipramine	74	167	2.26	1	0.188
	Bufuralol	45	99	2.20	1	0.238
	Propofol	2773	5052	1.82	2	0.016
	Alprazolam	2.1	3.7	1.76	1	1.000
	Midazolam	200	314	1.57	1	0.076
	Chlorpromazine	188	267	1.42	1	0.043
	Methylprednisolone	33	45	1.36	1	0.220
	Antipyrine	0.67	0.69	1.03	1	0.970
	Caffeine	2.1	2	0.95	1	0.651
	Prednisolone	30	27	0.90	1	0.100
	Theophylline	2.6	2.1	0.81	1	0.530
	Naloxone	284	200	0.70	1	0.459
	Codeine	35	19	0.54	1	0.930

Author (System)	Drug	CL Predicted	CL Observed	Fold Dif	BDDCS Class	$f_{u,B}$
Hallifax et al. (17)						
(Microsomes)						
	Prochlorperazine	199	29240	146.93	1	0.003
	Theophylline	0.03	2.61	87.00	1	0.53
	Felodipine	98	4300	43.88	2	0.003
	Mianserin	34.6	1463	42.28	1	0.14
	FK1052	40	1600	40.00	-	0.021
	Amitriptyline	13	490	37.69	1	0.058
	Clozapine	4.4	160	36.36	2	0.051
	Propranolol	7.8	267	34.23	1	0.14
	Mexiletine	0.77	26	33.77	1	0.39
	Lidocaine	3.1	82.1	26.48	1	0.33
	Methoxsalen	38	1000	26.32	2	0.13
	Promazine	62.8	1595	25.40	1	0.029
	Phenytoin	0.16	4	25.00	2	0.12
	Labetalol	18.4	450	24.46	1	0.32
	Ondansetron	1.7	31.8	18.71	1	0.27
	Imipramine	18	318	17.67	1	0.13
	Promethazine	76.3	1318	17.27	1	0.023
	Lorcainide	48	710	14.79	1	0.30
	Phenacetin	42.3	615	14.54	2	0.60
	Dofetilide	0.4	4.5	11.25	3	0.36
	Quinidine	3.2	34.2	10.69	1	0.15
	Warfarin	0.49	4.5	9.18	2	0.005
	Indinavir	16	130	8.13	2	0.39
	Prednisone	2.6	21	8.08	2	0.10
	Omeprazole	67	520	7.76	1	0.068
	Desipramine	16	118	7.38	1	0.25
	Ibuprofen	8.2	59.1	7.21	2	0.015
	Nilvadipine	1200	8400	7.00	2	0.016
	FK480	51	340	6.67	-	0.008
	Glyburide	57.9	385	6.65	2	0.004
	Caffeine	0.43	2.82	6.56	1	0.65
	Trimipramine	205	1344	6.56	2	0.051
	Buprenorphine	449	2938	6.54	1	0.040
	Clomipramine	192	1047	5.45	1	0.022
	Fluphenazine	302	1581	5.24	2	0.012
	Dexamethasone	2.9	14	4.83	1	0.34
	Ketamine	28.6	138	4.83	1	0.59
	Antipyrine	0.14	0.6	4.29	1	0.97
	Diclofenac	108	418	3.87	2	0.014
	Methohexital	47	180	3.83	1	0.39

Author (System)	Drug	CL Predicted	CL Observed	Fold Dif	BDDCS Class	$f_{u,B}$
	Diltiazem	40.6	143	3.52	1	0.20
	Metoprolol	18	62.2	3.46	1	0.80
	Fenoprofen	13.5	34.3	2.54	2	0.018
	Flunitrazepam	5	12.7	2.54	1	0.28
	Propafenone	133	328	2.47	2	0.059
	Alprenolol	48.5	117	2.41	1	0.27
	Tolbutamide	1.2	2.82	2.35	2	0.16
	Chlorpheniramine	2	4.62	2.31	1	0.30
	Gemfibrosil	30.1	68.4	2.27	2	0.036
	Tenoxicam	1.6	3.33	2.08	1	0.013
	Verapamil	193	310	1.61	1	0.12
	Bepridil	992	1583	1.60	1	0.005
	Nicardipine	1200	1900	1.58	1	0.068
	Amobarbital	0.89	1.4	1.57	1	0.26
	Diazepam	10	15.3	1.53	1	0.036
	Zolpidem	23.1	31.9	1.38	1	0.17
	Chlorpromazine	208	287	1.38	1	0.053
	Bupivacaine	83	110	1.33	1	0.068
	Tenidap	7.9	8.3	1.05	2	0.001
	Alprazolam	2	2.08	1.04	1	0.64
	Risperidone	43.3	43	0.99	1	0.17
	YW796	15	14	0.93	-	0.63
	Sildenafil	121	89.8	0.74	1	0.094
	Triazolam	43.5	30.6	0.70	1	0.17
	Domperidone	520	275	0.53	2	0.060
	Trazodone	65.4	32.3	0.49	2	0.061
	Midazolam	708	134	0.19	1	0.072
	Glimepiride	35.4	5.1	0.14	2	0.14
Hallifax et al. (17)						
(Hepatocytes)						
	Prochlorperazine	45.6	29240	641.23	1	0.003
	Furosemide	0.91	84.9	93.30	4	0.022
	Buprenorphine	40	2938	73.45	1	0.040
	Mianserin	22.3	1463	65.61	1	0.14
	Fluoxetine	5.3	228	43.02	1	0.060
	Levoprotiline	8.1	261	32.22	1	0.19
	Labetalol	16.4	450	27.44	1	0.32
	Promazine	64.6	1595	24.69	1	0.029
	Fluphenazine	69.9	1581	22.62	2	0.012
	Glyburide	17.2	385	22.38	2	0.004
	Phenacetin	36.2	615	16.99	2	0.60

Author (System)	Drug	CL Predicted	CL Observed	Fold Dif	BDDCS Class	$f_{u,B}$
	Montelukast	96.3	1503	15.61	2	0.001
	Lorazepam	1	14.2	14.20	1	0.090
	Promethazine	101	1318	13.05	1	0.023
	Metoprolol	5.3	62.2	11.74	1	0.80
	Cyclosporin A	13.5	152	11.26	2	0.040
	Flumazenil	16.3	183	11.23	1	0.52
	Timolol	4.4	49.3	11.20	1	0.48
	Trimipramine	138	1344	9.74	2	0.051
	Clomipramine	109	1047	9.61	1	0.022
	Verapamil	33.4	310	9.28	1	0.12
	Propranolol	29.2	267	9.14	1	0.14
	Temazepam	5.7	51.4	9.02	1	0.027
	Diltiazem	16	143	8.94	1	0.20
	Ondansetron	3.9	31.8	8.15	1	0.27
	Clozapine	20.8	160	7.69	2	0.051
	Imipramine	42.8	318	7.43	1	0.13
	Tolbutamide	0.38	2.82	7.42	2	0.16
	Glipizide	7.1	50.3	7.08	2	0.020
	Ketoprofen	11	77.5	7.05	2	0.017
	Prazosin	6.2	39.7	6.40	1	0.085
	Diphenhydramine	16	94.2	5.89	1	0.19
	Oxazepam	6.9	38.5	5.58	2	0.045
	Lidocaine	15.3	82.1	5.37	1	0.33
	Diclofenac	86.8	418	4.82	2	0.014
	Bepridil	337	1583	4.70	1	0.005
	Indomethacin	27.1	126	4.65	2	0.020
	Propafenone	76.4	328	4.29	2	0.059
	Naproxen	1.4	5.86	4.19	2	0.018
	Oxaprozin	24.4	100	4.10	2	0.001
	Zolpidem	8	31.9	3.99	1	0.17
	Sildenafil	24.4	89.8	3.68	1	0.094
	Diflunisal	9.9	34.3	3.46	2	0.005
	Ketamine	40.5	138	3.41	1	0.59
	Bupivacaine	32.6	110	3.37	1	0.068
	Triprolidine	39.6	130	3.28	1	0.10
	Domperidone	88.1	275	3.12	2	0.060
	Ritonavir	30.5	86.1	2.82	2	0.015
	Flunitrazepam	4.5	12.7	2.82	1	0.28
	Morphine	64.6	179	2.77	1	0.77
	Gemfibrosil	24.9	68.4	2.75	2	0.036
	Desipramine	45.3	118	2.60	1	0.25
	Acetaminophen	2.5	6.28	2.51	1	0.79
	Triazolam	12.3	30.6	2.49	1	0.17

Author (System)	Drug	CL Predicted	CL Observed	Fold Dif	BDDCS Class	$f_{u,B}$
	Diazepam	6.6	15.3	2.32	1	0.036
	Irbesartan	58.8	118	2.01	2	0.040
	Quinidine	18	34.2	1.90	1	0.15
	Trazodone	17.4	32.3	1.86	2	0.061
	Alprenolol	64.5	117	1.81	1	0.27
	Ibuprofen	32.6	59.1	1.81	2	0.015
	Carvedilol	282	500	1.77	2	0.030
	Oxprenolol	14.9	26.2	1.76	1	0.30
	S-Warfarin	1.9	3.31	1.74	2	0.018
	Chlorpromazine	182	287	1.58	1	0.053
	Ranitidine	3	4.38	1.46	3	0.77
	Bufuralol	45	64.5	1.43	1	0.24
	Methylprednisolone	33	45	1.36	1	0.22
	Scopolamine	19.6	26.7	1.36	1	0.88
	Caffeine	2.1	2.82	1.34	1	0.65
	Nifedipine	146	196	1.34	2	0.068
	Fenoprofen	27.4	34.3	1.25	2	0.018
	Cimetidine	3.4	4.21	1.24	3	0.90
	Pindolol	7.8	9.58	1.23	1	0.55
	Metoclopramide	10	11.6	1.16	1	0.76
	Betaxolol	7.4	8.58	1.16	1	0.56
	Granisetron	29.7	33.5	1.13	1	0.70
	Acebutolol	5.1	5.33	1.05	1	0.96
	Theophylline	2.6	2.61	1.00	1	0.53
	Alprazolam	2.1	2.08	0.99	1	0.64
	Midazolam	138	134	0.97	1	0.072
	Prednisolone	30	27.1	0.90	1	0.10
	Antipyrine	0.67	0.6	0.90	1	0.97
	Etodolac	81.2	69.9	0.86	2	0.020
	Glimepiride	9.4	5.1	0.54	2	0.14
	Codeine	35	18.9	0.54	1	0.93
	Chlorpheniramine	9.4	4.62	0.49	1	0.30
	Nadolol	7.7	3.48	0.45	3	0.97
	Tenoxicam	8.8	3.33	0.38	1	0.013
	Carbamazepine	5.9	1.32	0.22	2	0.31
Ito et al. (18)						
(Microsomes)						
	Theophylline	0.033	3.5	106.06	1	
	Felodipine	98	4300	43.88	2	
	FK1052	40	1600	40.00	-	
	Amitriptyline	13	490	37.69	1	
	r-Warfarin	0.15	5.4	36.00	2	

Author (System)	Drug	CL Predicted	CL Observed	Fold Dif	BDDCS Class	$f_{u,B}$
	Mexiletine	0.77	26	33.77	1	
	Methoxsalen	38	1000	26.32	2	
	Diphenhydramine	2	52	26.00	1	
	Phenytoin	0.16	4	25.00	2	
	Propafenone	160	4000	25.00	2	
	Ketamine	26	550	21.15	1	
	Ondansetron	1.7	33	19.41	1	
	Diclofenac	35	630	18.00	2	
	Lidocaine	3.1	55	17.74	1	
	Imipramine	18	310	17.22	1	
	Chlorpromazine	24	370	15.42	1	
	Verapamil	120	1800	15.00	1	
	Lorcainide	48	710	14.79	1	
	Clozapine	4.4	59	13.41	2	
	Dofetilide	0.4	4.5	11.25	3	
	Tenidap	7.9	80	10.13	2	
	Ibuprofen	8.2	83	10.12	2	
	Desipramine	16	150	9.38	1	
	Warfarin	0.49	4.5	9.18	2	
	Caffeine	0.43	3.5	8.14	1	
	Indinavir	16	130	8.13	2	
	Prednisone	2.6	21	8.08	2	
	Zolpidem	20	160	8.00	1	
	Omeprazole	67	520	7.76	1	
	Nilvadipine	1200	8400	7.00	2	
	Quinidine	3.2	22	6.88	1	
	FK480	51	340	6.67	-	
	Midazolam	44	270	6.14	1	
	s-Warfarin	1	5.7	5.70	2	
	Dexamethasone	2.9	14	4.83	1	
	Methohexital	47	180	3.83	1	
	Propranolol	90	340	3.78	1	
	Hexobarbital	2.2	8.2	3.73	1	
	Diltiazem	81	300	3.70	1	
	Antipyrine	0.14	0.51	3.64	1	
	Diazepam	4.1	13	3.17	1	
	Triazolam	13	38	2.92	1	
	Phenacetin	19	46	2.42	2	
	Flunitrazepam	5	11	2.20	1	
	Diazepam	10	21	2.10	1	
	Tolbutamide	1.2	2	1.67	2	
	Nicardipine	1200	1900	1.58	1	
	Amobarbital	0.89	1.4	1.57	1	

Author (System)	Drug	CL Predicted	CL Observed	Fold Dif	BDDCS Class	$f_{u,B}$
	Alprazolam	2	3.1	1.55	1	
	Metoprolol	18	26	1.44	1	
	Tenoxicam	1.6	2.2	1.38	1	
	YW796	15	14	0.93	-	
McGinnity et al. (19)						
(Hepatocytes)						
	Imipramine	21	113	5.38	1	
	Fluoxetine	2.6	13	5.00	1	
	Desipramine	7.9	30	3.80	1	
	Propranolol	26	80	3.08	1	
	Morphine	63	180	2.86	1	
	Omeprazole	4.5	12	2.67	1	
	Ondansetron	3.7	8.4	2.27	1	
	Metoprolol	19	37	1.95	1	
	Zileuton	5.5	8.6	1.56	2	
	Doxepin	34	47	1.38	1	
	Bepridil	5.3	7.2	1.36	1	
	Ranitidine	2.6	3.4	1.31	3	
	Verapamil	46	60	1.30	1	
	Scopolamine	19	24	1.26	1	
	Diltiazem	24	30	1.25	1	
	Diphenhydramine	16	19	1.19	1	
	Cimetidine	3.2	3.8	1.19	3	
	Triprolidine	11	13	1.18	1	
	Triazolam	2.6	2.9	1.12	1	
	Acebutolol	4.8	5.2	1.08	1	
	Granisetron	24	24	1.00	1	
	Nifedipine	15	15	1.00	2	
	Clozapine	16	12	0.75	2	
	Betaxolol	6.6	4.8	0.73	1	
	Pindolol	7.4	5.3	0.72	1	
	Cyclosporin A	9.2	6.1	0.66	2	
	Bromocriptine	98	60	0.61	1	
	Prazosin	6.1	3.1	0.51	1	
	Diazepam	0.8	0.4	0.50	1	
	Dextromethorphan	20	8.6	0.43	1	
	Lorazepam	2.6	1.1	0.42	1	
	Ethinylestradiol	19	7.4	0.39	1	
	Bisoprolol	4.2	1.4	0.33	3	
	Isradipine	47	13	0.28	2	
	Midazolam	37	9.9	0.27	1	

Author (System)	Drug	CL Predicted	CL Observed	Fold Dif	BDDCS Class	$f_{u,B}$
	Caffeine	8.7	2.3	0.26	1	
	Temazepam	5.3	1.4	0.26	1	
	Ritonavir	5.5	1.3	0.24	2	
	Codeine	61	12	0.20	1	
	Chlorpheniramine	7.4	1.4	0.19	1	
	Carvedilol	93	15	0.16	2	
	Propofol	283	24	0.08	2	
	Carbamazepine	5.3	0.4	0.08	2	
	Naloxone	570	37	0.06	1	
Obach et al. (20)						
(Microsomes)						
($f_{u,B}$ and $f_{u,inc}$)						
	Zolpidem	0.5	5.7	11.40	1	0.105
	Ibuprofen	0.2	1.5	7.50	2	0.018
	Tolbutamide	0.07	0.36	5.14	2	0.073
	Diclofenac	1.6	7.6	4.75	2	0.009
	Diphenhydramine	2.2	9.5	4.32	1	0.338
	Warfarin	0.02	0.08	4.00	2	0.018
	Methoxsalen	4.5	18	4.00	2	0.134
	Dexamethasone	1	3.8	3.80	1	0.344
	Tenidap	0.03	0.1	3.33	2	0.001
	Diltiazem	3.6	12	3.33	1	0.220
	Diazepam	0.2	0.6	3.00	1	0.018
	Amitriptyline	4.2	12	2.86	1	0.058
	Hexobarbital	1.4	3.6	2.57	1	0.530
	Quinidine	1.4	2.7	1.93	1	0.141
	Imipramine	6.6	12	1.82	1	0.091
	Lorcainide	9.9	18	1.82	1	0.195
	Clozapine	1.9	2.9	1.53	2	0.057
	Propafenone	13	19	1.46	2	0.057
	Verapamil	13	19	1.46	1	0.130
	Methohexital	11	16	1.45	1	0.386
	Prednisone	3.4	4.9	1.44	2	0.301
	Triazolam	3.3	4.7	1.42	1	0.161
	Desipramine	8.8	12	1.36	1	0.188
	Ketamine	15	20	1.33	1	1.073
	Chlorpromazine	8.6	11	1.28	1	0.064
	Amobarbital	0.32	0.35	1.09	1	0.260
	Tenoxicam	0.03	0.03	1.00	1	0.013
	Midazolam	9.4	8.7	0.93	1	0.094
	Alprazolam	0.95	0.76	0.80	1	0.410

Author (System)	Drug	CL Predicted	CL Observed	Fold Dif	BDDCS Class	$f_{u,B}$
Obach et al. (20)						
(Microsomes)						
($f_{u,B}$)						
	Zolpidem	0.3	5.7	19.00	1	0.105
	Amitriptyline	0.8	12	15.00	1	0.058
	Diazepam	0.04	0.6	15.00	1	0.018
	Diphenhydramine	0.7	9.5	13.57	1	0.338
	Tenidap	0.01	0.1	10.00	2	0.001
	Clozapine	0.3	2.9	9.67	2	0.057
	Warfarin	0.01	0.08	8.00	2	0.018
	Ibuprofen	0.2	1.5	7.50	2	0.018
	Imipramine	1.6	12	7.50	1	0.091
	Chlorpromazine	1.5	11	7.33	1	0.064
	Prednisone	0.8	4.9	6.13	2	0.301
	Quinidine	0.5	2.7	5.40	1	0.141
	Tolbutamide	0.07	0.36	5.14	2	0.073
	Diclofenac	1.6	7.6	4.75	2	0.009
	Desipramine	2.8	12	4.29	1	0.188
	Methoxsalen	4.3	18	4.19	2	0.134
	Diltiazem	2.9	12	4.14	1	0.220
	Dexamethasone	1	3.8	3.80	1	0.344
	Hexobarbital	1.2	3.6	3.00	1	0.530
	Propafenone	6.5	19	2.92	2	0.057
	Lorcainide	6.7	18	2.69	1	0.195
	Verapamil	9	19	2.11	1	0.130
	Triazolam	2.7	4.7	1.74	1	0.161
	Ketamine	12	20	1.67	1	1.073
	Methohexital	9.9	16	1.62	1	0.386
	Tenoxicam	0.02	0.03	1.50	1	0.013
	Amobarbital	0.24	0.35	1.46	1	0.260
	Alprazolam	0.64	0.76	1.19	1	0.410
	Midazolam	8.8	8.7	0.99	1	0.094
Obach et al. (20)						
(Microsomes)						
(no binding)						
	Diphenhydramine	1.9	9.5	5.00	1	0.338
	Zolpidem	2.5	5.7	2.28	1	0.105
	Prednisone	2.4	4.9	2.04	2	0.301
	Hexobarbital	2.1	3.6	1.71	1	0.530
	Ketamine	12	20	1.67	1	1.073

Author (System)	Drug	CL Predicted	CL Observed	Fold Dif	BDDCS Class	$f_{u,B}$
	Amitriptyline	8.2	12	1.46	1	0.058
	Dexamethasone	2.6	3.8	1.46	1	0.344
	Diltiazem	8.7	12	1.38	1	0.220
	Methoxsalen	14	18	1.29	2	0.134
	Desipramine	9.4	12	1.28	1	0.188
	Imipramine	10	12	1.20	1	0.091
	Lorcainide	15	18	1.20	1	0.195
	Methohexital	15	16	1.07	1	0.386
	Verapamil	18	19	1.06	1	0.130
	Propafenone	19	19	1.00	2	0.057
	Chlorpromazine	11	11	1.00	1	0.064
	Quinidine	2.9	2.7	0.93	1	0.141
	Clozapine	3.8	2.9	0.76	2	0.057
	Alprazolam	1.5	0.76	0.51	1	0.410
	Triazolam	10	4.7	0.47	1	0.161
	Midazolam	19	8.7	0.46	1	0.094
	Tolbutamide	0.86	0.36	0.42	2	0.073
	Diclofenac	19	7.6	0.40	2	0.009
	Amobarbital	0.9	0.35	0.39	1	0.260
	Diazepam	2.1	0.6	0.29	1	0.018
	Ibuprofen	6.2	1.5	0.24	2	0.018
	Warfarin	0.46	0.08	0.17	2	0.018
	Tenidap	5.9	0.1	0.02	2	0.001
	Tenoxicam	1.6	0.03	0.02	1	0.013
Riley et al. (21)						
(Microsomes)						
	Methoxsalen	43	1340	31.16	2	
	Phenacetin	9.9	212.5	21.46	2	
	Propranolol	16.3	284.5	17.45	1	
	Fluvastatin	75.4	1052	13.95	1	
	Propafenone	644.9	6650	10.31	2	
	Lorcainide	97.1	924	9.52	1	
	Diclofenac	183.8	1667.3	9.07	2	
	FK1052	182	1525	8.38	-	
	Ibuprofen	12.3	102.4	8.33	2	
	Phenytoin	0.5	4	8.00	2	
	Diphenhydramine	7.3	53.5	7.33	1	
	Zolpidem	17.9	115.5	6.45	1	
	Amitriptyline	94.3	516	5.47	1	
	Omeprazole	101	502.7	4.98	1	
	Tolbutamide	1.3	6.4	4.92	2	

Author (System)	Drug	CL Predicted	CL Observed	Fold Dif	BDDCS Class	$f_{u,B}$
	Dexamethasone	3	13.6	4.53	1	
	Methohexital	57.6	207.4	3.60	1	
	Imipramine	106.6	330	3.10	1	
	Tenidap	26.2	80.4	3.07	2	
	Diltiazem	77.7	232.6	2.99	1	
	Metoprolol	6.8	20.2	2.97	1	
	Hexobarbital	2.9	8.3	2.86	1	
	Diazepam	11.8	28	2.37	1	
	Nilvadipine	3867	8123.4	2.10	2	
	Quinidine	10.7	22.1	2.07	1	
	Desipramine	81.8	160	1.96	1	
	Verapamil	553.6	935.3	1.69	1	
	Chlorpromazine	229.6	381.3	1.66	1	
	Clozapine	35.7	59	1.65	2	
	Prednisone	13.6	21.5	1.58	2	
	Triazolam	24.6	38.1	1.55	1	
	Amobarbital	1.2	1.4	1.17	1	
	Tenoxicam	2.2	2.2	1.00	1	
	Midazolam	183.7	163.2	0.89	1	
	Alprazolam	2.4	1.9	0.79	1	
	FK480	662	327.3	0.49	-	
	Nicardipine	13460	1806.7	0.13	1	
Riley et al. (21)						
(Hepatocytes)						
	FK1052	32.38	1570	48.49	-	0.021
	Troglitazone	306.36	10000	32.64	2	0.0017
	Montelukast	96.27	1495.15	15.53	2	0.0009
	Cyclosporin A	13.46	155.27	11.54	2	0.04
	FK079	56.38	636	11.28	-	0.0288
	Lorazepam	1.16	12.38	10.67	1	0.094
	Sildenafil	24.35	214.29	8.80	1	0.04
	Glipizide	7.13	60.52	8.49	2	0.02
	Nifedipine	32.6	253.7	7.78	2	0.05
	Prazosin	6.16	42.23	6.86	1	0.07
	FK480	49.41	336	6.80	-	0.008
	Naloxone	150.28	924.35	6.15	1	0.56
	Midazolam	40.08	246.27	6.14	1	0.04
	Indomethacin	27.13	145.77	5.37	2	0.02
	Propranolol	59.2	291.87	4.93	1	0.12
	Diazepam	6.41	31.29	4.88	1	0.012
	Oxazepam	8.23	38.8	4.71	2	0.03

Author (System)	Drug	CL Predicted	CL Observed	Fold Dif	BDDCS Class	$f_{u,B}$
	Ketoprofen	22.44	103.95	4.63	2	0.02
	Zidovudine	9.87	42.1	4.27	1	0.8
	Oxaprozin	24.4	100.36	4.11	2	0.0007
	Lidocaine	24.61	100.68	4.09	1	0.3
	Furosemide	5.95	22.85	3.84	4	0.029
	Fenoprofen	56.52	216.15	3.82	2	0.01
	Quinidine	12.95	48.63	3.76	1	0.15
	Diflunisal	9.86	34.8	3.53	2	0.0053
	Timolol	6.55	22.75	3.47	1	0.4
	Diclofenac	618.36	2083.46	3.37	2	0.0055
	Triprolidine	39.61	133.33	3.37	-	0.1
	Metoprolol	13.87	40.62	2.93	1	0.747
	Ritonavir	30.51	86.26	2.83	2	0.0148
	Phenacetin	76.01	212.5	2.80	2	0.594
	Acetaminophen	2.53	6.71	2.65	1	0.79
	Buspirone	613.8	1582	2.58	2	0.05
	Gemfibrozil	325.82	773.37	2.37	2	0.005
	Ondansetron	5.23	12.4	2.37	1	0.68
	Irbesartan	58.75	131.31	2.24	2	0.04
	Warfarin	3.69	8.22	2.23	2	0.018
	Chlorpromazine	230.33	502.92	2.18	1	0.03
	Carvedilol	281.58	521.97	1.85	2	0.03
	Diltiazem	77.81	143.61	1.85	1	0.22
	Prednisolone	35.54	59.22	1.67	1	0.26
	Ranitidine	3	4.4	1.47	3	0.77
	Methylprednisolone	37.08	52.17	1.41	1	0.23
	Verapamil	278.92	388.33	1.39	1	0.115
	Imipramine	92.57	125.59	1.36	1	0.1
	Tolbutamide	6.91	8.99	1.30	2	0.04
	Cimetidine	3.35	4.23	1.26	3	0.9
	Granisetron	29.72	35.14	1.18	1	0.7
	Ibuprofen	71.34	82.7	1.16	2	0.0182
	Etodolac	81.2	82.84	1.02	2	0.02
	Theophylline	1.67	1.68	1.01	1	0.4
	Desipramine	127.16	124.92	0.98	1	0.17
	Antipyrine	0.82	0.69	0.84	1	0.94
	Caffeine	2.89	2.25	0.78	1	0.685
	Pindolol	9.28	5.91	0.64	1	0.9
	Tenoxicam	8.77	4.46	0.51	1	0.0164

Author (System)	Drug	CL Predicted	CL Observed	Fold Dif	BDDCS Class	$f_{u,B}$
Riley et al. (21)						
(Hepatocytes)						
(serum)						
	Tolcapone	6.41	1650.32	257.46	2	0.0018
	Mibefradil	41.3	4888.9	118.38	2	0.005
	Felodipine	72.08	6111.11	84.78	2	0.004
	Bosentan	0.67	42.1	62.84	2	0.02
	Diltiazem	8.45	205.44	24.31	1	0.22
	Oxazepam	1.52	36.94	24.30	2	0.03
	Midazolam	25.74	599.04	23.27	1	0.04
	Propranolol	21.67	388.75	17.94	1	0.1
	Warfarin	0.34	6.02	17.71	2	0.018
	Lorazepam	1.24	16.71	13.48	1	0.094
	Diazepam	3.44	42.78	12.44	1	0.012
	Theophylline	0.35	1.55	4.43	1	0.4
	Caffeine	0.37	1.4	3.78	1	0.83
	Antipyrine	0.23	0.6	2.61	1	0.94

Publishing Agreement

It is the policy of the University to encourage the distribution of all theses, dissertations, and manuscripts. Copies of all UCSF theses, dissertations, and manuscripts will be routed to the library via the Graduate Division. The library will make all theses, dissertations, and manuscripts accessible to the public and will preserve these to the best of their abilities, in perpetuity.

Please sign the following statement:

I hereby grant permission to the Graduate Division of the University of California, San Francisco to release copies of my thesis, dissertation, or manuscript to the Campus Library to provide access and preservation, in whole or in part, in perpetuity.

Christine Bowman
Author Signature

6/14/19
Date